Quantum propagation and initial value problems in curved space.

Stanley, Ross James

Quantum Propagation and Initial Value Problems in Curved Space

Ross James Stanley

Thesis 2012
January

by

Ross J. Stanley

Swansea University
Prifysgol Abertawe

Submitted in conformity with the requirements
for the degree of Doctor of Philosophy
Department of Physics
Swansea University

Abstract

Quantum Propagation and Initial Value Problems in Curved Space

Ross James Stanley

Thesis 2012
January
Ross J. Stanley

Quantum field theory is studied within the semi-classical gravity approximation. The quantum correction to the propagation of both photons and gravitons in a general curved space background is calculated showing a non-trivial spacetime refractive index as well as a dynamical dressing (or undressing) of the particle state. The initial interacting particle's 'dressing', the cloud of virtual particles that surrounds it, may receive corrections from an infinite number of modes even for flat space. When gravitational tidal effects remove this dressing, squeezing it back into the bare particle, this leads to an amplification in a way consistent with unitarity.

There is a possible shift discovered in the graviton wavefront velocity related to higher order curvature couplings, although in this calculation there is also a logarithmic divergence at high frequencies, leading to a breakdown of the perturbative approximation.

Next we consider initial value problems and the stability of de Sitter space. Here the self decay of a massive scalar in de Sitter space is proposed to lead to a particle explosion where divergent growth of the field expectation value is observed.

Directly investigating this divergent field expectation value a one loop calculation is completed for a massive scalar particle in 3-dimensional de Sitter space. This result has characteristic secular growth that can be summed into a rapidly decaying exponential by using the dynamical renormalisation group.

Finally the evolution of two point functions is studied, by numerically solving their equations of motion using the Kaydanoff-Baym equations in 2-dimensional de Sitter space. Here we see a decay of the vacuum state due to the coupling. This appears to be related to the choice of initial conditions be chosen to match the free field vacuum plus non-interacting particles. This choice is made inappropriate by the dynamical dressing of the bare particle states.

Declaration

This work has not previously been accepted in substance for any degree and is not being concurrently submitted in candidature for any degree.

Signed ..... (candidate)
Date 24th February 2012

This thesis is the result of my own investigations, except where otherwise stated.
Other sources are acknowledged by footnotes giving explicit references. A bibliography is appended.

Signed ..... (candidate)
Date 24th February 2012

I hereby give consent for my thesis, if accepted to be available for photocopying and for inter-library loan, and for the title and summary to be made available to outside organisations.

Signed ..... (candidate)
Date 24th February 2012

Contents

Acknowledgments

With regards to the content of the thesis I would like to thank Tim Hollowood, my supervisor; Graham Shore, coauthor on my first paper and Ed Bennett for his help with the C coding used in Chapter.9.

I would also like to thank the STFC for giving me the money to do this work and the Physics Department at Swansea University for giving me somewhere to do it.

Further more I would like to thank my office mates over the years, Omar Al-Hartomy, Jéŕôḿé Gáílláŕd, Jonathan Lloyd, Jamie Nemeth, Jim Rafferty, Robert Rickman and Mark Round for putting up with the mess. A big shout out goes to everyone who made it to a steak friday.

Obviously much thanks must go to my friends and family who have supported me throughout the PhD.

Chapter 1

Introduction

The ultimate aim of modern theoretical physics is, ostensibly at least, to discover the so called Theory Of Everything. This would be a single theory with the capability to describe, accurately and self-consistently, any possible observable quantity.

Our current understanding of the universe is based around two different theories; General Relativity (GR) and Quantum Field Theory (QFT), specifically the Standard Model of particle physics. Both of these theories are hugely successful, although neither can lay claim to being a complete description of physics.

General Relativity, Einstein's theory of gravity first published in 1916, gives accurate predictions for measurements over an incredible range of distances, from less than around 60 micrometers [1] to the largest observable scales of tens of billions of light years [2].

Within General Relativity gravity is an exclusively attractive force, which allows it to describe the motions of objects. This is, of course, incomplete as it does not describe any of the usual quantum fields. One issue of a particular conceptual concern is the existence of black hole solutions. These include

singularities where we find infinite densities of matter and infinite curvature, indicating a break down of the theory.

The Standard Model which consists of Quantum Chromo-Dynamics (QCD) and Electro-Weak theory, is an example of a QFT and describes the most fundamental particles in nature that we know of. In principle the Standard Model could be used to derive, among other theories, condensed matter and atomic physics as well as all the theories reliant on these, although in practice this is not required and is unlikely to be undertaken. The Standard Model may, however, be used to directly describe the strong and weak nuclear forces as well as electro-magnetism (Electro-Weak theory describes the unification of the latter two), with some of the most accurate, verified, predictions in science [3,4]. The Standard Model and QFTs in general do not describe gravity or gravitational effects such as a field in a general curved background, or the gravitational back-reaction of particles, limiting the validity of the model to a fixed, flat space.

One should also be aware that the Standard Model is an effective theory. As such it has a limited range of energy scales over which it is valid. This leaves it unable to explain very high energy effects. On the other hand any Theory of Everything must be valid for the highest (possibly infinite) energy scales and as such would not be an effective theory.

The Theory of Everything would have to combine the successes of both General Relativity and the Standard Model, presumably by having both of these theories as limiting theories in particular kinematic and curvature regimes. This theory would also have to be meaningful in all regimes and capable of calculating the gravitational back-reaction of the fields on the geometry. As this must include both of these original gravitational and quantum mechanical descriptions the theory is often, *in absentia*, known as Quantum-Gravity (QG).

Attempts to create a working theory of Quantum-Gravity have proven notoriously difficult and are hindered greatly (and in a Popperist/positivist ap-

proach near terminally) by the lack of experimental measurements describing events and effects where it could be expected that these Quantum-Gravity influences become important, e.g. the regions where either General Relativity or quantum field theories on their own breakdown. Even black holes which are objects that are known to exist [5] do not present us with measurements that can not be explained using current theoretical techniques

There are however several potential theories of Quantum-Gravity, the most successful of which is String Theory. As of yet however none of these potential descriptions of Quantum-Gravity has been shown to be adequate as they introduce new computational and conceptual problems, or fail to correctly match experimental results. However further discussion of these issues is beyond the scope of this thesis.

There is another approach that may be taken when working with Quantum-Gravity as opposed to tackling it head on. In parameter space there are large areas where it is expected that non-trivial curvature and quantum effects should occur. Some of these regions of parameter space are still well within the ranges where we expect both GR and our known QFTs to be valid. Specifically this is when there is weak curvature and the energy scales are low. It is in these areas where it is possible to examine the interplay between these two theories. Using such an approach would lead to several potential benefits. Firstly it is this regime that becomes important when one is studying the early universe. Secondly it would give a larger variety of known results. These results would be valuable as non-trivial test in the development of a full theory of Quantum-Gravity such that new limits could be taken to match these weak curvature, low energy, effects. Of more immediate importance to this approach is that it could also lead to the identification of regions in parameter space where Quantum-Gravity effects become important that have not been identified though other means. One might hope that such regions are potentially accessible to modern experimental techniques.

Furthermore by understanding both QFTs and GR in a more general environment it could be expected that some general techniques and methodologies

would be developed. These techniques would not require a special set of circumstances to be of any use.[1] This could be of great benefit to our theoretical understanding of any physical situation, even within existing well-developed theories.

Probably the simplest way of making progress in this direction is by using an approximation scheme known as semi-classical gravity. Within this scheme a full QFT is taken to live on a fixed, curved, background space. In other words the fluctuations of the quantum fields dominate over the fluctuations of the spacetime metric (gravitons).

In fact one should be aware that the semi-classical gravity approximation is used whenever standard quantum field theory results are calculated, as these consist of calculations on a flat Minkowski, or very nearly flat, space background where any effects of gravitational back reaction are ignored. It could be claimed therefore that all the successes of particle physics are also successes of the concept of semi-classical gravity. As it is believed that the universe has a de Sitter geometry semi-classical gravity tells us that curvature effects only play a part in calculations at a level suppressed by inverse powers of the de Sitter radius and as such are irrelevant. The applicability of this argument is itself evidence supporting the semi-classical approximation.

It is the study of semi-classical gravity, both its predictions and the study of its range of validity, that forms the basis of this thesis. In particular we study the evolution of field vacuum and excitation states in the presence of curved backgrounds. These initial value problems require the review of several novel techniques [6–9] that are to be described in the following chapters. Firstly in Chapter.2 the semi-classical approximation [10] is described in greater detail and it is seen that some of our usual intuition from flat space particle physics is no longer applicable or useful here. Most notably the uniquely defined

[1]Note that many of our conceptual and intuitive ideas about quantum field theories come from the specific symmetry properties of flat space that do not hold in a general curved space, this includes the concept of globally defined particles and certain conservation laws e.g. the conservation of energy and momentum.

concept of a particle become more nebulous. Here several important problems are encountered, among which is the removal of new curvature dependent divergences from the stress-tensor, which requires the renormalization of the higher order curvature 'couplings' appearing in the effective action [10].

As it is general curved spaces that are being investigated it becomes necessary to deal with dynamical backgrounds. In such a situation the usual quantum field theoretical concept of the S-matrix may become inappropriate for calculations as the in and out states (if such states are even known) no longer share the same Hilbert space.

To this ends it is the evolution of 'In-In' state field expectation values that become our main consideration. To allow this a technique developed for non-equilibrium situations known variously as the 'In-In' [11], 'Closed Time Path' [8] , 'Real Time' [12], 'Causal' or 'Schwinger-Keldysh' [13] formalism is described in Chapter.3 and used in Chapters.(4,5,6,8,9).

Using the techniques shown in Chapters.(2,9) in Chapter.4 we develope the formalism [14] required in the new and original calculation of the the propagation of interacting particles in curved spaces. This requires examining the high frequency limit of the effective refractive index of a given spacetime and introduces us the a dynamical dressing or undressing of the composite particles seen in interacting theories. The general techniques and formalism required in this calculation are shown using the example of scalar fields in Chapter.4.

In Chapter.5 an existing calculation in scalar Quantum Electro-Dynamics [15] (sQED) is extended to the real world theory of Quantum Electro-Dynamics (QED) [16]. This shows how the spinor electron/positron loop (to lowest order in the coupling) modifies the propagation of a photon through curved space. This result is presented in the form of a refractive index and some phenomenologically relevant examples are given.

Chapter.6 shows the calculation of the propagation of a graviton, coupled

to a massive scalar field, through curved space. This introduces a frequency independent shift in the low frequency phase velocity and new curvature dependent divergences that lead to a breakdown of this perturbative scheme [17].

When working with curved spaces it is sensible to look at the simplest examples, with the highest degree of symmetry, first. This leads us to the three maximally symmetrical solutions to Einstein's vacuum equations: Minkowski (M), de Sitter (dS) and anti-de Sitter (AdS) spaces. These have zero, positive and negative scalar curvatures respectively. Minkowski space is standard flat space. Here special attention is given to the phenomenologically important de Sitter space.

De Sitter space is of particular interest as it is a dynamical spacetime maintaining the same number of symmetry generators as Minkowski space, although our understanding of physics in this background is not so well developed. De Sitter space is also of importance is cosmology, being the vacuum solution for both inflation [18] and the dark energy [19] solution in which late time accelerated cosmological expansion is observed. This background information forms the basis of Chapter.7

In the examination of QFTs living in de Sitter space we encounter the controversial question of whether de Sitter space is a stable background for a scalar quantum field theory. Some calculations show destabilizing growing modes [20], due to the apparent divergent growth of some initial non-vacuum state. This potential growth is physically justified by the fact that self decay, of a particle into multiple copies of itself, is now kinematically allowed [21].

The possibility of these growing field amplitudes is investigated in Chapter.8. Here in a 3 dimensional example the calculation of the one point field amplitude is examined, partially extending results from [7] to the case of massive field. The results obtained show a field amplitude whose absolute value grows rapidly with time. This growth shows a secular behaviour that characteristically appears in non-equilibrium calculations. These secular terms may be summed into a rapidly decaying exponential form by the use of the dynamical

renormalisation group [22].

In Chapter.9 we go beyond the results calculated in Chapter.8 by using using the Kadanoff-Baym (sometimes referred to as the Real Time Schwinger-Dyson) equations, which use a 2PI expansion, truncated here in a coupling expansion at 3 loop level. These are used to compute the evolution of the statistical and spectral 2-point functions in 2 dimensional de Sitter space. This allows us to see the evolution of specific occupation states and even the vacuum state in the presence of an interaction as well as potentially describing thermalisation. This technique is also capable of calculating the stress tensor for the field, the relevant quantity when back-reaction effects are being considered.

Finally in Chapter.10 these results are brought together and conclusions are made. Chapters.(1,2,3,7) review existing material, Chapters.(4,5,6) cover the original results presented in [16] [17] and finally Chapters.(8, 9) show unpublished results.

Chapter 2

Curved Space Quantum Field Theory

There are many conceptual problems that one encounters when considering calculations in curved spaces, such as those that are the basis of this thesis. Therefore in this chapter some of these concepts are reviewed.

2.1 Particles in Curved Space

In flat space the solutions to the field equations may be written in term of a superposition of positive and negative frequency plane wave modes. An 'in'('out') state is is one that is described entirely in terms of positive frequency plane wave modes, when these modes are viewed in the asymptotic past(future).

For a free field theory in flat space these in and out states will share the same Hilbert space, such that an in state describing a stable particle will evolve with time into an out state describing the same particle. In curved space the asymptotic past and future will not give plane wave solutions to the field equations so our usual definitions of in and out states are no longer applicable.

Furthermore even if some suitable generalisation of in and out states is chosen these will not in general share the same Hilbert space, leading to any definition of a particle ambiguous. In fact an in state corresponding to a vacuum may result in an out state with non-zero occupation numbers in a way that may be seen as particle creation from the vacuum. In Chapters.(4,5,6) we bypass this problem insisting that our space be asymptotically flat, although such an assumption can not be used in Chapters.(7,8,9) involving de Sitter space.

A further consideration when working in curved space is that the symmetries and their corresponding conservation rules, which are used to greatly simplify flat space calculations, are now lost. Some of these global concepts, such as asymptotic states and energy conservation may however be replaced with their local equivalents (i.e. states defined on local Cauchy surfaces and the conservation of the energy momentum tensor).

2.2 Semi-Classical Gravity and the large-N limit

As it is not known what the correct theory of Quantum-Gravity is for calculating 'real' quantum gravitational effects, that we expect to be true (that is we are not making 'guesses' about the nature of QG), it becomes necessary to use some suitable approximation of the full theory. The most obvious, low energy, weak curvature, scheme for doing this known as the semi-classical gravity approximation.

For a complete theory of Quantum-Gravity it is expected that all quantities undergo quantum fluctuations such that field fluctuations back-react with the geometry, which in turn affects the fields and so on. This a non-linear effect so at best difficult to compute exactly. The semi-classical gravity approximation avoids these problems as, put simply, it states that quantum field fluctuations dominate over fluctuations of the gravitational background. This allows the calculation of the back-reaction to be well controlled.

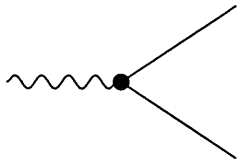

Figure 2.1: The diagrammatic form of the coupling between a the electron and photon fields. This vertex introduces a factor of $\alpha \simeq \frac{1}{137}$ into calculations. This graph may also be used to represent an electron emitting a photon or a photon decaying into an electron-positron pair.

This is a reasonable assumption to make in almost any situation where it is possible to make a physical measurement. The reason for this becomes clear the coupling of a typical QFT is compared with the 'coupling' which occurs in gravitational situations.

Taking, for instance, QED we have the cubic coupling between the fermionic electron field and the photon field as shown in Figure.2.1. This vertex is proportional to the coupling, which is in QED given by the dimensionless quantity known as the fine structure constant, $\alpha \simeq 1/137$. This in turn means that the one vertex tree level effect, such as the emission of a photon by an electron, is suppressed by this factor. For more complicated diagrams, with multiple appearances of this coupling, this is suppressed by a greater power of the coupling. It is this small factor that justifies the use of our perturbation scheme.[1]

For a perturbative expansion involving gravitons our couplings are proportional to the ratio between the energy scale of interested and the Planck mass, μ/G_{pl} such that a dimensionless expansion parameter is found. This coupling appears in calculations when a field back-reacts with the curvature, which diagrammatically leads to graphs of the form Figure.2.2.

When we are considering QFT effects, for what is experimentally considered a high energy scale of 1TeV, this gives relative a relative suppression factor of $\sim 10^{-15}$. Thus it is expected that QED effects are greater than gravitational

[1]The renormalisation group running of this constant is ignored in this argument, restricting its range of validity to low energy scales.

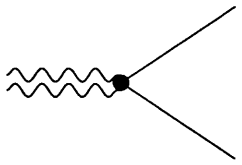

Figure 2.2: The coupling between a scalar/fermion field and a graviton. The coupling is proportional to the inverse of the Planck mass, measured in the units of the energy scale in which the expansion is being made at i.e. $\frac{\mu}{G_{pl}}$

back-reaction effects by a factor of approximately 10^{15} times. This explains why any such gravitational contributions are not included in any 'real world' calculations in particle physics. This also explains why when corrections to the stress tensor are considered they are expected to be very small, unless for some reason the perturbative techniques used break down.

However from a mathematical view point this still poses some troubling questions. For instance the coupling only acts as a multiplicative factor of a perturbative calculation in which it may be possible that this calculation gives a result that becomes large, despite the suppression factor from the coupling. There is also the possibility of non-perturbative and strong coupling effects becoming important. Furthermore we would like the validity of our approximation to be independent of the values of the particular constants appearing in our theory, e.g. it should not require a gravitational coupling that is small in comparison to the QFT couplings. Such a coupling independent scheme or approximation would allow more rigorous conclusions to be drawn from semi-classical gravity. In Chapter.6 such an approximation scheme is required as it is the propagation of gravitons that is calculated.

It is possible, to achieve a coupling independent approximation, in a formal sense at least, by taking N identical copies of the field in question. When N is allowed to become large this controlled approximation is observed. This may be made clear by examining this the simple case of a massive scalar field with the action

$$S = \int d^4x\sqrt{g}\left[\frac{1}{16\pi G}\left(R - 2\Lambda\right) + \mathcal{L}_{matter}\right] . \tag{2.1}$$

Taking N copies of the field multiplies the matter part of the action by N which gives

$$S_N = \int d^4x\sqrt{g}\left[\frac{1}{16\pi G}(R - 2\Lambda) + N\mathcal{L}_{matter}\right] . \tag{2.2}$$

Expanding this action in powers of N^{-1}, a parameter that is independent of our energy scalar or couplings, shows that to leading order the action is dominated by the matter contribution, regardless of the size of any of the couplings. This therefore matches the action of semi-classical gravity approximation. This can also viewed as taking the gravitational correction terms that are ignored in semi-classical gravity to be suppressed by positive factors N. The use of this large N scheme becomes a necessity when we wish to discuss the validity of the semi-classical approximation as, within this framework, any divergences found for gravitons must arise due to a breakdown of the approximation scheme and not the particular perturbation theory being used [23].

2.3 Curved Space Stability

When curved spacetimes are being considered as a background for QFTs the question of whether the spacetime presents a stable ground state for the field theory must be asked. As the semi-classical approximation assumes a fixed curved background if the situation being studied contains gravitational back-reaction due to the presence of matter fields one would expect the calculation to break down.

An example of this type of back-reaction is the 4 dimensional Schwartzschild black-hole. In the presence of some quantum field the curvature of the black hole induces particle production known as Hawking radiation [24]. The emission of these particles causes the black hole to lose mass until it eventually 'evaporates away'. This change in background shows how the semi-classical approximation that assumes a fixed background must breakdown.

A more dramatic kind of instability exists in which a spacetime may via an instantonic tunneling process decay into a different spacetime. One important example of this is the decay of the Kaluza-Klein spacetime into the so called bubble of nothing solution [25]. For such a spacetime it would make no sense to even try to consider to the behaviour of a field theory on this kind of fixed background as due to the 'spacetime decay rate' in the asymptotic future the original spacetime would no longer be present.

In general it is not immediately clear if a given spacetime is stable or not. Within the semi-classical approximation it is not possible to clearly show these instabilities, although indications may be expected. Specifically for an initial value problem with some small metric perturbation one would expect that these graviton modes would become divergently growing [23]. However even if such modes were to be discovered they would only indicate a breakdown of the approximation scheme, whether or not this is caused by a background instability. Knowing the limits of the semi-classical gravity approximation is, in itself however, still a useful result.

2.4 Stress Tensor Renormalisation

In Chapter.6 the coupling between a massive scalar field and a graviton is examined such that the simplest form of back-reaction may be considered.

Field expectation values, such as the field two-point stress tensor $\langle\phi(x)\phi(y)\rangle$, have the property that they diverge in the limit $x \to y$. In flat space these divergences are removed in a process known as normal ordering. This is equivalent isolating our attention to differences in energy levels as opposed to their absolute values. This is fine as in non-gravitating systems this difference is all that can be observed, however for gravitational systems this divergent absolute value for an expectation value would lead to infinite curvature and a break down of our theory, due to the stress tensor appearing as a source term in the Einstein field equations.

Therefore it becomes necessary to develop a method for renormalising these divergent quantities in a curved background. There are, for free fields in curved space, regularization and renormalisation methods. Of these the most useful for us here is the technique of dimensional regularisation. These methods are now well known and developed (see for instance [10]). As the coupling between a free field and a graviton is given by the stress tensor, it is the calculation of the renormalisation of this quantity that allows us to calculate the counter terms that appear in the calculation of the modification to graviton propagation appearing in Chapter.(6).

We summarise this stress tensor renormalisation in the Section.(2.4.1).

2.4.1 Renormalisation of the scalar field stress tensor in 4-D.

In this section we explicitly describe the calculation of the renormalised stress tensor for a free 4-D massive scalar field. To begin the matter part of the free scalar field action with the scalar coupling ξ is

$$\mathcal{L}_{matter} = \frac{1}{2}\left[g^{\mu\nu}\nabla_\mu\phi\nabla_\nu\phi - \left(m^2 + \xi R\right)\phi^2\right] \ , \tag{2.3}$$

for a mass m field in a curved background with scalar curvature R. As this is a massive theory we may redefine the mass in such a way as to absorb the factor ξR, although this would generally introduce a spacetime dependence for the mass which would not be natural. We ultimately avoid this problem by choosing to work in the minimally coupled case. The coupling between a free scalar field and a graviton can be found by the metric variation of this action, giving the classical stress-energy-momentum tensor of the scalar field

$$\begin{aligned} T_{\mu\nu} =& (1-2\xi)\nabla_\mu\phi\nabla_\nu\phi + \left(2\xi - \frac{1}{2}\right) g_{\mu\nu}\nabla_\sigma\phi\nabla^\sigma\phi \\ & - 2\xi\phi\nabla_\mu\nabla_\nu\phi + 2\xi g_{\mu\nu}\phi\nabla_\sigma\nabla^\sigma\phi - \frac{1}{2}g_{\mu\nu}m^2\phi^2 \ . \end{aligned} \tag{2.4}$$

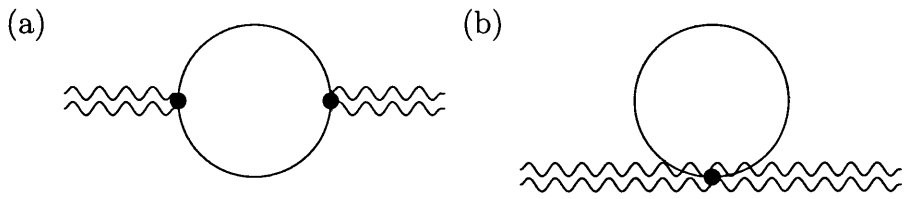

Figure 2.3: The lowest, one-loop, order contribution to the two point function of the graviton due to interactions with the scalar field. This may be seen as the coupling of a massive free scalar field to the gravitational background, via interactions with gravitons.

For simplicity we now switch to the minimally coupled case ($\xi = 0$) which gives,

$$T_{\mu\nu} = \nabla_\mu\phi\nabla_\nu\phi - \frac{1}{2}g_{\mu\nu}\nabla_\sigma\phi\nabla^\sigma\phi - \frac{1}{2}g_{\mu\nu}m^2\phi^2 \ , \tag{2.5}$$

from which the coupling between the scalar field and gravitons may be directly read off.

As it is the one-loop contribution to the vacuum polarisation that is the ultimate purpose of the calculation one must consider the Feynman diagrams shown in Figure.2.3. The second of these, the tadpole diagram, contains only a single local four-point coupling. Taking the second variation of the effective action with respect to the metric would find the four-point interaction. This contribution is not explicitly required in this calculation however, as it is local so has no curvature dependence so does not capture any of the curvature effects we are trying to examine. As this term is irrelevant when one is considering curvature effects it may be removed via the introduction of appropriate local contact terms during the regualrisation and renormalisation of the effective action.

These quantum loops introduce divergences that appear in the effective action. These are well known and have been calculated for a free scalar field in a general spacetime, as have appropriate regularisation methods. This can be seen, for example, in the monograph by Birrell and Davies [10]. For completeness some relevant parts of this discussion, including of course the final

result, are sketched here.

By considering the effective action in path integral formalism it may be shown

$$\mathcal{L}_{eff}(x) = \frac{i}{2}\lim_{y\to x}\int_{m^2}^{\infty} dm^2 G_F(x,y) \ . \tag{2.6}$$

where we now require a specific form for the Feynman Green's function. As we are interested in the short distance UV divergences we use the the asymptotic expansion known as the De Witt-Schwinger Green's function. This allows us to write the D dimensional effective action, $\mathcal{L}_{eff}$ as the sum,

$$\mathcal{L}_{eff} \approx -\lim_{x\to y}\frac{\sqrt{\det\Delta(x,y)_{\mu\nu}}}{2(4\pi)^{D/2}}\sum_{j=0}^{\infty} a_j(x,y)\int_0^{\infty}(iT)^{j-1-\frac{D}{2}}e^{-i(m^2T-\frac{\sigma}{2T})}idT \ . \tag{2.7}$$

where $\sigma(x,y) = \frac{1}{2}y_\sigma y^\sigma$ is half the geodesic distance between x and y and $\Delta(x,y) = \partial_\mu\partial_\nu\sigma(x,y)$ is the Van Vleck Morette matrix. The $a_j(x,y)$ terms appearing here are the so called HaMiDeW coefficients.[2]

To obtain the asymptotic expansion appear in (2.7) we begin by first expanding the metric $g(x)$ around the point x in Riemann normal coordinates, giving a metric of the form

$$g_{\mu\nu} = \eta_{\mu\nu}+\frac{1}{3}R_{\mu\sigma\nu\rho}y^\sigma y^\rho-\frac{1}{6}R_{\mu\sigma\nu\rho;\lambda}y^\sigma y^\rho y^\lambda+\left[\frac{1}{20}R_{\mu\sigma\nu\rho;\lambda\delta}+\frac{2}{45}R_{\sigma\mu\rho\gamma}R^{\gamma}_{\lambda\nu\delta}\right]y^\sigma y^\rho y^\lambda y^\delta... \tag{2.8}$$

where the coefficients are evaluated at $y = 0$.

When a kind of local momentum given by $ky = \eta^{\sigma\rho}k_\sigma y_\rho$ is introduced it is possible to (asymptotically) expand the local momentum space Green's

[2]Note that in some sources the VVM determinant prefactor is absorbed into the definition of the HaMiDeW coefficients. The technical advantages of this definition are of no benefit here, so we use the more 'old fashioned' notation.

functions as

$$G_F(k) \approx \left(k^2-m^2\right)^{-1} - \left(\frac{1}{6}-\xi\right) R \left(k^2-m^2\right)^{-2} + \frac{1}{2} i \left(\frac{1}{6}-\xi\right) R_{;\sigma} \partial^\sigma \left(k^2-m^2\right)^{-2} - \frac{1}{3} a_{\sigma\rho} \partial^\sigma \partial^\rho \left(k^2-m^2\right)^{-2} + \left[\left(\frac{1}{6}-\xi\right)^2 R^2 + \frac{2}{3}\alpha_\gamma^\gamma\right] \left(k^2-m^2\right)^{-3} \tag{2.9}$$

where $\partial_\sigma = \partial/\partial k^\sigma$. By using the prescription $m^2 \to m^2 - i\epsilon$ (other prescriptions here would allow for the derivation of other 2-point functions of this kind) and the integral representation

$$\left(k^2-m^2+i\epsilon\right)^{-1} = -i\int_0^\infty dT e^{iT(k^2-m^2+i\epsilon)} \tag{2.10}$$

this allows the Feynman propagator to be written as

$$G_F^{DS}(x,y) = -\sqrt{\Delta(x,y)} \int_0^\infty \frac{dT}{(4\pi T)^2} i e^{-im^2T + \frac{i}{2T}\sigma(x,y)} \Omega(x,y|T) \ . \tag{2.11}$$

Finally there is the asymptotic expansion

$$\Omega(x,y \mid T) \approx a_0(x,y) + a_1(x,y) iT + a_2(x,y)(iT)^2 + ... \tag{2.12}$$

This expansion may now be used to in (2.6) to find the expansion (2.7).

Using this form of the effective action we now wish to isolate and remove the UV divergences. The first $D/2+1$ terms that appear in the series appearing in (2.7) become divergent as $\sigma \to 0$. One may use dimensional regularisation to obtain these divergences in D dimensions. The coincidence limit in which the points x and y approach each other is given by

$$\begin{aligned} \mathcal{L}_{eff} &\approx \frac{1}{2}(4\pi)^{-D/2} \sum_{j=0}^\infty a_j(x) \int_0^\infty (iT)^{j-1-D/2} e^{-im^2T} i dT \\ &= \frac{1}{2}(4\pi)^{-D/2} \sum_{j=0}^\infty a_j(x) (m^2)^{D/2-j} \Gamma(j-D/2) \end{aligned} \tag{2.13}$$

where $a_j = a_j(x) = a_j(x,x)$. Up until this point the calculation has been valid for all D, but from now on the example of final spacetime dimension 4 is used, as this appears in the calculation in Chapter.6. To maintain the correct mass dimension of $(\text{length})^{-4}$ for the Lagrangian we introduce an arbitrary mass scale μ such that

$$\mathcal{L}_{eff} \approx -\frac{1}{2}(4\pi)^{-D/2}(m/\mu)^{D-4}\sum_{j=0}^{\infty} a_j(x) m^{4-2j}\Gamma(j-D/2)\ . \tag{2.14}$$

Around the point $D-4=\eta$ divergences occur due to the poles in the gamma function given by

$$\begin{aligned}
\Gamma(-D/2) &= \frac{4}{D(D-2)}\left(\frac{2}{\eta}-\gamma_E\right)+O(\eta)\ , \\
\Gamma(1-D/2) &= \frac{2}{2-D}\left(\frac{2}{\eta}-\gamma_E\right)+O(\eta)\ , \\
\Gamma(2-D/2) &= \frac{2}{\eta}-\gamma_E+O(\eta)\ .
\end{aligned} \tag{2.15}$$

Collecting these divergences together in a term that will be called $\mathcal{L}_{div}$ gives

$$\mathcal{L}_{div} = -(4\pi)^{-D/2}\left[\frac{1}{\eta}+\frac{1}{2}\left[(\gamma_E+\ln\left(\frac{m^2}{\mu^2}\right)\right]\right]\left(\frac{4m^4a_0}{D(D-2)}-\frac{2m^2a_1}{D-2}+a_2\right)\ . \tag{2.16}$$

The first three HaMiDeW coefficients, those appearing as the divergent terms in this expression, are given for any value of ξ by

$$\begin{aligned}
a_0 &= 1\ , \\
a_1 &= \left(\frac{1}{6}-\xi\right)R\ , \\
a_2 &= \frac{1}{180}R_{\mu\nu\sigma\rho}R^{\mu\nu\sigma\rho}-\frac{1}{180}R^{\mu\nu}R_{\mu\nu}-\frac{1}{6}\left(\frac{1}{5}-\xi\right)\Box R+\frac{1}{2}\left(\frac{1}{6}-\xi\right)^2R^2\ ,
\end{aligned} \tag{2.17}$$

where $R_{\mu\nu\sigma\rho}$ is the Riemann tensor, $R_{\mu\nu}$ is the Ricci tensor and R is the Ricci scalar.

As these divergent parts of the effective action are proportional to purely geometric quantities these terms are best seen as belonging to the gravitational, as opposed to the matter, part of the action. These new geometric terms modify the Einstein-Hilbert action to give

$$S_{Geo} = \int d^4x\sqrt{g}\left[\frac{1}{16\pi G_{Newton}}(R-2\Lambda) + c_1 R_{\mu\nu\sigma\rho}R^{\mu\nu\sigma\rho} + c_2 R^{\mu\nu}R_{\mu\nu} + c_3 R^2 + ...\right], \tag{2.18}$$

where the dots indicate the higher order curvature corrections.

It is not, however, the effective action that is of direct concern to us, but instead the equations of motion obtained via the effective action's variation with respect to the graviton. In four dimensions the generalised Gauss-Bonnet theorem state $\int d^4x\sqrt{g}\left(R_{\mu\nu\sigma\rho}R^{\mu\nu\sigma\rho} + R^2 - 4R_{\mu\nu}R^{\mu\nu}\right)$,

$$\int d^4x\sqrt{g}\left(R_{\mu\nu\sigma\rho}R^{\mu\nu\sigma\rho} + R^2 - 4R_{\mu\nu}R^{\mu\nu}\right), \tag{2.19}$$

must vanish as this is the Euler characteristic for the spacetime a topological invariant. This result allows us to eliminate one of these three new coupling terms from the action (2.18).

Now that the divergences of the effective action may be evaluated it is possible to calculate the counter terms appearing in the calculation of the one loop stress tensor.

The variation of the divergent part of the Lagrangian proceeds as follows,

$$\begin{aligned}
&\frac{1}{\sqrt{g}}\frac{\delta}{\delta g^{ab}}\int d^4x\sqrt{g}\mathcal{L}_{div} \\
&= \frac{1}{\sqrt{g}}\frac{\delta}{\delta g^{ab}}\int d^4x\sqrt{g}\left(\frac{1}{4\pi^2}\left(\frac{1}{\eta}-\frac{1}{2}\left(\gamma_E+\ln\frac{m^2}{\mu^2}\right)\right)\right. \\
&\quad\left.\times\left(\frac{m^4}{2}+\frac{R_{\mu\nu\sigma\rho}R^{\mu\nu\sigma\rho}}{180}-\frac{R_{\mu\nu}R^{\mu\nu}}{180}\right)\right) \\
&= \frac{1}{\sqrt{g}}\frac{\delta}{\delta g^{ab}}\int d^4x\sqrt{g}\left(\frac{1}{4\pi^2}\left(\frac{1}{\eta}-\frac{1}{2}\left(\gamma_E+\ln\frac{m^2}{\mu^2}\right)\right)\right. \\
&\quad\left.\times\left(\frac{m^4}{2}+\frac{R_{\mu\nu\sigma\rho}R^{\mu\nu\sigma\rho}}{240}+\frac{1}{720}\left(R_{\mu\nu\sigma\rho}R^{\mu\nu\sigma\rho}-4R_{\mu\nu}R^{\mu\nu}\right)\right)\right).
\end{aligned} \tag{2.20}$$

Renormalisation of the bare cosmological constant term, Λ_B, and the bare Newton's gravitational constant, G_B, from the unrenormalised Einstein equations, can be used to regularise the non-curvature dependent HaMiDeW coefficient, a_0. The other divergent terms, a_1 and a_2 can not be regularised by renormalisation of the existing constant terms in the Einstein field equations. This is because these remaining divergences are of the order of the fourth derivative of the metric, which requires the renormalisation of the c_i constants appearing in (2.18). When (2.19) is applied here the values of

$$\begin{aligned}
c_1 &= -\frac{1}{(4\pi)^2}\cdot\frac{1}{360}\left[\alpha_1+\log\left(\frac{m^2}{\mu^2}\right)\right], \\
c_2 &= \frac{1}{(4\pi)^2}\cdot\frac{1}{360}\left[\alpha_2+\log\left(\frac{m^2}{\mu^2}\right)\right], \\
c_3 &= 0,
\end{aligned} \tag{2.21}$$

for the terms appearing in (2.18) are found.

This leaves us with two, small, finite terms appearing in the effective action, α_1 and α_2.

It is known that the magnitude of these new physical constants must be

small to be consistent with observation for instance in [26] corrections to the Newtonian potential due to higher derivative corrections to the Einstein Hilbert action are considered. The physical effect of these constants in the calculation in Chapter.6 is to add a curvature dependent shift in the phase velocity. As this does not depend on the frequency, this shift also applies to the wavefront velocity. This appears to modify the causal structure of the spacetime for the graviton, for a non-zero value of these constants.

In fact whenever higher derivative corrections are considered massless particles not follow the GR light cone [27, 28] furthermore when gravitational fluctuations are considered on a spacetime the light cones are modified [29,30] as $g_{\mu\nu} + h_{\mu\nu}$ not $g_{\mu\nu}$ determines the causal structure [31]. Such modifications have been discussed in various settings, including with the AdS/CFT correspondence where the inclusion of bulk space curvature corrections lead to various modifications of the causal structures in this space [28,32–35].

It should also be expected that any corrections to the causal structure will only be applicable to spaces that are stably causal [36], should this not be the case then one might assume that these corrections either lead to acausality or a break down of the model being used, e.g. semi-classical gravity.

Chapter 3

Schwinger Keldysh Formalism

3.1 Evolution of States and Operators

The Schwinger-Keldysh (or 'in-in' or 'causal' or 'real-time') formalism is used to describe the time evolution of the expectation value of a field or operator set up in some arbitrary initial configuration.

This is a formalism developed for non-equilibrium calculations and has applications in thermal physics and has been successfully extended to include applications curved space physics, where it is commonly used in cosmology calculations [6].

As this calculation is taken from a fixed time until some arbitrary end point we have no need to define global in and out states as we do not integrate over the whole spacetime manifold, allowing us to work in situations where these states are not known. It also provides a framework in which one may uniquely define asymptotic in and out states by allowing the initial and final times tend to past and future infinity respectively (these positive or negative states are defined with respect to the imposed initial and final surfaces).

Although this formalism may be derived via a path integral approach for clarity and brevity we follow the operator formalism derivation appearing in the appendix of [6] here.[1]

To begin we take the field $\phi(\mathbf{x},t)$ and its conjugate momentum $\pi(\mathbf{x},t)$. These obey the canonical commutation relations

$$\begin{aligned}[\phi(\mathbf{x},t),\pi(\mathbf{y},t)] &= i\delta^{D-1}(\mathbf{x}-\mathbf{y}) \ , \\ [\phi(\mathbf{x},t),\phi(\mathbf{y},t)] &= [\pi(\mathbf{x},t),\pi(\mathbf{y},t)] = 0 \ .\end{aligned} \tag{3.1}$$

The dynamics of these fields are controlled by the Hamiltonian, H, such that

$$\begin{aligned}\dot{\phi}(\mathbf{x},t) &= i\left[H\left[\phi(t),\pi(t)\right],\phi(\mathbf{x},t)\right] \ , \\ \dot{\pi}(\mathbf{x},t) &= i\left[H\left[\phi(t),\pi(t)\right],\pi(\mathbf{x},t)\right] \ .\end{aligned} \tag{3.2}$$

As it is the fluctuations that are being studied a classical, c-number, result given by $\bar{\phi}$ and $\bar{\pi}$ is perturbed around such that $\phi = \bar{\phi} + \delta\phi$, $\phi = \bar{\pi} + \delta\pi$, where the classical solutions have equations-of-motion given by

$$\begin{aligned}\dot{\bar{\phi}}(\mathbf{x},t) &= \frac{\delta H\left[\bar{\phi}(t),\bar{\pi}(t)\right]}{\delta\bar{\pi}(\mathbf{x},t)} \ , \\ \dot{\bar{\pi}}(\mathbf{x},t) &= \frac{\delta H\left[\bar{\phi}(t),\bar{\pi}(t)\right]}{\delta\bar{\phi}(\mathbf{x},t)} \ .\end{aligned} \tag{3.3}$$

As these classical solutions are c-number solutions $\delta\phi$ and $\delta\pi$ follow the commutation relations (3.1), where we use the replacements $\phi \to \delta\phi$ and $\pi \to \delta\pi$.

Now, to separate out the fluctuations, the Hamiltonian H is expanded in powers of the perturbations to find

$$\begin{aligned}H\left[\phi(t),\pi(t)\right] = H[\bar{\phi}(t),\bar{\pi}(t)] + \frac{H\left[\bar{\phi}(t),\bar{\pi}(t)\right]}{\delta\bar{\phi}(\mathbf{x},t)}\delta\phi(\mathbf{x},t) + \frac{H\left[\bar{\phi}(t),\bar{\pi}(t)\right]}{\delta\bar{\pi}(\mathbf{x},t)}\delta\pi(\mathbf{x},t) \\ + \tilde{H}\left[\delta\phi(t),\delta\pi(t);t\right] \ ,\end{aligned} \tag{3.4}$$

[1]The path integral approach would increase the number of available gauge choices (depending on the fields) as well as allowing non-perturbative calculations.

where $\tilde{H}$ contains all the Hamiltonian terms that are second or higher order in the perturbations.

It is $\tilde{H}$ that determines the equations-of-motion of $\delta\phi$ and $\delta\pi$ as can be seen by subtracting the equations-of-motion for $\bar{\phi}$ and $\bar{\pi}$ from ϕ and π, which leaves

$$\begin{aligned} \delta\dot{\phi}(\mathbf{x},t) &= i\left[\tilde{H}\left[\bar{\phi}(t),\bar{p}(t);t\right],\delta\phi(\mathbf{x},t)\right] , \\ \delta\dot{\pi}(\mathbf{x},t) &= i\left[\tilde{H}\left[\bar{\phi}(t),\bar{p}(t);t\right],\delta\pi(\mathbf{x},t)\right] . \end{aligned} \tag{3.5}$$

Now, moving towards the initial value problem that is the purpose of this methodology, the following equations may be written,

$$\begin{aligned} \delta\phi(t) &= U^{-1}(t,t_0)\delta\phi(t_0)U(t,t_0) , \\ \delta\pi(t) &= U^{-1}(t,t_0)\delta\pi(t_0)U(t,t_0) . \end{aligned} \tag{3.6}$$

The unitary operator $U(t,t_0)$ used here is defined by the equation

$$\frac{d}{dt}U(t,t_0) = -i\tilde{H}\left[\delta\phi(t),\delta\pi(t);t\right]U(t,t_0) \tag{3.7}$$

along with the initial condition $U(t_0,t_0)=1$.

It is useful now to switch to the interaction picture. This may be done by separating out the quadratic, kinematic, piece of $\tilde{H}$, labelled here as H_0, leaving the interaction term H_I

$$\tilde{H}\left[\delta\phi(t),\delta\pi(t);t\right] = H_0\left[\delta\phi(t),\delta\pi(t);t\right] + H_I\left[\delta\phi(t),\delta\pi(t);t\right] . \tag{3.8}$$

U may be computed as a power series in the interaction Hamiltonian H_I. Working towards this ends the interaction operators $\delta\phi_I(t)$ and $\delta\pi_I(t)$ are introduced. These operators have the equations-of-motion that are given by

$$\begin{aligned} \delta\dot{\phi}_I(t) &= i\left[H_0\left[\delta\phi_I(t),\delta\pi_I(t);t\right],\delta\phi_I(t)\right] , \\ \delta\dot{\pi}_I(t) &= i\left[H_0\left[\delta\phi_I(t),\delta\pi_I(t);t\right],\delta\pi_I(t)\right] , \end{aligned} \tag{3.9}$$

where the initial conditions

$$\delta\phi_I(t_0) = \delta\phi(t_0) \ , \qquad \delta\pi_I(t_0) = \delta\pi(t_0) \ , \tag{3.10}$$

have been chosen.

Due to the explicit dependence of the kinematic Hamiltonian H_0 in (3.9) on t, the interaction operators may be chosen to be taken any time. Therefore by choosing $t = t_0$, using (3.10) the relation

$$H_0\left[\delta\phi_I(t), \delta\pi_I(t); t\right] = H_0\left[\delta\phi(t), \delta\pi(t); t\right] \ , \tag{3.11}$$

is found.

The solution of (3.9) may be written as a unitary transform of some initial state

$$\begin{aligned} \delta\phi_I(t) &= U_0^{-1}(t, t_0)\delta\phi(t_0)U_0(t, t_0) \ , \\ \delta\pi_I(t) &= U_0^{-1}(t, t_0)\delta\pi(t_0)U_0(t, t_0) \ . \end{aligned} \tag{3.12}$$

where U_0 is defined by

$$\frac{d}{dt}U(t, t_0) = -iH_0\left[\delta\phi(t), \delta\pi(t); t\right] U_0(t, t_0) \tag{3.13}$$

and the initial condition $U_0(t_0, t_0) = 1$.

Now, by combining (3.7) and (3.13) it is found that

$$\frac{d}{dt}\left[U_0^{-1}(t, t_0)U(t, t_0)\right] = -iU_0^{-1}(t, t_0)H_I\left[\delta\phi(t), \delta\pi(t); t\right] U(t, t_0) \ . \tag{3.14}$$

This result, by use of (3.12), implies that

$$U(t, t_0) = U_0(t, t_0)K(t, t_0) \ , \tag{3.15}$$

where

$$\frac{d}{dt}K(t, t_0) = -iH_I(t)K(t, t_0) \ , \qquad K(t_0, t_0) = 1 \ . \tag{3.16}$$

This includes H_I which is in turn given by

$$H_I(t) = U_0(t,t_0)H_I\left[\delta\phi(t_0),\delta\pi(t_0);t\right]U_0^{-1}(t,t_0) = H_I\left[\delta\phi_I(t),\delta\pi_I(t);t\right] \ . \tag{3.17}$$

The solution for K is of a well known form given by

$$K(t,t_0) = T\exp\left(-i\int_{t_0}^{t} H_I(t)dt\right) \ , \tag{3.18}$$

such that for an operator $Q(t)$ constructed from products of $\delta\phi(t)$ and $\delta\pi(t)$ we find the time evolution equation

$$Q(t) = \left[\bar{T}\exp\left(i\int_{t_0}^{t} H_I(t)dt\right)\right] Q_I(t) \left[T\exp\left(i\int_{t_0}^{t} H_I(t)dt\right)\right] \ . \tag{3.19}$$

$\bar{T}$ is the anti-time ordering operator, Q is constructed from some product of $\delta\phi$ and $\delta\pi$, with Q_I being the same product as Q using $\delta\phi_I$ and $\delta\pi_I$ instead of $\delta\phi$ and $\delta\pi$.

3.2 Diagrammatic Rules and Two Point Functions

By assuming that the interaction Hamiltonian may be constructed perturbatively, in the coupling, the usual Wick contractions may be used to construct a set of diagrammatic rules for the calculation of a time dependent expectation value, as shown in (3.19). Due to the time ordering and anti-time ordering operators (3.19) may be interpreted as as a contour integral in the complex t plane with integrations in both the forward $+$ and backward $-$ time directions as shown in Figure.(3.1).

The two point functions appearing in this expansion have a more complicated structure than those of the usual Feynman approach in which all of the expansion terms may be written in terms of the Feynman propagators. This

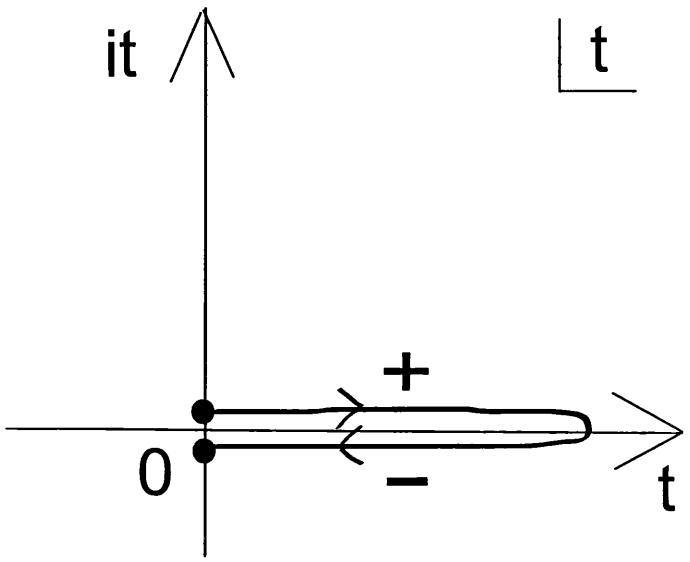

Figure 3.1: The contour integral described in (3.19). The time ordered (T) branch labeled with, +, is given the $+i\epsilon$ prescription and the anti-time ordered ($\bar{T}$) branch is labeled with a, −, and is given the $-i\epsilon$ prescription. The integral is taken from $t = t_0$ to $t = t$, via abuse of notation.

is a result of the presence of both time and anti-time ordered fields in (3.19) which effectively introduces two copies of the field, $\delta\phi_I$ labelled with a + and −. These labels are allocated according to the field insertions are in the + or − branch of the integral shown in Figure.3.1 respectively.

Therefore as the Wick contractions are over all bilinear field combinations the two point functions inherit a a set of labels $G^{AB}(x, y)$, in which $A, B = +, -$.[2] Note that the mixed index two point functions $G^{+-}(x, y)$, $G^{-+}(x, y)$ are not Green's functions as they are solutions to the homogeneous equations-of-motions.

These two point functions may be related to each other and the usual

[2]The fact we only include the bilinear contractions is due to the assumption that the fields perturbations obey a Gaussian distribution. This is a good approximation when we only consider small perturbations as is the case here.

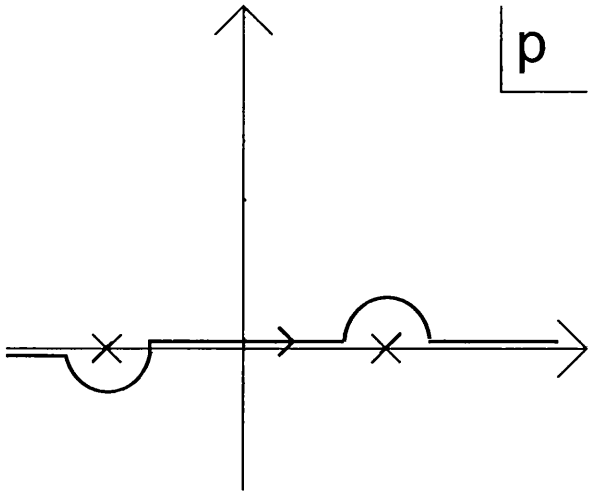

Figure 3.2: The Feynman propagator as momentum space contour integrals. The corresponding anti-Feynman propagator takes the opposite prescription, above $p = -p_0$ and below $p = p_0$. The prescription is therefore given by $+ip\epsilon$ for the Feynman and $-ip\epsilon$ for the anti-Feynman.

Feynman propagator and Wightman functions using

$$G^{++}(x,y) = \langle T\phi(x)\phi(y)\rangle = G_F(x,y) \tag{3.20a}$$

$$G^{--}(x,y) = \langle \bar{T}\phi(x)\phi(y)\rangle = \overline{G_F}(x,y) \tag{3.20b}$$

$$G^{+-}(x,y) = \langle \phi(x)\phi(y)\rangle \ = G_+(x,y) \tag{3.20c}$$

$$G^{-+}(x,y) = \langle \phi(y)\phi(x)\rangle \ = G_-(x,y) \tag{3.20d}$$

The momentum space contours representing this two point functions (in flat space) are given in Figure.3.2 for the Feynman Propagator and Figure.3.3 for the Wightman functions, showing their 'ϵ' prescriptions.

Although these functions form a complete basis and are those that are

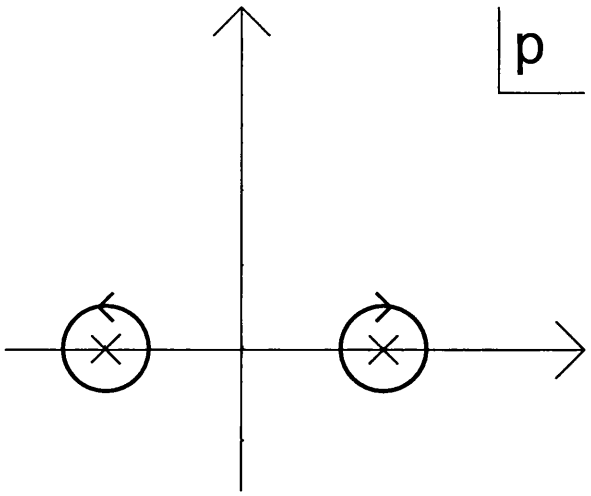

Figure 3.3: The Positive and Negative frequency Wightmann functions as momentum space contour integrals. The positive (negative) frequency function is the contour taken around the pole at $p = p_0$ ($p = -p_0$).

directly encountered though the Wick contractions over field pairs it is also possible to write these functions in terms of a different basis of two point functions known as the Keldysh basis as shown in, for instance, [37] and references therein. It is useful to show this other set of two point functions here as these become the appropriate choice of basis for the Kadanoff-Baym equations appearing in Chapter.9. This Schwinger basis is given by the 2-point functions

$$iG_S(x,y) = \langle[\phi(x)\phi(y)]\rangle = G^{+-}(x,y) - G^{-+}(x,y) = F(x,y) \quad (3.21a)$$

$$G^{(1)}(x,y) = \langle\{\phi(x)\phi(y)\}\rangle = G^{+-}(x,y) + G^{-+}(x,y) = \rho(x,y) \quad (3.21b)$$

$$G_R(x,y) = -\Theta(x_0 - y_0)G_S(x,y) \quad (3.21c)$$

$$G_A(x,y) = \Theta(y_0 - x_0)G_S(x,y)\ , \quad (3.21d)$$

where $G_S(x,y)$ is the Schwinger Function, with the momentum space contour shown in Figure.3.4 (also known as the statistical function), $G^{(1)}(x,y)$ is Hadamard's elementary function also shown in Figure.3.4 (also known as the spectral function), $G_R(x,y)$ is the Retarded propagator and $G_A(x,y)$ is the advanced propagator where the momentum space contours representing both

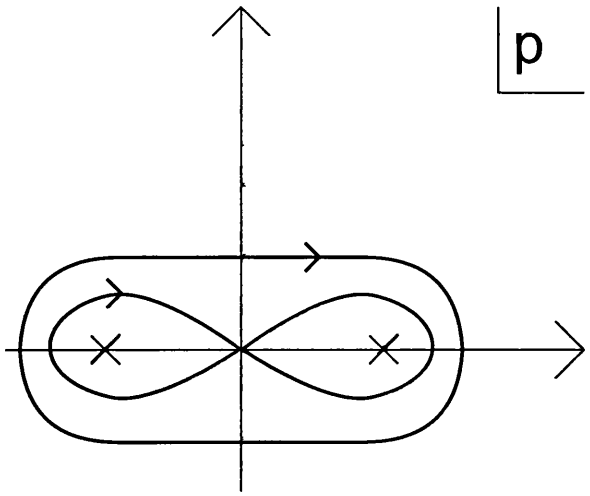

Figure 3.4: The Schwinger and Hadamard functions as momentum space contour integrals. The Schwinger function here is the 'figure of eight' contour here and the Hadamard function is the outer circular contour.

are shown in Figure.3.5.

Here we describe the diagrammatic rules used in the Feynman/Wightman basis of propagators [6]. It is perfectly possible to formulate such diagrammatic rules in the Keldysh basis [38]. To calculate the to nth order in the interaction coupling one starts by taking n vertices, each labeled with a space and time coordinate. Lines are connected to these vertices and represent the fields. For each field δ_I appearing in Q_I we have an external leg, with only one end connected to a vertex. The rest of the lines are internal and must begin and end on a vertex. The interaction in the theory tells us how many lines can or must be attached to each vertex.

Each vertex is assigned a $(+/-)$ and the sum over all 2^n possible configurations must be taken. For a vertex labeled with a $+$ the coupling is multiplied

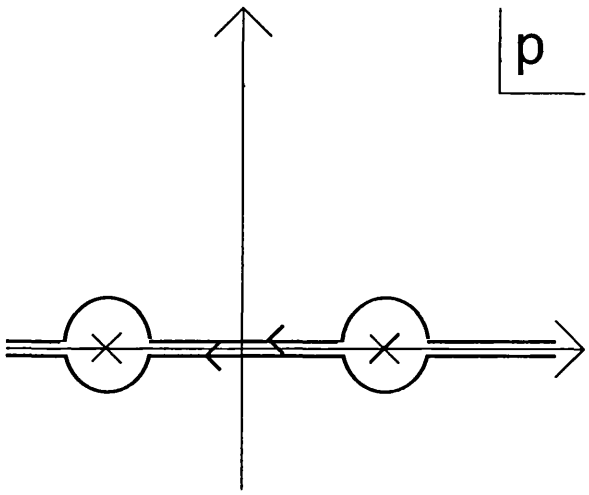

Figure 3.5: The Advanced and Retarded propagators as momentum space contour integrals. For the Advanced Propagator we have the $+i\epsilon$ prescription and the $-i\epsilon$ prescription is used for the Retarded propagator.

by a factor of $+i$ and for vertex labeled with a $-$ this factor is now $-i$.

When there is a line that connecting a $+$ vertex to a $+$ vertex a standard Feynman propagator $G_F(x,y)$ should be included. When a line connects a $-$ vertex to a $-$ vertex an 'anti-Feynman' propagator $\overline{G_F}(x,y)$ should be included. For a line that connects a $-(+)$ vertex to a $+(-)$ vertex or vice a versa a Wightman functions, $G^{+(-)}(x,y)$ must be included. Finally when there is a $+(-)$ vertex attached to an external leg a $\phi^{+(-)}(x)$ field insertion is included. Now one must integrate over space and the vertex times between t_0 and t, to find the diagrammatic contribution.

Chapter 4

Curved Space Quantum Particle Propagation

Now that the techniques of semi-classical gravity and the Schwinger-Keldysh formalism have been developed, they can be applied to the calculation of the effect of curvature on the propagation of interacting particles. This line of research was motivated by the possibility of superluminal propagation of particles suggested by the Drummond Hathrell effect [39].

The Drummond Hathrell effect explains how the one (electron-positron) loop effective action in a low frequency approximation can lead to modifications of the phase velocity of a propagating photon. Since this was first discovered it lead to discussions about possible violations of causality [36, 40–43].

The superluminal low frequency propagation of photons can be extracted from the effective action for QED in curved spacetime taken to linear order in the curvature:

$$S = \int d^4x \sqrt{g}\Big[-\frac{1}{4e^2} F_{\mu\nu}F^{\mu\nu} + a_1 R F_{\mu\nu}F^{\mu\nu} + a_2 R_{\mu\nu}F^{\mu\lambda}F^{\nu}{}_{\lambda} + a_3 R_{\mu\nu\lambda\rho}F^{\mu\nu}F^{\lambda\rho} + \cdots \Big] . \tag{4.1}$$

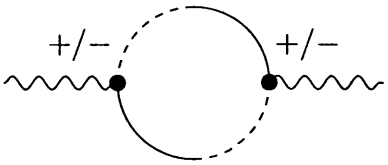

Figure 4.1: The, one loop, sunset diagram that contributes to the 1-loop 2PI effective action of QED, where the $+/-$ are summed over giving four diagrams using the rules desribed in Chapter.3. The variation with respect to one of the external legs (specifically $\delta^+(x)$)of these diagrams (integrated over all space) is used to calculate the correction to the scalar equations of motions Schwinger-Keldysh formalism.

The terms involving the curvature here are caused by vacuum polarization and the dots indicate that this effective action is the first term in a curvature/derivative expansion, so results deduced from it are valid only for low frequency propagation. At one-loop order, the Schwinger-Keldysh diagram that contributes is shown in Figure 4.1 is non-local and so sensitive to the background curvature. The effective action (4.1) has been renormalized and the one-loop divergence has been absorbed into the definition of the renormalized electric charge.

The refractive index derived from (4.1) for a photon with wave-vector $k^\mu = \omega\hat{k}^\mu$, where ω is the frequency, is

$$n_{ij} = \delta_{ij} + \frac{\alpha}{m^2}\left(c_1\delta_{ij}R_{\mu\nu}\hat{k}^\mu\hat{k}^\nu + c_2R_{\mu i\nu j}\hat{k}^\mu\hat{k}^\nu\right) , \tag{4.2}$$

where the indices i, j label the two spacelike polarisation directions. The constant coefficients c_1, c_2 are simply related to the known coefficients a_2, a_3 in the effective action (4.1)(see for example [15]). If an affine coordinate u is introduced along the null geodesic, with tangent vector k^μ, where the geodesic is denoted by γ, one may write (4.2) as

$$n_{ij}(u) = \delta_{ij} + \frac{\alpha}{m^2}\left(c_1\delta_{ij}R_{uu}(u) + c_2R_{iuju}(u)\right) . \tag{4.3}$$

This makes it clear that the Drummond-Hathrell result depends on the cur-

vature components $R^i{}_{uju}(u)$ and $R_{uu}(u)$ evaluated along the null geodesic γ describing the photon's classical trajectory. These are exactly the same geometric quantities required to describe the Penrose limit [44] taken along the same geodesic.

There are three scales in the problem, ω, m and $\mathfrak{R}$, the latter being the scale of a typical element of the Riemann tensor of mass dimension $[M^{-2}]$. The Drummond-Harthrell result based on the effective action in (4.1) is valid in the limit $m^2 \gg \mathfrak{R}$ and $\omega^2\mathfrak{R}/m^4 \ll 1$, while the description of the photon in terms of classical ray optics in curved space requires that $\omega^2 \gg \mathfrak{R}$, so that the wavelength is large compared with the length scale over which the curvature varies. It is by using this ray optics limit that allows the results presented here to go beyond those of this Drummond-Hathrell result.

As this Drummond-Hathrell result brings about questions regarding causality it is useful to clarify what we mean in such a context. When one is discussing causality in curved space QED the relevant 'speed of light' to consider is the wavefront velocity [36].[1]The wavefront velocity may be defined as the infinite frequency limit of the phase velocity. This requires a calculation in the limit $\omega^2\mathfrak{R}/m^4 \gg 1$, which is compatible with the ray optics limit.

As the Drummond Hathrell effect is a low frequency result it does not directly relate to causality. However in flat space we have the Kramers-Kronig dispersion relations which relate the zero frequency phase velocity to the wavefront velocity, using the imaginary contribution to the vacuum polarisation.

$$n(\infty) = n(0) - \int_0^\infty \frac{d\omega}{\omega} \mathrm{Im}\left(n(\omega)\right) \ , \tag{4.4}$$

where the refractive index $n(\omega)$ is related to the phase velocity $v_{ph}(\omega)$ by the relation $n(\omega) = c/v_{ph}(\omega)$. For a non-dispersive medium the optical theorem states that $\mathrm{Im}\left[n(w)\right]$ must always be positive, such that if $v_{ph}(0)$ is greater than c, then so must be $v_{wf} = c/n(\infty)$.

[1]This is as any information must be carried in some sharp fronted wave packet, where this sharp front is dominated by the highest frequency modes.

The resolution to this problem relies on the fact that spacetime acts as a dispersive optical medium, although to show this, the phase velocity must be calculated in some scheme valid at high frequencies. This was achieved in a series of papers [14–17, 45–47]. These results include the calculation of a spacetime refractive index, showing that a superluminal signal speed does not occur, although spacetime is found to act as a dispersive medium with a not trivial refractive index. This dispersion itself introduces either growth or decay of the particle amplitude. Although this seems to violate unitarity it was further shown to be a dynamical process of either 'dressing' or 'undressing' the bare, free-field particle states.

This variable dressing of states may be understood be re-evaluating our understanding of (4.4). Here it is usually assumed that the imaginary part of the decay rate is identified with the dispersion of the photon field due to scattering in the medium, or in this case the decay of the photon into an electron positron pair. However one must consider that an interacting particle is dressed by a cloud of virtual particles. In some cases this dressing of the field may be divergent even in flat space. This cloud is non-local and as such is exposed to the tidal forces arising due to spatial curvature. Conceptually these tidal forces may either be convergent, squashing this cloud undressing the photon, or divergent, stretching this dressing cloud leading to a greater amount of dressing. It is this curvature dependence of balancing between the dressing and the bare field that is described by the imaginary part of the refractive index.

The results presented in the following chapters are calculated at one loop level and are valid within the ray optics also called the WKB approximation, $\omega^2 \gg \mathfrak{R}$. In this chapter the example of the propagation of a massless scalar coupled to a massive scalar is calculated.

In Chapter.5 the effect of the spin-$\frac{1}{2}$ electron on the propagation of a photon is considered, extending previous calculations conducted with the less physically important scalar QED. Chapter.6 investigates the propagation of a graviton coupled to N scalar fields in a curved background.

The scalar field equations-of-motion are given by the Klein-Gordon equation

$$\Box A(x) = 0 \, . \tag{4.5}$$

In a general background spacetime, it is not possible to solve for these scalar modes exactly. However we will work in the WKB approximation which is valid when the frequency is much greater than the scale over which the curvature varies, $\omega^2 \gg \mathfrak{R}$. In this case, we can write the field in the form

$$A(x) = \mathcal{A}(x) e^{i\Theta(x)} \, , \tag{4.6}$$

where the eikonal phase Θ is $\mathcal{O}(\omega)$ and the scalar amplitude $\mathcal{A}$ is $\mathcal{O}(\omega^0)$ and given by

$$\mathcal{A}(x) = \frac{1}{g(x)^{1/4}}, \tag{4.7}$$

where $g(x)$ is the usual determinant of the metric tensor.

Substituting this into the equation-of-motion, and expanding in powers of $1/\omega$, the leading order term yields the *eikonal equation* for the phase:

$$\partial\Theta \cdot \partial\Theta = 0 \, ; \tag{4.8}$$

which implies that the gradient $k^\mu = \partial^\mu \Theta$ is a null vector field. This vector field defines a *null congruence*, that is a family of null geodesics whose tangent vectors are identified with the vector field k^μ. This vector can also be identified with the 4-momentum of photons: in this sense the eikonal approximation is the limit of classical ray optics.

We can then pick out a particular null geodesic, or classcal ray, in the congruence. Our goal is to find how this particular ray γ is affected by the $\mathcal{O}(\mathfrak{R}^2)$ terms in the action. There are a set of coordinates $(u, \hat{v}, x^a)$ which are specifically adapted to the null congruence: these will become the Rosen coordinates of the Penrose limit (4.11). In these adapted coordinates the geodesics are simply lines of constant $(\hat{v}, x^a)$ and u is the affine parameter. We will choose the ray γ to be the one with $x^a = \hat{v} = 0$. In these coordinates

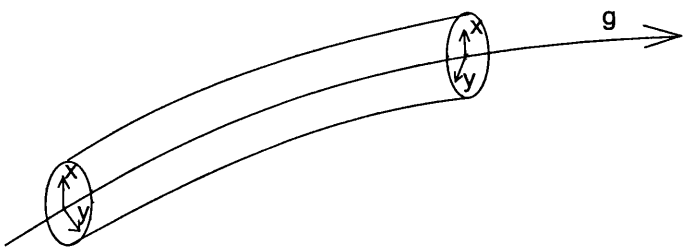

Figure 4.2: The small region around the geodesic, g, which is Gaussian in the curvature is expanded to cover the whole of space within the Penrose limit, i.e. x and y are expanded such that the tubular region in the diagram fills the whole manifold. It is this region that contains the null congruence.

the eikonal phase is simply,

$$\Theta = \omega \hat{v} \ . \tag{4.9}$$

4.1 Curved Space Particle Propagation

Schematically the free field eikonal modes and propagators are used to calculate the one loop correction to the eikonal phase velocity of the original modes. This calculation is controlled by the fact that the loop particles are massive and therefore their contribution is dominated by the spacetime curvature in the region directly surrounding the propagating particle's geodesic. This this region is described by the Penrose limit [44] as is shown in Figure.4.2.

In these calculations the Penrose limit arises naturally as we explain later in this chapter. The Penrose limit may be seen as the spacetime observed by an observer following a null geodesic. In the taking of this limit one will always find a result in the form of a plane wave geometry.

To describe such plane wave spaces two coordinate systems are commonly used, these are known as Brinkmann and Rosen coordinates, although other coordinate systems do exist. A useful review of plane wave geometries and Penrose limits may be found in [48,49]. The general form of such a plane wave

may be given by the following metrics

$$ds^2 = 2dudv - h_{ij}(u)z^i z^j du^2 + \delta_{ij}dz^i dz^j \tag{4.10}$$

in Brinkman coordinates and

$$ds^2 = 2dud\tilde{v} + C_{ab}(u, x^a)dx^a dx^b \tag{4.11}$$

in Rosen coordinates. The u coordinate that is shared between both sets of coordinates is an affine 'time' parameter along the direction of the propagation of the wave. It should be noted that $h_{ij}(u)z^i z^j = -R^i_{uju}z^i z^j$.

It is possible to switch between these two sets of coordinates, with the transforms from Rosen to Brinkman shown here, by using the following relations

$$\begin{aligned} \tilde{v} &\to v + \frac{1}{2}\Omega_{ij}(u)z^i z^j \\ x^a &\to E^a_i(u)z^i \ . \end{aligned} \tag{4.12}$$

The zweibeins $E^i_a(u)$ appearing in these equations are the solutions to the equation

$$C_{ab}(u) = E_{ia}(u)\delta^{ij}E_{jb}(u) \ , \tag{4.13}$$

along with the condition

$$\Omega_{ij} = \frac{dE_{ia}(u)}{du}E^a_j(u) \ . \tag{4.14}$$

These zweibeins $\boldsymbol{E}$ are uniquely specified by the requirement that $\boldsymbol{\Omega}$ is symmetrical under interchange of indices.

To see how the Penrose limit of a general spacetime is taken it is convenient to notice that any metric may be rewritten in the form

$$ds^2 = dud\tilde{v} + C(u, \tilde{v}, x^a)d\tilde{v}^2 + 2C_a(u, \tilde{v}, x^b)dx^a d\tilde{v} + C_{ab}(u, \tilde{v}, x^c)dx^a dx^b \tag{4.15}$$

Note that u is an affine parameter here, such that the length dimension of u is $[L^0]$, the length dimension of $\tilde{v}$ is$[L^2]$ and the dimension of x is $[L^1]$. Therefore we expand all the terms in (4.15) to second order in the length scale, where this is valid when these distances are small is with respect to the curvature scale $\mathfrak{R}$. This expansion gives us

$$ds^2 = 2dud\tilde{v} + C_{ab}(u)dx^a dx^b + ... \tag{4.16}$$

which, when the higher order corrections are ignored gives us the plane wave Penrose limit in terms of Rosen coordinates.

A quantity that we will find useful in later calculations is the "Van Vleck-Morette (VVM) matrix" $\Delta_{ij}(u,u')$ and its determinant $\Delta(u,u') \equiv \det \Delta_{ij}(u,u')$. The determinant $\Delta(u,u')$ is a bi-scalar quantity that can be written for arbitrary coordinates as

$$\Delta(u,u') \equiv \Delta(x(u),x(u')) \ , \qquad \Delta(x,x') = -\frac{1}{\sqrt{g(x)g(x')}}\det\frac{\partial^2\sigma(x,x')}{\partial x^\mu \partial x'^\nu} \ , \tag{4.17}$$

where $\sigma(x,x')$ is the geodesic interval between points x and x', defined in (4.23)). In Brinkmann coordinates it follows that

$$\Delta(u,u') = \det \Delta_{ij}(u,u') \ . \tag{4.18}$$

This only depends on the curvature components $R^i{}_{uju}(u)$ of the full metric evaluated along γ and physically it encodes the tidal forces that are experienced along γ. In order to investigate these tidal forces, consider the geodesic equations for the transverse Brinkmann coordinates, or "Jacobi fields", $z^i(u), i = 1,2$,

$$\frac{d^2z^i}{du^2} + R^i{}_{uju}(u)z^j = 0 \ . \tag{4.19}$$

The VVM matrix can then be defined in terms of the Jacobi fields as follows. If the solution for the Jacobi field $z^i(u)$ is written in terms of some initial data

at u',[2]

$$z^i(u) = \mathscr{B}_{ij}(u,u')z^j(u') + \mathscr{A}_{ij}(u,u')\dot{z}^j(u') \ , \tag{4.20}$$

where we note that these geometric $\mathscr{A}$ and $\mathscr{B}$ matrices are important for describing our results in Chapter.6. Now one may write [15]

$$\Delta_{ij}(u,u') = (u-u')\mathscr{A}^{-1}_{ji}(u,u') \ , \tag{4.21}$$

so that the VVM matrix depends on the Jacobi fields that describe infinitesimal deformations of geodesic γ, specifically at the 'times' u and u'. The VVM matrix here, is of course, specifically defined in Brinkmann coordinates. For later use, we quote an important identity [15]

$$\mathscr{B}_{ij}(u,u') + \mathscr{A}_{ik}(u,u')\Omega_{kj}(u') = E_{ia}(u)E_j{}^a(u') \ . \tag{4.22}$$

The geodesic interval between the points x and x' $\sigma(x,x')$ may be explicitly written as,

$$\sigma(x,x') = \frac{1}{2}\int_0^1 d\tau \, g_{\mu\nu}(x)\dot{x}^\mu\dot{x}^\nu \ , \tag{4.23}$$

where $x^\mu = x^\mu(\tau)$ is the geodesic joining $x = x(0)$ and $x' = x(1)$.

4.2 The WKB approximation and the Penrose Limit

In chapters.(5,6) the consequences of a one loop effective action, schematically of the form

$$S_{eff} = \int d^4x d^4x' \sqrt{g(x)}\sqrt{g(x')}A(x)\Pi(x,x')A(x') \ , \tag{4.24}$$

on the propagation of particles is considered.

[2]Note that the transverse Brinkmann coordinates are raised and lowered with $\delta^i{}_j$ and so one does not need to distinguish upper and lower indices.

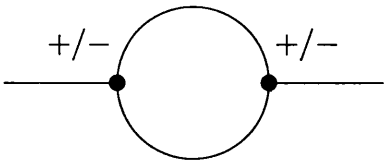

Figure 4.3: The, one loop, sunset diagram that contributes to the scalar effective action. This may be described using the Schwinger Keldysh formalism in the same way as Figure.4.1

In this chapter the propagation of a massless scalar particle with a self-energy resulting from a cubic coupling with a massive scalar field.

For a cubic coupling the self-energy is given varying the 1-loop 2PI effective action by the Schwinger-Keldysh graph shown in Figure.4.3. The variation is with respect to a '+' field at the point (x) such that the two contributing amputated self-energies are collected in

$$\begin{aligned} \Pi^{one-loop}(x,x') &= \lambda^2 \left(G_F^2(x,x') + G_-^2(x,x')\right) \ , \\ &= -\lambda^2 \Theta(u-u') \left(G_+^2(x,x') - G_-^2(x,x')\right) \ . \end{aligned} \tag{4.25}$$

As the Feynman propagator may be written in terms of the positive and negative frequency Wightman functions ((3.20a), (3.21a)) we have rewritten the second line of (4.25) in terms of these independent functions. This leads to corrections to the equations-of-motion of the form

$$\Box A(x) = -\lambda^2 \int d^4x' \sqrt{g(x')} \Theta(u-u') \left(G_+^2(x,x') - G_-^2(x,x')\right) A(x') \ , \tag{4.26}$$

where the 'time' integration is taken between t_0 and t or u_0 and u when null lightcone coordinates are used.

As shown in (4.6) we know that when $\omega^2 \gg \Re$ we may write our mode functions in the eikonal form we mas also use the De Witt propagators given in the form of (2.11).

As we will find it easier to calculate using the Feynman propagators. However the Schwinger-Keldysh formalism gives a result in the form of Wightman functions. It is possible, in the null lightcone coordinates we are using to find a relation between the two within an integral of the form (4.26).

Again by using the results in Chapter.3 we note that

$$\int d^4x' \left(G_F^2(x,x')\right) A(x') = \int d^4x' \left(\Theta(u-u')G_+^2(x,x') + \Theta(u'-u)G_+^2(x,x')\right) A(x') \,. \tag{4.27}$$

Now as our fields are positive frequency Eikonal modes and propagators of the form (2.11) we see that due to the conservation of ω at the vertex, itself caused by the $\partial_{\tilde{v}}$ isometry of the plane wave background, that

$$\int d\tilde{v}' \left(G_-^2(x,x')\right) A(x') = 0 \,. \tag{4.28}$$

From here it is clear that we may now replace the self-energy in (4.26) with that from the usual Feynman techniques. This shows the equivalence between the Feynman and Schwinger-Keldysh methods in this calculation The expression of these Feynman propagators (2.11) has a nice interpretation in the worldline formalism, in which the propagator between two points x and x' is determined by a sum over worldlines $x^\mu(\tau)$ that connect $x = x(0)$ and $x' = x(T)$ weighted by $\exp iS[x]$ with the action

$$S[x] = -m^2T + \frac{1}{4}\int_0^T d\tau \, g_{\mu\nu}(x)\dot{x}^\mu\dot{x}^\nu \,. \tag{4.29}$$

Here, T is the worldline length of the loop which is an auxiliary parameter that must be integrated over. The expression (2.11) corresponds to the expansion of the resulting functional integral around the stationary phase solution, which is simply the classical geodesic that joins x and x'. In particular, the classical geodesic has an action $S[x] = \sigma(x,x')/2T - m^2T$ giving the exponential terms in (2.11). The VVM determinant comes from integrating over the fluctuations around the geodesic to Gaussian order while the term

$\Omega(x,x'|T) = 1 + \sum_{n=1}^{\infty} a_n(x,x')T^n$ encodes all the higher non-linear corrections. These terms are effectively an expansion in $\mathfrak{R}/m^2$, so the form for the propagator is useful in the limit of weak curvature compared with the Compton wavelength of the scalar particle. Of course, this is precisely the limit being used in here and this goes hand-in-hand with the fact that in the plane wave limit this factor is trivial $\Omega(x,x'|T) = 1$ due to the WKB exactness of the scalar propagator in a plane wave background.

The weak curvature limit $\mathfrak{R} \ll m^2$ leads to a considerable simplification as is now explained. Denoting the worldline lengths of each of the scalar propagators as T_1 and T_2, the terms in the exponent of the integrals in (4.26) are

$$\exp\Big[- im^2T + \frac{i}{2}\Big(\frac{1}{T_1} + \frac{1}{T_2}\Big)\sigma(x,x') + i\omega\hat{v}'\Big] \ . \tag{4.30}$$

For later use, we find it convenient to change variables from T_1 and T_2 to $T = T_1 + T_2$ and $\xi = T_1/T$, so $0 \leq \xi \leq 1$. The parameter ξ is identified as a conventional Feynman parameter. Expressed the other way

$$T_1 = T\xi \ , \qquad T_2 = T(1-\xi) \ . \tag{4.31}$$

The Jacobian is

$$\int_0^\infty \frac{dT_1}{T_1^2}\frac{dT_2}{T_2^2} = \int_0^\infty \frac{dT}{T^3}\int_0^1 \frac{d\xi}{[\xi(1-\xi)]^2} \ . \tag{4.32}$$

In the limit $\mathfrak{R} \ll m^2$ the integral over x' is dominated by a stationary phase determined by extremizing the exponent (4.30) with respect to x':

$$\frac{1}{2T\xi(1-\xi)}\partial'_\mu\sigma(x,x') + \omega\partial'_\mu\hat{v}' = 0 \ . \tag{4.33}$$

Since $\partial'^\mu\sigma(x,x')$ is the tangent vector at x' of the geodesic passing through x' and x, the stationary phase solution corresponds to a geodesic with tangent vector $\propto \partial'^\mu\hat{v}'$. This means that x and x' must lie on a null geodesic. If we choose x to be the point $(u,0,0,0)$ then x' must have Rosen coordinates

$(u', 0, 0, 0)$ and so x' and x lie on the geodesic γ and

$$\partial_{\hat{v}'}\sigma(x, x') = u - u' \; ; \tag{4.34}$$

so the $\hat{v}'$ component of (4.33) becomes

$$\frac{u' - u}{2T\xi(1-\xi)} + \omega = 0 \tag{4.35}$$

and hence

$$u' = u - 2\omega T\xi(1-\xi) \; . \tag{4.36}$$

In the equivalent worldline picture, the stationary phase solution which dominates in the limit $\mathfrak{R} \ll m^2$ describes a situation where the incoming massless particle propagating along γ decays to pair of massive particles at the point $u' = u - 2\omega T\xi(1-\xi)$ which then propagate along the null geodesic γ to the point u and then combine into the massless scalar again as is depicted in Figure.4.4. This was a key step in the derivation of the refractive index in the worldline formalism in [14, 45].

The plane-wave limit of the full metric provides precisely the data that is needed to perform the saddle-point approximation to leading order. In other words, for a plane wave background the problem is exact at Gaussian order. For the remainder of the calculation, we now simply assume a plane-wave metric knowing that the result will apply to the full metric when $\mathfrak{R} \ll m^2$. The meat of the calculation involves performing the Gaussian integral over x' where the exponential factor has the form (4.30). In the plane-wave background the geodesic interval has a simple form quadratic in the transverse Rosen coordinates

$$\sigma(x, x') = (u - u')(\hat{v} - \hat{v}') + \tfrac{1}{2}\Delta_{ab}(u, u')(x - x')^a(x - x')^b \; , \tag{4.37}$$

where

$$\Delta_{ab}(u, u') = (u - u')\left[\int_{u'}^{u} C^{-1}(u'')du''\right]^{-1}_{ab} \; . \tag{4.38}$$

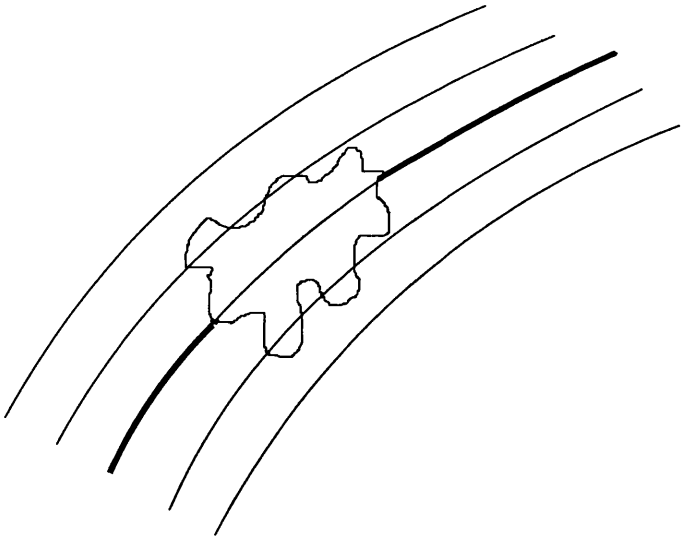

Figure 4.4: The original massless scalar's worldline, with the one loop massive scalar correction. It is the limit $\omega^2 \gg \mathfrak{R}$ that allows us to choose a single geodesic for the uncorrected incoming particle, i.e. the ray optics limit. It is the limit $m^2 \gg \mathfrak{R}$ that restricts the loop contribution to the region around this initial geodesic given by the null congruence.

is the transverse part of the VVM matrix in Rosen coordinates. It is related to the same quantity in the Brinkmann coordinates by the zweibein

$$\Delta_{ij}(u,u') = E_i{}^a(u) E_j{}^b(u') \Delta_{ab}(u,u') \ . \tag{4.39}$$

The integrals over $\hat{v}'$ and u' are trivial, the former leading to a delta function constraint

$$\int d\hat{v}' \, \exp\left[\frac{i(u'-u)\hat{v}'}{2T\xi(1-\xi)} + i\omega\hat{v}'\right] = 4\pi T\xi(1-\xi)\delta\big(u'-u+2\omega T\xi(1-\xi)\big) \tag{4.40}$$

which then saturates the integral over the latter. The condition on u' is precisely the saddle-point condition (4.36).

What remains is the integration over the transverse coordinates. For the

scalar case we may complete this integral using the identity

$$I^{(1)} = \int d^2x' \, e^{\frac{i}{4T\xi}x'\Delta(u,u')\cdot x'} \, e^{\frac{i}{4T(1-\xi)}x'\cdot\Delta(u,u')\cdot x'} = \frac{4iT\pi\xi(1-\xi)}{\sqrt{\det \Delta_{ab}(u,u')}} \, , \quad (4.41)$$

Using the fact that for a plane wave space the scalar amplitude of the photon is given by

$$\mathcal{A}(x) = \frac{1}{\sqrt{\det E^i_\mu(u)}} \quad (4.42)$$

allows us to write our correction to the equation of motion as

$$\Box A(x) = \frac{\lambda^2}{2\pi\omega^2} \int_0^{\frac{u_0}{2\omega\xi(1-\xi)}-i\epsilon} \frac{dT}{T} e^{-im^2T} \int_0^1 d\xi \left[\sqrt{\det\Delta(u,u')}\right]_{u'=u-2\omega T\xi(1-\xi))} \quad (4.43)$$

This result is divergent in the limit that $u' \to u$. However this is a local, non curvature dependent divergence and as such may be removed by subtracting the flat space result to leave us with the curvature dependent part.

It is in this integration over the transverse directions where we see the main computational differences with respect to this scalar example in the calculations appearing in Chapters.5&6, as this part of the calculation is dependent on the form of the couplings and propagators in the theory for which the calculation is preformed.

Within this calculation we used the fact that the function $\Omega(x,x'|T) = 1$ for the scalar propagator (2.11) on a plane wave backgorund. This same WKB exactness applies to the spinor case but not to higher spin particles [50]. This would mean that to extend the calculation to, for example, a vector loop particle would result in the loss of this correspondence between the WKB approximation and the Penrose limit.

A subtle point that has been ignored in the calculation until now it that in these light cone coordinates the initial value surface is a null surface. This means that it is not a Cauchy surface and does not completely specify all

relevant information. Cauchy surfaces are defined by a surface which any non-spacelike inextensible curve crosses exactly once, or in other words any particle's world line must cross this surface exactly once. For a null surface parallel null worldlines never cross this surface. This would imply that our initial value surface is incomplete as particles that are not specified in the initial value surface could still have some impact on our final result.

This problem with light-cone coordinates is well known and the technique of discrete light cone quantisation (DLCQ) has been developed to resolve these issues. Some basic ideas from DLCQ may be applied to the problem in question. By adding periodic (for scalars) boundary conditions to the transverse directions at some finite separation scale L, this leaves us with an initial value surface describing all relevant quantities at the expense of introducing corrections proportional to some negative power of L. If it is assumed that L is much larger than any other scale appearing in the problem however these corrections may be safely ignored.

Chapter 5

Photon Propagation in Curved Spacetime

Nearly all measurements taken in astronomy are made by detecting incoming photons. These may have traveled as far as 13.7×10^9 light-years to reach the detector from all directions in the sky. Such photons will have had ample opportunity to experience a variety of spatial curvatures. This means that, phenomenologically speaking, it is by understanding these photons where we find perhaps our greatest chance of seeing any low-energy signals of Quantum-Gravity.

Furthermore as discussed in Chapter.4 the resolution to the problems raised by the Drummond Hathrell effect requires the calculation of the effect of curvature on the propagation of photons.

This is completed here using Schwinger-Keldysh perturbation theory, as developed in Chapter.3 to find the one loop correction to the propagation of a photon in curved space, using full Quantum Electro-Dynamics (QED). These results are available in [16], the corresponding calculation for scalar QED may be seen in [15]. In [16] and this chapter the step of extending the result of the scalar QED calculation to include spinors is taken. This is an important result

as, for the first time, the calculation is conducted using a 'real world' theory.

The one loop correction to the effective action of QED is

$$S_{cor} = \int \sqrt{g(x)}\sqrt{g(x')}d^4x d^4x' A(x)^\mu \Pi(x,x')_{\mu\nu} A(x')^\nu \ , \tag{5.1}$$

such that the photon equations-of-motion are given by

$$\nabla_\nu F(x)^\nu_\mu = 4 \int \sqrt{g(x')}\Pi(x,x')_{\mu\nu} A(x')^\nu d^4x' \tag{5.2}$$

where in the Schwinger-Keldysh formalism the 'time' integral is restricted to be taken between u_0 and u, the initial and final surfaces. The one loop vacuum polarisation is given by

$$\begin{aligned} \Pi(x,x')_{\mu\nu} &= e^2 \mathrm{Tr}\left[\gamma_\mu \mathbb{S}_R(x,x')\gamma_\nu \mathbb{S}_R(x,x')\right] \\ \Pi(x,x')_{\mu\nu} &= \Theta(u-u')e^2 \mathrm{Tr}\left[\gamma_\mu \mathbb{S}(x,x')\gamma_\nu \mathbb{S}(x,x')\right] \ , \end{aligned} \tag{5.3}$$

where the the second line uses the fact that light-cone coordinates have been used. The $\mathbb{S}_R(x,x')$ are the retarded spinor propagators, the $\mathbb{S}(x,x')$ appearing here are the Feynman spinor propagators. γ_μ is the curved space gamma matrix. As we are working in the WKB regime may use the vector eikonal modes, similar to the scalar modes given in (4.6) which take the form

$$A_{\mu s}(x) = \mathcal{A}(x)\epsilon_{i\mu}(x) e^{i\Theta_{ss'}(u)} P^i_{s'} \tag{5.4}$$

where $\Theta(u)$ is the eikonal phase, $\mathcal{A}(x)$ is the scalar amplitudewhich is the same as for the scalar, which for a plane wave background is given by (4.7) and $\epsilon_{i\mu}$ is the polarisation tensor given by the zweibeins ($E_{i\mu}$) defined in (4.13). P^i_s gives the physical polarisations with $P^i_1 = \left(\frac{1}{0}\right)$ and $P^i_2 = \left(\frac{0}{1}\right)$ chosen such that the polarisations lie in the transverse Brinkman directions. The eikonal phase is the same as in the scalar case, although we now add polarisation indices such that

$$\Theta_{ss'}(u) = \delta_{ss'}\omega\tilde{v} \ . \tag{5.5}$$

The effect of taking the one loop correction is the same as taking the eikonal phase off-shell,

$$\Theta_{ss'}(u) \to \Theta_{ss'}(u) - \vartheta_{ss'}(x;\omega), \tag{5.6}$$

Substituting (5.6) into (5.2) the corrected equations-of-motion for the photon are

$$\nabla_\nu F(x)_s^{\nu\mu} = 2\omega^2 \frac{\partial \vartheta_{ss'}(x_0,x;\omega)}{\partial u} \mathcal{A}(u)\epsilon_{s'}^\nu e^{i\omega v} \ , \tag{5.7}$$

where the dependence on x_0 is introduced by the initial value surface and the notation $P_s^i \epsilon_i^\nu = \epsilon_s^\nu$ is used. Assuming that these results are only perturbatively off-shell it is possible to write

$$n(x_0,x;\omega) = 1 + \frac{\partial \vartheta(x_0,x;\omega)}{\partial u} \tag{5.8}$$

This allows us to relate the one loop correction to the effective action to the correction to the mode function by equating the right hand side of (5.7) to that of (5.2), giving the effective refractive index for a photon propagating from the initial value surface at the point x_0.

$$n_{ss'}(x_0,x;\omega) = \delta_{ss'} - \frac{2}{\omega^2}\int_{u_0}^{u} du' \int d^3x' \sqrt{g(x')} \frac{\mathcal{A}(x')}{\mathcal{A}(x)} \tilde{\epsilon}_s^\mu(x) \Pi_{\mu\nu}^{1-loop}(x,x') \epsilon_{s'}^\nu e^{i\omega(\tilde{v}-\tilde{v}')} \ . \tag{5.9}$$

As we can see the calculation of this correction is dependent on the evaluation of the one loop vacuum polarisation appearing in Figure.4.1.One should recall that we are working in the limit $\omega^2 \gg \mathfrak{R}$, so we progress by using the techniques developed in Chapter.4, by completing the calculation on a plane wave background.

5.1 One-Loop Spinor Calculation

5.1.1 Spinor propagator in a plane wave spacetime

To allow the completion of the integrations appearing in (5.9) it is necessary to describe spinors in curved backgrounds. In order to do this a local pseudo-orthonormal frame at each point in space by means of a vierbein:

$$g_{\mu\nu} = e_\mu{}^A e_\nu{}^B \eta_{AB} \,, \tag{5.10}$$

where the null structure is preserved in the local frame by taking

$$\eta_{AB} = \begin{pmatrix} 0 & 1 & 0 & 0 \\ 1 & 0 & 0 & 0 \\ 0 & 0 & 1 & 0 \\ 0 & 0 & 0 & 1 \end{pmatrix} . \tag{5.11}$$

For a plane wave spacetime, in Rosen coordinates, the vierbeins are explicitly

$$e^A{}_\mu = e_\mu{}^A = \begin{pmatrix} \mathbf{1} & 0 \\ 0 & E^i{}_a \end{pmatrix} . \tag{5.12}$$

In the local frame we denote the indices as $A = (+, -, i)$. Notice that the indices $i, j = 1, 2$ are common to the local frame and the Brinkmann coordinates in the transverse space. The γ matrices are defined in the local frame and satisfy

$$\{\gamma^A, \gamma^B\} = -2\eta^{AB} . \tag{5.13}$$

In particular, along the null directions the gamma matrices are nilpotent, $\gamma^+\gamma^+ = \gamma^-\gamma^- = 0$. This is a crucial simplification, as we see below.

The next step is to define the spin connection. From the metric condition $\nabla_\mu e^\nu{}_B = 0$, this is:

$$\omega_{\mu AB} = e_{A\nu}\partial_\mu e^\nu{}_B + e_{A\nu}\Gamma^\nu{}_{\mu\rho} e^\rho{}_B \,, \tag{5.14}$$

and has non-vanishing components

$$\omega_{a\,i+} \;=\; -\,\omega_{a\,+i} \;=\; -\,\dot{E}_{ia}(u)\;. \tag{5.15}$$

One can verify explicitly that the connection is torsion free: $de_A + \omega_{AB} \wedge e^B = 0$, or in components,

$$\partial_{[\mu} e_{A\nu]} + \omega_{[\mu\,AB} e^{B}{}_{\nu]} = 0\;. \tag{5.16}$$

The covariant derivative on spinors is defined as

$$\nabla_\mu = \partial_\mu + \tfrac{1}{2}\omega_{\mu\,AB}\sigma^{AB}\;, \tag{5.17}$$

where $\sigma^{AB} = \frac{1}{4}[\gamma^A, \gamma^B]$. In Rosen components, this gives

$$\nabla_\mu = \left(\partial_u, \partial_V, \partial_a - \tfrac{1}{2}\dot{E}_{ia}(u)\gamma^i\gamma^+\right)\;, \tag{5.18}$$

so the Dirac operator is

$$\not{\nabla} = \gamma^A e_A{}^\mu \nabla_\mu = \gamma^+\partial_u + \gamma^-\partial_V - \gamma^i E_i{}^a(u)\partial_a + \tfrac{1}{2}E_i{}^a(u)\dot{E}_{ja}(u)\gamma^i\gamma^j\gamma^+\;. \tag{5.19}$$

The spinor parallel transporter is a bi-spinor that parallel transports a spinor along a given path, in our case the null geodesic γ joining x and x'. It satisfies the two conditions

$$\partial^\mu\sigma(x,x')\nabla_\mu \mathbb{U}(x,x') = 0\;, \qquad \mathbb{U}(x,x) = \mathbb{I}\;, \tag{5.20}$$

and has an explicit representation in terms of the spin connection by the path ordered expression

$$\mathbb{U}(x,x') = \mathcal{P}\exp -\frac{1}{2}\int_{u'}^{u} \omega_{\mu AB}\sigma^{AB}\,dx^\mu\;, \tag{5.21}$$

where the integral is taken along γ. The key observation is that since the spin connection involves the nilpotent γ^+, we can expand the exponential and only terms up to linear order in the spin connection contribute (in particular the

issue of path ordering is moot):

$$\mathbb{U}(x,x') = \mathbb{I} + \tfrac{1}{2}\gamma^i\gamma^+ \int_{Y'^a(u')}^{Y^a(u)} \dot{E}_{ia}(u)\, dY^a \ , \tag{5.22}$$

where the Y^as here correspond to the transverse directions in Rosen coordinates. To evaluate this, write

$$\int_{Y'^a}^{Y^a} \dot{E}_{ia}(u)\, dY^a = \int_{u'}^{u} du\, \dot{E}_{ia}(u)\, \dot{Y}^a(u) \ . \tag{5.23}$$

and use the geodesic equation $\dot{Y}^a = C^{ab}\xi_b$, which has the solution

$$(Y - Y')^a = \int_{u'}^{u} du'' C^{ab}(u'')\xi_b \ . \tag{5.24}$$

Since $\boldsymbol{C} = \boldsymbol{E}^\top \boldsymbol{E}$ and $\boldsymbol{\Omega} = \dot{\boldsymbol{E}}\boldsymbol{E}^{-1}$ are both symmetric, we can write

$$\begin{aligned} \int du\, \dot{\boldsymbol{E}}\boldsymbol{E}^{-1}\big(\boldsymbol{E}^{-1}\big)^\top &= \int du\, \big(\boldsymbol{E}^{-1}\big)^\top \dot{\boldsymbol{E}}^\top \big(\boldsymbol{E}^{-1}\big)^\top \\ &= -\int du\, \big(\dot{\boldsymbol{E}}^{-1}\big)^\top = -\big(\boldsymbol{E}^{-1}\big)^\top \ . \end{aligned} \tag{5.25}$$

Hence

$$\begin{aligned} \int_{Y'^a}^{Y^a} \dot{E}_{ia}(u)\, dY^a &= -\big(E_i{}^a(u) - E_i{}^a(u')\big)\xi_a \\ &= -\big(E_i{}^a(u) - E_i{}^a(u')\big)\frac{\Delta_{ab}(u,u')}{u-u'}(Y-Y')^b \ , \end{aligned} \tag{5.26}$$

using (5.24) and (4.38). This gives the following explicit form for the spinor parallel transporter in terms of the VVM matrix:

$$\mathbb{U}(x,x') = \mathbb{I} - \tfrac{1}{2}\gamma^i\gamma^+\big(E_i{}^a(u) - E_i{}^a(u')\big)\frac{\Delta_{ab}(u,u')}{u-u'}(Y-Y')^b \ . \tag{5.27}$$

Finally, we need the Feynman propagator $\mathbb{S}(x,x')$ for the spinor electron. This can be written in terms of the propagator $G(x,x')$ for a massive scalar

field and the spinor parallel transporter $\mathbb{U}(x,x')$ as follows:

$$\mathbb{S}(x,x') = (\not{\nabla} - m)G(x,x')\mathbb{U}(x,x') \ . \tag{5.28}$$

5.1.2 Vacuum polarization in spinor QED

With this form for the spinor propagator in a plane wave spacetime, it is now possible to calculate the vacuum polarization and refractive index following by following the methods developed in Chapter.4. Inserting the vacuum polarization given in (5.3) into (5.9)

$$n_{ss'}(x_0,x;\omega) = \delta_{ss'} + \frac{2e^2}{\omega^2}\int_{u_0}^{u} du' \int d^3x' \sqrt{g(x')}\,\frac{\mathcal{A}(x')}{\mathcal{A}(x)}\,\mathrm{Tr}\left[\gamma_s \mathbb{S}(x,x')\gamma_s' \mathbb{S}(x',x)\right] e^{i\omega(\tilde{v}-\tilde{v}')} \ , \tag{5.29}$$

where we have used the notation $P_s^i\gamma_i = \gamma_s$. The calculation is best performed in Rosen coordinates although the end result is most naturally expressed in terms of tensors with Brinkmann indices. We take $x = (u,0,0,0)$ for convenience which implies $x' = (u',\tilde{v},\vec{x}')$.

Now notice that the terms which are linear in m involve an odd number of gamma matrices and so do not contribute to the trace. There are two remaining contributions to the trace of the form

$$\begin{aligned} &\mathrm{Tr}\Big[\gamma_s \not{\nabla}\left(G(x,x')\mathbb{U}(x,x')\right)\gamma_{s'}\not{\nabla}'\left(G(x',x)\mathbb{U}(x',x)\right)\Big] \\ &+ m^2\mathrm{Tr}\Big[\gamma_s G(x,x')\mathbb{U}(x,x')\gamma_{s'}G(x',x)\mathbb{U}(x',x)\Big] \ . \end{aligned} \tag{5.30}$$

The explicit expression for the spinor parallel transporter is given in (5.27). The x^a integrals are Gaussian and easily evaluated using the relationships

$$I^{(1)} = \int d^2x'\, e^{\frac{i}{4T\xi}x'\Delta(u,u')\cdot x'}\, e^{\frac{i}{4T(1-\xi)}x'\cdot\Delta(u,u')\cdot x'} = \frac{4iT\pi\xi(1-\xi)}{\sqrt{\det\Delta_{ab}(u,u')}} \tag{5.31}$$

and

$$I^{(2)}_{ab} = \int d^2x' \frac{\partial}{\partial x'^a} e^{\frac{i}{4T\xi}x'\cdot\Delta(u,u')\cdot x'} \frac{\partial}{\partial x'^b} e^{\frac{i}{4T(1-\xi)}x'\cdot\Delta(u,u')\cdot x'} = \frac{2\pi\xi(1-\xi)\Delta_{ab}(u,u')}{\sqrt{\det\Delta_{ab}(u,u')}} , \tag{5.32}$$

where the choice of which integral depends on the number of derivatives in the transverse directions acting on the scalar propagators.

while the $\tilde{v}'$ integral is trivial and simply produces a delta function constraint(4.40), also allowing the completion of the u' integral.

Noting that

$$\not{\nabla}\mathbb{U}(x,x')\not{\nabla}'\mathbb{U}(x',x) = 0 , \tag{5.33}$$

due to the fact that $\gamma^+\gamma^+ = 0$, there are three types of contribution in (5.30) which, suppressing the calculational details which are not in themselves enlightening, yield:

$$\begin{aligned}&\int_{u_0}^{u} du' \int d^3x' \sqrt{g(x')}\, e^{-i\omega\tilde{v}'} \frac{\mathcal{A}(x')}{\mathcal{A}(x)} \mathrm{Tr}\Big[\gamma_s G(x,x')\mathbb{U}(x,x')\gamma_{s'} G(x',x)\mathbb{U}(x',x)\Big] \\ &= 64\pi T^2\xi^2(1-\xi)^2\sqrt{\det\boldsymbol{\Delta}(u,u')} ,\end{aligned} \tag{5.34}$$

along with

$$\begin{aligned}&\int_{u_0}^{u} du' \int d^3x' \sqrt{g(x')}\, e^{-i\omega\tilde{v}'} \frac{\mathcal{A}(x')}{\mathcal{A}(x)} \mathrm{Tr}\Big[\gamma_s \not{\nabla} G(x,x')\mathbb{U}(x,x')\gamma_{s'} \not{\nabla}' G(x',x)\mathbb{U}(x',x)\Big] \\ &= 16i\pi T\xi(1-\xi)\sqrt{\det\boldsymbol{\Delta}(u,u')}\Big\{\Big(-8\xi(1-\xi) \\ &- (1-2\xi(1-\xi))(u-u')\mathrm{Tr}\left(\partial_{u'}\boldsymbol{\Delta}_{ss'}(u,u')\boldsymbol{\Delta}^{-1}_{ss'}(u,u')\right)\Big)\delta_{ss'} + 4\xi(1-\xi)\Delta_{ss'}(u,u')\Big\}\end{aligned} \tag{5.35}$$

where we have introduced $P^i_s \Delta_{ij}(u,u') P^j_{s'} = \Delta_{ss'}(u,u')$ and

$$\begin{aligned}
&\int_{u_0}^{u} du' \int d^3x' \sqrt{g(x')}\, e^{-i\omega\bar{v}'} \frac{\mathcal{A}(x')}{\mathcal{A}(x)} \mathrm{Tr}\Big[\gamma_s \nabla\!\!\!/ G(x,x') \mathbb{U}(x,x') \gamma_{s'} G(x',x) \nabla\!\!\!/' \mathbb{U}(x',x) \\
&\quad + \gamma_s G(x,x') \nabla\!\!\!/ \mathbb{U}(x,x') \gamma_{s'} \nabla\!\!\!/' G(x',x) \mathbb{U}(x',x)\Big] \\
&= 16 i\pi T \xi(1-\xi) \delta_{ss'} \sqrt{\det \mathbf{\Delta}(u,u')} \\
&\quad \times \mathrm{Tr}\left(\delta_{ss'} - \mathbf{\Delta}_{ss'}(u,u') + (u-u') \partial_{u'} \mathbf{\Delta}_{ss'}(u,u') \mathbf{\Delta}^{-1}_{ss'}(u,u')\right) .
\end{aligned} \tag{5.36}$$

In all these expression u' is constrained via (4.36).

Putting everything together, the final result for the refractive index is

$$\begin{aligned}
n^{\text{spinor}}_{ss'}(u_0,u;\omega) = \delta_{ss'} &- \frac{\alpha}{2\pi\omega^2} \int_0^{\frac{u_0}{2\omega\xi(1-\xi)}} \frac{dT}{T^2}\, i e^{-im^2T} \\
&\times \int_0^1 d\xi \sqrt{\det \mathbf{\Delta}(u,u')} \Big[\Big(4iTm^2 + \frac{1}{\xi(1-\xi)} \mathrm{Tr}\left(\mathbf{\Delta}_{ss'}(u,u') - \delta_{ij}\right) \\
&- 2(u-u') \mathrm{Tr}\left(\partial_{u'} \mathbf{\Delta}_{ss'}(u,u') \mathbf{\Delta}^{-1}_{ss'}(u,u')\right) + 8\Big)\delta_{ss'} - 4\mathbf{\Delta}_{ss'}(u,u')\Big]
\end{aligned} \tag{5.37}$$

evaluated with $u' = u - 2\omega T\xi(1-\xi)$or equivalently,

$$\begin{aligned}
n^{\text{spinor}}_{ss'}(u_0,u;\omega) = \delta_{ss'} &- \frac{\alpha}{2\pi\omega^2} \int_0^{\frac{u_0}{2\omega\xi(1-\xi)}} \frac{dT}{T^2}\, i e^{-im^2T} \\
&\times \int_0^1 d\xi \sqrt{\det \mathbf{\Delta}(u,u')} \Big[\Big(\frac{1}{\xi(1-\xi)} \mathrm{Tr}\left(\mathbf{\Delta}_{ss'}(u,u') - \delta_{ss'}\right) \\
&- 4(u-u') \mathrm{Tr}\left(\partial_{u'} \mathbf{\Delta}_{ss'}(u,u') \mathbf{\Delta}^{-1}_{ss'}(u,u')\right) + 4\Big)\delta_{ss'} - 4\mathbf{\Delta}_{ss'}(u,u')\Big]
\end{aligned} \tag{5.38}$$

again using $u' = u - 2\omega T\xi(1-\xi)$. In the second expression, we have taken the first term and integrated by parts in T and ignored the singular boundary term which is curvature independent. The result is then manifestly UV finite, *i.e.* there is no singularity of the integrand at small T.

Finally, changing variables to $t = 2\omega\xi(1-\xi)T$ and writing the refractive index in the form

$$n^{\text{spinor}}_{ss'}(u_0,u;\omega) = \delta_{ss'} - \frac{\alpha}{2\pi\omega}\int_0^1 d\xi\,\xi(1-\xi)\mathcal{F}^{\text{spinor}}_{ss'}\Big(u_0,u;\frac{m^2}{2\omega\xi(1-\xi)}\Big)\,, \quad (5.39)$$

where

$$\mathcal{F}^{\text{spinor}}_{ss'}(u;z) = \int_0^{u_0-i\epsilon}\frac{dt}{t^2}\,ie^{-izt}\sqrt{\det\boldsymbol{\Delta}_{ss'}(u,u-t)}\Big[\Big(\frac{1}{\xi(1-\xi)}\mathrm{Tr}\,(\boldsymbol{\Delta}_{ss'}(u,u-t)-\delta_{ss'}) + 4t\,\mathrm{Tr}\,(\partial_t\boldsymbol{\Delta}_{ss'}(u,u-t)\boldsymbol{\Delta}^{-1}_{ss'}(u,u-t))+4\Big)\delta_{ss'} - 4\boldsymbol{\Delta}_{ss'}(u,u-t)\Big]\,. \quad (5.40)$$

Notice that $\Delta(u,u')$ is singular when u and u' are conjugate points on the geodesic γ, that is when the geodesic through u and u' can be infinitesimally deformed. Hence, the integral in (5.40) is only defined with an appropriate prescription which involves deforming the contour into the upper half complex plane, as indicated.

The integral in (5.40) is then convergent as long as the geometry becomes flat in the asymptotic past $u' \to -u_0 \to -\infty$. Notice that the result above for the refractive index is perfectly causal in that the refractive index at a point $u \in \gamma$ only depends on the curvature along γ in the past $u' < u$.

The leading low-frequency term in the expansion of $\boldsymbol{n}(u_0,u;\omega)$ may be verified when the initial value surface is taken to be in the asymptotic past ($u_0 \to \infty$). Substituting the expansion of $\Delta_{ij}(u,u-t)$ in powers of $\omega^2\mathfrak{R}/m^4$ given by,

$$\Delta_{ij}(u,u-t) = \delta_{ij} + \frac{1}{6}R_{uiuj}(u)t + \ldots \quad (5.41)$$

into (5.40), it is found that

$$n^{\text{spinor}}_{ss'}(u;\omega) = \delta_{ss'} - \frac{\alpha}{180\pi m^2}\big(13\delta_{ss'}R_{uu} - 4R_{usus'}\big) + \frac{R}{m^2}\mathcal{O}\Big(\frac{\omega^2 R}{m^4}\Big)\,, \quad (5.42)$$

in agreement with the original Drummond-Hathrell formula [39] .

As causality is determined by the wavefront velocity we are interested in the high frequency limit ($\omega \to \infty$). This limit may be taken by expanding the RHS of (5.40) for small z. Here we use the example of the conformally flat plane wave spacetime. This spacetime arises naturally as the Penrose limit of $AdS_2 \times S^2$ as well as the Einstein static universe, $R \times S^3$ [50]. Its metric is given by

$$ds^2 = dudv - \sigma^2 z^2 du^2 + dz^2 \tag{5.43}$$

in Brinkmann coordinates, where σ is a constant. Now we find that the VVM matrix is given by

$$\Delta_{ij}(u-u') = \delta_{ij}\frac{\sigma^2(u-u')}{\sin\sigma(u-u')} \tag{5.44}$$

Putting this VVM matrix into (5.39) and again taking the inital value surface at $-\infty$ allows us to find the analytic result for (5.40)

$$\begin{aligned}\mathcal{F}^{spinor}(z) = 8\Big(&-\sigma - 3z + 3\sigma\log(2\pi) - 6\sigma\log\Gamma\left(\frac{1}{2}+\frac{z}{2\sigma}\right) \\ &z\psi\left(1+\frac{z}{2\sigma}\right) + 2z\psi\left(\frac{1}{2}+\frac{z}{2\sigma}\right)\Big) \\ &+ \frac{4}{\xi(1-\xi)}\left(\sigma + z - \sigma\log(2\pi) + 2\sigma\log\Gamma\left(\frac{1}{2}+\frac{z}{2\sigma}\right) - z\psi\left(1+\frac{z}{2\sigma}\right)\right) ,\end{aligned} \tag{5.45}$$

expanding this in powers of small z one finds

$$\mathcal{F}^{spinor}(z) \approx 8\left(-\sigma + 3\sigma\log(2)\right) + \frac{4\sigma}{\xi(1-\xi)}\left(1-\log(2)\right) + \mathcal{O}(z) \ . \tag{5.46}$$

Now by inserting this result back into (5.39) we find that

$$\lim_{\omega\to\infty}\left(1 - \frac{\alpha}{2\pi\omega}\int_0^1 d\xi\xi(1-\xi)\mathcal{F}\left(\frac{m^2}{2\omega\xi(1-\xi)}\right)\right) = 1 \ , \tag{5.47}$$

as the correction terms are suppressed by a factor of $1/\omega$. This result is typical for these calculations in QED; there is no correction to the wavefront velocity so there is no violation of causality.

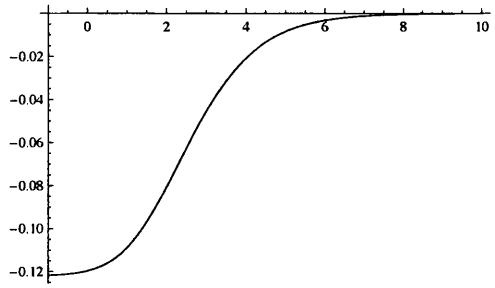

Figure 5.1: The refractive index $n(\omega)-1$ of a conformally flat symmetric plane wave, in units of $\alpha\sigma^2/(2\pi m^2)$, plotted as a function of $\log\omega\sigma/m^2$ for spinor QED.

Now moving back to considering the full result for the conformally symmetric plane wave using (5.45) we obtain the refractive index shown in Figure.5.1.

This result shows no imaginary contributions showing that this space is non-dispersive. It also shows that for lower frequencies there is an acceleration of the incoming phase velocity, but the wavefront velocity remains unchanged at c.

5.2 Further Examples

Here we extend the 'phenomenology' found by solving (5.39) in a selection of specific spacetime examples. In these examples we take the inital value surface $u_0 = -\infty$. These results and several more examples may be seen in more detail in [16].

After the examination of the conformally flat symmetric plane wave in the previous section we look at the Ricci flat symmetric plane wave. This arises as the Penrose limit of $dS_3 \times R$ where there has been some recent interest in field theory on this background, for example [51, 52]. The metric is given by

$$ds^2 = dudv - (\sigma_1^2 z_1^2 + \sigma_2^2 z_2^2)du^2 + dz^2 \tag{5.48}$$

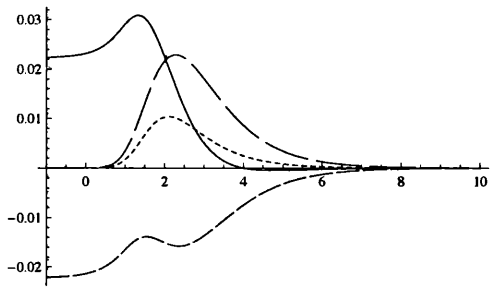

Figure 5.2: The refractive index $n(\omega) - 1$ of a Ricci flat symmetric plane wave, in units of $\alpha\sigma^2/(2\pi m^2)$, plotted as a function of $\log \omega\sigma/m^2$ for spinor QED: continuous (real part, polarisation i=1); big dashes (imaginary part, i=1); small dashes (real part, polarisation i=2) and dots (imaginary part, i=2).

in Brinkman coordinates. Here we have $\sigma_2 = i\sigma_1$, where $\sigma_1 = \sigma$ a real constant.

This has the VVM matrix given by

$$\begin{aligned} \Delta_{11}(u-u') &= \frac{\sigma(u-u')}{\sin\sigma(u-u')} \\ \Delta_{22}(u-u') &= \frac{\sigma(u-u')}{\sinh\sigma(u-u')} \ . \end{aligned} \tag{5.49}$$

Using this VVM matrix one finds the refractive index given in Figure.5.2

Here we see that there is an imaginary contribution, due to the poles of (5.49) along the imaginary axis of the integral in (5.39). Birefringence is also observed in this case as the different polarisations experience a different refractive index.

Next we consider the near singularity Penrose limit of a Schwartzschild black hole. Such limits are of particular interest as this is approach the regime where we expect quantum-gravitational effects to start appearing.

This gives us a specific example of a singular Ricci flat singular plane wave, were the metric we obtain is given by

$$ds^2 = dudv - h_{ij}z^i z^j du^2 + dz^2 \ . \tag{5.50}$$

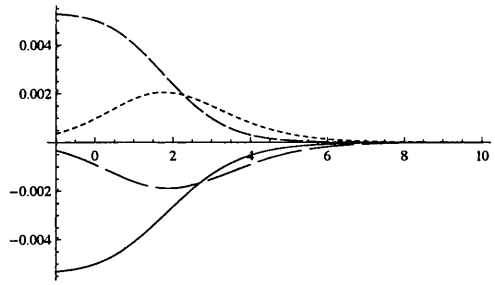

Figure 5.3: The refractive index $n(\omega) - 1$ for the near singularity region of a Schwartzschild black hole plotted as a function of a function of $\log\omega$ for spinor QED: continuous (real part, polarisation i=1); big dashes (imaginary part, i=1); small dashes (real part, polarisation i=2) and dots (imaginary part, i=2).

h_{ij} is diagonal with $h_{11} = -h_{22}$ and $h_{11} = -\frac{6}{25}\frac{1}{u^2}$.

This leads to the VVM matrix given by

$$\begin{aligned} \Delta_{11}(u-u') &= \frac{7(uu')^{1/5}(u-u')}{5(u^{7/5}-u'^{7/5})} \\ \Delta_{22}(u-u') &= \frac{u-u'}{5(uu')^{2/5}(u^{1/5}-u'^{1/5})} \end{aligned} \quad . \tag{5.51}$$

From this VVM one finds the refractive index seen in Figure.5.3. This again shows both imaginary contributions and birefringence, with these results being antisymmetric with respect to interchange of polarisation such that positive and negative corrections are found to both the real and imaginary parts of the refractive index, depending on the polarisation.

5.3 Comments

Even in the few, simple, examples shown in Section.5.2 several interesting effects are observed. There are both increases and decreases of the low frequency phase velocity observed, as well as birefringence effects. In all cases however

the wavefront velocity remains unaffected by the curvature.

It is also seen that both positive and negative contributions to the imaginary part of the refractive index. Although in flat space this would usually be related to particle decay rates, here it should be seen as a balancing of the virtual electron cloud dressing the bare photon [46, 53].

Chapter 6

Graviton Propagation

To examine the back-reaction of quantum fields on curved spaces, within the framework of the semi-classical approximation requires the examination of the propagation of gravitons [23]. This could potentially allow the identification of the regime of validity of the semi-classical gravity approximation for other fields, by using a calculation conducted within the approximation itself.

This may be undertaken by using the techniques developed in Chapters. 4&5, with gravitons replacing photons and the interaction is with some massive scalar fields. To maintain the semi-classical approximation it is assumed that the number of scalar fields N is large enough so that the effect of matter loops is much larger than graviton loops, although in a more complete analysis gravi-

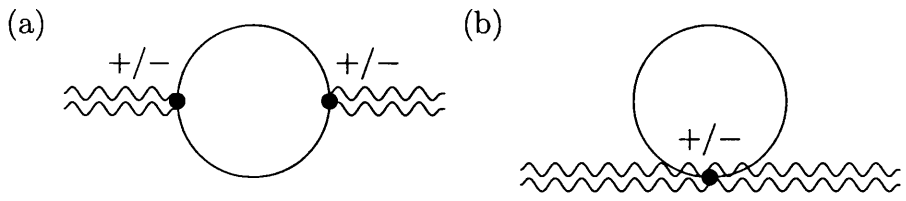

Figure 6.1: The one-loop Schwinger-Keldysh graphs that contribute to vacuum polarization of the graviton due to a free massive scalar field. Only the first loop (a) is non-local in spacetime and so sensitive to the background curvature.

ton loops could also be considered. The low frequency effective action that should be considered for a graviton includes those terms involving at most two powers of the curvature:[1]

$$S = \int d^4x\,\sqrt{g}\Big[\frac{1}{16\pi G}(R-2\Lambda)+c_1 R_{\alpha\beta\gamma\delta}R^{\alpha\beta\gamma\delta}+c_2 R_{\alpha\beta}R^{\alpha\beta}+c_3 R^2+\cdots\Big]\,. \quad (6.1)$$

This effective action is to be understood as being appropriately renormalized so that divergences are absorbed into the coupling G and the cosmological constant Λ. In $d = 4$ only two of the $\mathcal{O}(\mathfrak{R}^2)$ terms are independent as a consequence of the generalized Gauss-Bonnet theorem which implies that

$$\int d^4x\,\sqrt{g}\big(R_{\alpha\beta\gamma\delta}R^{\alpha\beta\gamma\delta} - 4R_{\alpha\beta}R^{\gamma\delta} + R^2\big) \quad (6.2)$$

is a topological invariant whose addition to the action cannot affect the equations-of-motion. The three couplings c_i depend logarithmically on the mass m and the renormalization scale μ. We will only need this dependence for the first two terms:

$$c_1 = -\frac{N}{(4\pi)^2}\cdot\frac{1}{360}\Big[\alpha_1 + \log\Big(\frac{m^2}{\mu^2}\Big)\Big]\,, \qquad c_2 = \frac{N}{(4\pi)^2}\cdot\frac{1}{360}\Big[\alpha_2 + \log\Big(\frac{m^2}{\mu^2}\Big)\Big]\,. \quad (6.3)$$

The constants α_i are the arbitrary finite parts of the counter terms and manifest the fact that gravity coupled to matter fields is not a perturbatively renormalizable theory and so at each order in perturbation theory new couplings appear.

In the next section, we investigate the effect of these terms of graviton propagation to find the gravitational analogue of the Drummond-Hathrell effect.

[1]For example, see the monograph [10].

6.1 The Gravitational Drummond-Hathrell Effect

The classical propagation of gravitons in curved space is determined by expanding around a solution to Einstein's equations to linear order $g_{\mu\nu} \to g_{\mu\nu} + h_{\mu\nu}$. As usual, one needs to fix a gauge in order to uncover the physical degree-of-freedom and to this end we impose the conventional transverse traceless gauge:[2]

$$\nabla_\mu h^{\mu\nu} = 0 \ , \qquad g_{\mu\nu} h^{\mu\nu} = 0 \ . \tag{6.4}$$

Just as in the massless scalar and photon cases we may describe the gravitons using eikonal modes given by

$$h_{\mu\nu}(x) = \varepsilon_{\mu\nu}(x) e^{i\Theta(u)} \tag{6.5}$$

where the eikonal phase take the usual form (4.9).

Once we have approximated the metric with Penrose limit, we can solve for the graviton modes exactly, these modes then correspond to the graviton modes of the full metric to leading order in the WKB approximation. There is a subtlety here in that to capture the leading order approximation involves keeping some of the components of the polarization tensor $\varepsilon_{\mu\nu}$ which are order ω^0 but also other components which are order ω^{-1}. This becomes clear when one solves for the exact complexified graviton modes in the plane-wave background:

$$h^{ab} = \frac{\mathbb{P}^{ij} E_i{}^a(u) E_j{}^b(u)}{\sqrt{\det E_{ia}(u)}} e^{i\omega\hat{v}} \ , \qquad h^{\hat{v}\hat{v}} = -\frac{i}{\omega} \frac{\mathbb{P}^{ij} \Omega_{ij}(u)}{\sqrt{\det E_{ia}(u)}} e^{i\omega\hat{v}} \ , \tag{6.6}$$

with the remaining components vanishing. The two independent polarization

[2] It is known that in some similar curved space examples the transverse-traceless gauge choice does not alway lead to gauge invariant results [54].

tensors $\mathbb{P}_s$, $s = 1, 2$, can be chosen as

$$\mathbb{P}_1^{ij} = \begin{pmatrix} 0 & 1 \\ 1 & 0 \end{pmatrix} , \qquad \mathbb{P}_2^{ij} = \begin{pmatrix} 1 & 0 \\ 0 & -1 \end{pmatrix} . \tag{6.7}$$

Notice that, as alluded to above, at leading order in the WKB approximation, we need to keep the component $h^{\hat{v}\hat{v}}$ even though it goes like ω^{-1}.

In order to describe the quantum corrections to graviton propagation, one takes the graviton modes off shell by modifying the eikonal phase via a u dependent factor:

$$\Theta \longrightarrow \omega\big(\hat{v} + \theta_{ss'}(u_0, u)\big) . \tag{6.8}$$

The corrected phase is a 2×2 matrix in the two-dimensional polarization space $s = 1, 2$. In general, $\theta_{ss'}(u_0, u)$ will have both a real and an imaginary part. The real part describes a local correction to the phase velocity of the graviton along γ and the imaginary part describes a local correction to the amplitude of the graviton along γ. Since $\theta_{ss'}(u_0, u)$ is perturbatively small, we can think of the result in terms of a matrix of refractive indices

$$n_{ss'}(u_0, u; \omega) = \delta_{ss'} + 2\frac{d\theta_{ss'}(u_0, u)}{du} . \tag{6.9}$$

The one-loop quantum corrections to the equations-of-motion that are linear in the curvature come from the last three terms in (6.1). It turns out that only the first two terms of order $\mathcal{O}(\mathfrak{R}^2)$ in (6.1) contribute to graviton propagation. The Gauss-Bonnet argument can then be used to reduce this to a single term involving the square of the Ricci tensor. So for a plane wave metric the renormalized effective action to this order takes the form

$$S = \int d^4x \sqrt{g}\Big[\frac{1}{16\pi G}(R - 2\Lambda) - \frac{N}{16\pi^2 \cdot 120}\lambda R_{\mu\nu}R^{\mu\nu}\Big] , \tag{6.10}$$

for a finite quantity λ which is an independent dimensionless coupling constant. Substituting the mode (6.6) with modified eikonal phase (6.8) into the equation-of-motion that follows from the above action at leading order in the

eikonal approximation and taking the initial value surface at $-\infty$ yields a simple equation of the form

$$\frac{d\theta_{ss'}(u)}{du} = \frac{\lambda G_{\text{eff}}}{120\pi} R_{uu}(u)\delta_{ss'} \ , \tag{6.11}$$

where we have used the effective Newton constant from (2.2) given by $G_{\text{eff}} = GN$.[3] Just as in the QED case, the result can be stated as a curvature induced contribution to the refractive index for graviton propagation along the geodesic γ,

$$n_{ss'}(u) = \left(1 + \frac{\lambda G_{\text{eff}}}{60\pi} R_{uu}(u)\right) \delta_{ss'} \ , \tag{6.12}$$

to $\mathcal{O}(G_{\text{eff}})$. The result is actually simpler than the QED case in (4.3) since the result is diagonal in the 2-dimensional polarization space. So the effective of curvature, in the limit $\omega^2 \gg \mathfrak{R}$, is to induce a frequency independent shift in the refractive index. Notice that this effect depends on the component of the Ricci tensor $R_{uu}(u)$ of the Penrose limit which is equal to the same components of the Ricci tensor of the full metric evaluated along γ.

6.2 One-Loop Vacuum Polarization

The aim of this section is to compute the effect of one-loop vacuum polarization of a massive scalar field on graviton propagation in the eikonal limit $\omega^2 \gg \mathfrak{R}$ and in the limit that $m^2 \gg \mathfrak{R}$.

At the one-loop level there are two graphs that contribute to the quantum equation-of-motion of the graviton field. The first is the important one from our point-of-view because it is non-local and therefore sensitive to the curvature. The second is local and we will be able to account for it by subtracting the contribution of the first in the flat space limit. So turning to the first graph. It involves the 2-point function of the energy-momentum tensor

[3]We are assuming that $N \gg 1$ so that graviton loops are suppressed relative to matter loops.

coupled to the external gravitons. Since we are interested in the quantum corrected equation-of-motion, the relevant 2-point function is the retarded one

$$\Pi_{\mu\nu\sigma\rho}(x,x') = \text{local} + \langle 0|T_{\mu\nu}(x)T_{\sigma\rho}(x')|0\rangle_{\text{ret}} \ . \tag{6.13}$$

The fact that the retarded Green function is needed ensures that the quantum equation-of-motion is causal, since it vanishes for x' lying outside the backward lightcone of x. In the above the energy-momentum tensor of the scalar field is

$$T_{\mu\nu} = \partial_\mu\phi\partial_\nu\phi - \tfrac{1}{2}g_{\mu\nu}(\partial^\rho\phi\partial_\rho\phi + m^2\phi^2) \ . \tag{6.14}$$

The linearized quantum-corrected equation-of-motion for the graviton modes takes the form

$$\Box h_{\mu\nu}(x) = 8\pi G_{\text{eff}} \int_{u_0}^{u} du' \int d^3x' \, \sqrt{g(x')}\, \Pi_{\mu\nu\sigma\rho}(x,x')h^{\sigma\rho}(x') \ , \tag{6.15}$$

with, on the left-hand side, the appropriate Laplacian for gravitons in a non-trivial background. The strategy is to solve this order-by-order in the coupling G_{eff}. At leading order, one takes the classical graviton mode (6.6) with the corrected eikonal phase (6.8) with θ of order G_{eff} one the left-hand side and on the right-hand side the classical graviton mode. This leads to the equation for the one-loop $\mathcal{O}(G_{\text{eff}})$ correction to the phase:

$$\frac{d\theta_{ss'}(u_0,u)}{du} = \text{local} + \frac{8\pi G_{\text{eff}}}{\omega^2} \int d^4x' \, \sqrt{g(x')}\, h_s^{*\mu\nu}(x)\partial_\mu\partial'_\sigma G(x,x')\, \partial_\nu\partial'_\rho G(x,x')h_{s'}^{\sigma\rho}(x') \ , \tag{6.16}$$

where we remember the u' integral is over the range u_0 to u. The insertions of the classical graviton modes involve, from (6.6),

$$h_s^{\mu\nu}\partial_\mu \otimes \partial_\nu = \mathbb{P}_s^{ij} \frac{e^{i\omega\hat{v}}}{\sqrt{\det E_{ia}}} \Big[E_i{}^a E_j{}^b \partial_a \otimes \partial_b - \frac{i}{\omega}\Omega_{ij}\partial_{\hat{v}} \otimes \partial_{\hat{v}} \Big] \ . \tag{6.17}$$

Note only the first term in the energy-momentum tensors contributes due to the gauge condition (6.4). In the above, $G(x,x')$ are the scalar propagators in the plane-wave background. These can be taken as Feynman propagators even though the retarded Green function is called for in (6.13), as is explained

in Chapter.4.

The scalar Feynman propagator in a general background spacetime can be written in the heat-kernel or "proper-time" formalism as shown in (2.11) and repeated here for clarity

$$G(x,x') = \sqrt{\Delta(x,x')}\int_0^\infty \frac{dT}{(4\pi T)^2}\, i e^{-im^2T+\frac{i}{2T}\sigma(x,x')}\Omega(x,x'|T)\ , \qquad (6.18)$$

subject to the usual $m^2 \to m^2 - i\epsilon$ prescription.

We follow the same calculational techniques as described in Chapter.4 and used in Chapter.5. As we have introduced more derivatives than in any of the other cases we introduce the following identities for completion of the integrals over the transverse coordinates x'^a. The Gaussian integrals that we need are of the form[4]

$$I^{(1)} = \int d^2x'\, e^{\frac{i}{4T\xi}x'\Delta(u,u')\cdot x'}\, e^{\frac{i}{4T(1-\xi)}x'\cdot\Delta(u,u')\cdot x'} = \frac{4iT\pi\xi(1-\xi)}{\sqrt{\det\Delta_{ab}(u,u')}}\ , \qquad (6.19)$$

along with

$$I^{(2)}_{ab} = \int d^2x'\, \frac{\partial}{\partial x'^a} e^{\frac{i}{4T\xi}x'\cdot\Delta(u,u')\cdot x'}\, \frac{\partial}{\partial x'^b} e^{\frac{i}{4T(1-\xi)}x'\cdot\Delta(u,u')\cdot x'} = \frac{2\pi\xi(1-\xi)\Delta_{ab}(u,u')}{\sqrt{\det\Delta_{ab}(u,u')}}\ , \qquad (6.20)$$

and

$$\begin{aligned} I^{(3)}_{abcd} &= \int d^2x'\, \frac{\partial^2}{\partial x'^a\partial x'^c} e^{\frac{i}{4T\xi}x'\cdot\Delta(u,u')\cdot x'}\, \frac{\partial^2}{\partial x'^b\partial x'^d} e^{\frac{i}{4T(1-\xi)}x'\cdot\Delta(u,u')\cdot x'} \\ &= -\frac{i\pi\xi(1-\xi)}{T\sqrt{\det\Delta_{ab}(u,u')}}\big(\Delta_{ab}(u,u')\Delta_{cd}(u,u') \\ &\qquad + \Delta_{ac}(u,u')\Delta_{bd}(u,u') + \Delta_{ad}(u,u')\Delta_{bc}(u,u')\big)\ , \end{aligned} \qquad (6.21)$$

where we have repeated the integrals (5.31) (5.32) here as (6.19) and (6.20) for clarity.

[4]Where the integrals are rendered convergent by the prescription $T \to T - i0^+$ and we define $x'\cdot\Delta(u,u')\cdot x' = x'^a\Delta_{ab}(u,u')x'^b$.

The contribution for indices $\{i,j,k,l\}$ involves the quantity

$$E_i{}^a(u)E_j{}^b(u)I^{(3)}_{abcd}(u,u')E_k{}^c(u')E_l{}^d(u')\ , \tag{6.22}$$

which, using (4.39) is proportional to

$$\begin{aligned} &E_j{}^a(u)E_{j'a}(u')\Delta_{ij'}(u,u')\Delta_{k'l}(u,u')E_{k'b}(u)E_k{}^b(u') \\ &\qquad + \Delta_{ik}(u,u')\Delta_{jl}(u,u') + \Delta_{il}(u,u')\Delta_{jk}(u,u')\ . \end{aligned} \tag{6.23}$$

The contribution form the other terms involving indices $\{i,j,\hat{v},\hat{v}\}$, $\{\hat{v},\hat{v},k,l\}$ and $\{\hat{v},\hat{v},\hat{v},\hat{v}\}$ is proportional to

$$\begin{aligned} &\Omega_{ij}(u)I^{(2)}_{cd}(u,u')E_k{}^c(u')E_l{}^d(u') + E_i{}^a(u)E_j{}^b(u)I^{(2)}_{ab}(u,u')\Omega_{kl}(u') \\ &\qquad + \frac{i(u-u')^2}{4\omega T^2\xi(1-\xi)}\Omega_{ij}(u)I^{(1)}(u,u')\Omega_{kl}(u')\ , \end{aligned} \tag{6.24}$$

which, using (4.36), (5.31) and (5.32), is proportional to

$$\Omega_{ij}(u)\mathscr{A}^{-1}_{lk'}(u',u)E_{k'b}(u)E_k{}^b(u')+E_j{}^a(u)E_{j'a}(u')\mathscr{A}^{-1}_{j'i}(u',u)\Omega_{kl}(u')+\Omega_{ij}(u)\Omega_{kl}(u')\ . \tag{6.25}$$

Using the identity (4.22), and being careful with the relative normalization, these terms combine nicely with the first term in (6.23), to give a net contribution involving the tensor[5]

$$\begin{aligned} &\big(\mathscr{B}(u,u')\mathscr{A}^{-1}(u,u')\big)_{ji}\big(\mathscr{A}^{-1}(u,u')\mathscr{B}(u,u')\big)_{lk} \\ &\qquad = \frac{1}{(u-u')^2}\big(\Delta(u,u')\mathscr{B}^\top(u,u')\big)_{ij}\big(\mathscr{B}^\top(u,u')\Delta(u,u')\big)_{kl}\ . \end{aligned} \tag{6.26}$$

In particular, if we had not included the $h^{\hat{v}\hat{v}}$ term in (6.6), we would not have been able to write the final result in terms of the matrices $\mathscr{A}$ and $\mathscr{B}$ which are defined in (4.20) and, for example, the result for a symmetric plane wave to be discussed below would not have involved a function of the difference $u-u'$ which on physical grounds we expect since this particular plane wave admits a Killing vector ∂_u. But with the contribution from $h^{\hat{v}\hat{v}}$, the final expression

[5]Here, we use the symmetry properties $\mathscr{A}_{ij}(u,u') = -\mathscr{A}_{ji}(u',u)$ and $\mathscr{B}_{ij}(u,u') = \mathscr{B}_{ji}(u',u)$.

depends only on the matrices $\mathscr{A}_{ij}(u,u')$ and $\mathscr{B}_{ij}(u,u')$ or $\Delta_{ij}(u,u')$ that are associated to the Jacobi fields. The final tensorial nature of the result can be summarized by the quantity

$$\Delta^{(2)}_{ijkl}(u,u') \stackrel{\text{def.}}{=} \frac{1}{16}\Big[(\Delta(u,u')\mathscr{B}^{\mathsf{T}}(u,u'))_{ij}(\mathscr{B}^{\mathsf{T}}(u,u')\Delta(u,u'))_{kl} + \Delta_{ik}(u,u')\Delta_{jl}(u,u') + \Delta_{il}(u,u')\Delta_{jk}(u,u')\Big] . \tag{6.27}$$

Collecting all the remaining factors together gives the result

$$\frac{d\theta_{ss'}(u_0,u)}{du} = \text{local} - \frac{G_{\text{eff}}}{16\pi\omega^2}\int_0^{\frac{u_0}{2\omega\xi(1-\xi)}-i0^+}\frac{dT}{T^3}\int_0^1 d\xi\, e^{-im^2T}\Delta^{(2)}_{ss'}(u,u')\sqrt{\Delta(u,u')}\Big|_{u'=u-2\omega T\xi(1-\xi)} , \tag{6.28}$$

where

$$\Delta^{(2)}_{ss'}(u,u') = \mathbb{P}^{ij}_s\Delta^{(2)}_{ijkl}(u,u')\mathbb{P}^{kl}_{s'} . \tag{6.29}$$

The local contribution comes from graph (b) in Figure 6.1. We can account for this contribution by subtracting the flat space limit of the non-local expression. This gives

$$\frac{d\theta_{ss'}(u_0,u)}{du} = -\frac{G_{\text{eff}}}{16\pi\omega^2}\int_0^{\frac{u_0}{2\omega\xi(1-\xi)}-i0^+}\frac{dT}{T^3}\int_0^1 d\xi\, e^{-im^2T} \times\Big[\Delta^{(2)}_{ss'}(u,u')\sqrt{\Delta(u,u')}-4\Big]_{u'=u-2\omega T\xi(1-\xi)} . \tag{6.30}$$

The contour for the T integral is taken just below to real axis in order to avoid the singularities of the VVM determinant when u and u' are conjugate points.

The resulting integral is still divergent as we can see by expanding the integrand in powers of ω. This is achieved by expanding in powers of $u-u'$:

$$\Delta^{(2)}_{ss'}(u,u')\sqrt{\Delta(u,u')} = \big(4+R_{uu}(u)(u-u')^2\big)\delta_{ss'}+\mathcal{O}(u-u')^3 . \tag{6.31}$$

This means that divergent contribution is of the form

$$\frac{d\theta_{ss'}(u_0u)}{du}\Big|_{\text{div.}} = -\frac{G_{\text{eff}}}{120\pi}R_{uu}(u)\delta_{ss'}\int_0^{\frac{u_0}{2\omega\xi(1-\xi)}-i0^+}\frac{dT}{T}e^{-im^2T}\,. \tag{6.32}$$

We can regularize by first rotating to Euclidean proper time $T \to -iT$ and then introducing a cut off δ

$$\frac{d\theta_{ss'}(u_0,u)}{du}\Big|_{\text{div.}} = \frac{G_{\text{eff}}}{120\pi}\Big[\gamma_E + \log(m^2\delta)\Big]R_{uu}(u)\delta_{ss'}\,. \tag{6.33}$$

We can subtract the divergence and introduce an arbitrary finite piece in the form of the coupling λ. The regularized expression is then

$$\begin{aligned}\frac{d\theta_{ss'}(u_0u)}{du} &= \frac{\lambda G_{\text{eff}}}{120\pi}R_{uu}(u)\delta_{ss'} - \frac{G_{\text{eff}}}{16\pi\omega^2}\int_0^{\frac{u_0}{2\omega\xi(1-\xi)}}\frac{dT}{T^3}\int_0^1 d\xi\, e^{-im^2T}\\ &\times\Big[\Delta^{(2)}_{ss'}(u,u')\sqrt{\Delta(u,u')} - (4+R_{uu}(u)(u-u')^2)\delta_{ss'}\Big]_{u'=u-2\omega T\xi(1-\xi)}\,,\end{aligned} \tag{6.34}$$

where the integrand is now regular at $u' = u$. In the low frequency limit, when we laet $u_0 \to \infty$ we have

$$\frac{d\theta_{ss'}(u)}{du} = \frac{\lambda G_{\text{eff}}}{120\pi}R_{uu}(u)\delta_{ss'} + \frac{m^4 G_{\text{eff}}}{\omega^2}\mathcal{O}\left(\frac{\omega\sqrt{\mathfrak{R}}}{m^2}\right)^4\,, \tag{6.35}$$

which matches the form extracted from the effective action (6.11) precisely.

We can express the result above as a matrix of refractive indices and change variables from T to u' to write the result in the same form as the QED result (5.39):

$$n_{ss'}(u_0,u;\omega) = \delta_{ss'} - \frac{G_{\text{eff}}}{2\pi}\int_0^1 d\xi\,[\xi(1-\xi)]^2\mathcal{F}_{ss'}\Big(u_0,u;\frac{m^2}{2\omega\xi(1-\xi)}\Big)\,, \tag{6.36}$$

where

$$\mathcal{F}_{ss'}(u_0,u;z) = -\lambda R_{uu}(u)\delta_{ss'} + \int_{-u_0+i0^+}^{u} \frac{du'}{(u-u')^3}\, e^{iz(u'-u)}\Big[\Delta^{(2)}_{ss'}(u,u')\sqrt{\Delta(u,u')} - (4+R_{uu}(u)(u-u')^2))\delta_{ss'}\Big] \,. \tag{6.37}$$

This result is the gravitational analogue of the formula for the refractive index of the photon in (5.39).

6.3 Properties of the Gravitational Refractive Index

In this section, we investigate some of the phenomenology of the gravitational refractive index where we work under the assumption that the initial value surface is taken at $-\infty$. In order to have a concrete example to hand, we first look at the simplest kind of plane-wave spaces for which the Riemann tensor components $R^i{}_{uju}$ are constant along the geodesic. These are the symmetric plane waves, or Cahen-Wallach spaces [55]. To simplify things further, we take the case where the two eigenvalues of the Riemann tensor are equal, so up to a choice of coordinates we can write $R^i{}_{uju} = \sigma^2\delta_{ij}$, for constant σ. In this case, the VVM matrix, and related tensor $\Delta^{(2)}$, are

$$\Delta_{ij}(u,u') = \frac{\sigma(u-u')}{\sin\sigma(u-u')}\delta_{ij} \,, \qquad \Delta^{(2)}_{ss'}(u,u') = \frac{4\sigma^2(u-u')^2}{\sin^2\sigma(u-u')}\delta_{ss'} \,. \tag{6.38}$$

In this case, everything is diagonal in polarization indices and so we will not show them where possible. Changing variable to $t = u - u'$, we have, from (6.37),

$$\begin{aligned}\mathcal{F}(z) &= -2\lambda\sigma^2 + \int_0^{\infty-i0^+} dt\, e^{-izt}\Big[\frac{4\sigma^3}{\sin^3\sigma t} - \frac{4}{t^3} - \frac{2\sigma^2}{t}\Big] \\ &= -2\lambda\sigma^2 - 4z\sigma + \frac{11\sigma^2}{3} + 2(z^2-\sigma^2)\Big[\log\Big(\frac{2\sigma}{z}\Big) + \psi\Big(\frac{3\sigma+z}{2\sigma}\Big)\Big] \,,\end{aligned} \tag{6.39}$$

where $\psi(x)$ is the di-gamma function. Notice that the integrand is a function of the difference $t = u - u'$ which is a special feature of a symmetric plane wave background which is translationally invariant under $u \to u + a$.

The first issue is to investigate is the behaviour of the refractive index at high and low frequencies, or more precisely large and small values of the dimensionless ration $\omega\sigma/m^2$. The low frequency behaviour is obtained by expanding (6.39) in powers of z^{-1}:

$$n(\omega) = 1 + \frac{G_{\text{eff}}}{2\pi}\Big(\frac{\lambda\sigma^2}{30} + \frac{17\sigma^4\omega^2}{4725m^4} + \frac{914\sigma^6\omega^4}{945945m^8} + \cdots\Big) \ . \tag{6.40}$$

So the low frequency limit of the refractive index is independent of ω and depends on the coupling constant α. Consequently, the low frequency phase velocity is not necessarily equal to c. As has been discussed in detail in [42], it is possible that $n(0) < 1$ since this does not imply a violation of causality because low frequency waves cannot be used to send information.

Causality actually depends on the high frequency limit of the refractive index, since this is what governs the propagation of a sharp wavefront. For our plane-wave example, this can be extracted by taking the $z \to 0$ limit of (6.39),

$$\mathcal{F}(z) \longrightarrow 2\sigma^2 \log z + \mathcal{O}(z^0) \ . \tag{6.41}$$

Therefore, the refractive index behaves as

$$n(\omega) \stackrel{\omega\to\infty}{=} 1 + \frac{G_{\text{eff}}\,\sigma^2}{60\pi} \log\Big(\frac{\omega\sigma}{m^2}\Big) + \cdots \ , \tag{6.42}$$

for large ω. This indicates that at some high frequency the perturbative expansion is breaking down and — at the very least — one would need to sum up an infinite class of higher terms in perturbation theory in order to get a sensible result. The result above, for the high frequency behaviour is in fact universal, since the origin of the logarithm is in the divergence at the upper limit of integration of the third term in the integrand (6.37) as $z \to 0$. The

general result for the high frequency limit, is therefore simply

$$n_{ss'}(u;\omega) \overset{\omega\to\infty}{=} \delta_{ss'} + \frac{G_{\text{eff}}}{120\pi} R_{uu}(u) \log\left(\frac{\omega\sigma}{m^2}\right) \delta_{ss'} + \cdots . \tag{6.43}$$

Interestingly, the logarithmic behaviour is increasing as long as the null energy condition is satisfied since this requires that $R_{uu} > 0$.

For our simple example of a symmetric plane-wave space, the refractive index is real, however, more generally the refractive index has both a real and an imaginary part. The real part represents a change in the phase velocity along the ray γ while the imaginary part represents the dissipative effect of propagation caused by decay into pairs of the scalar particle, although there is nothing to prevent an amplification, as we explain below. For instance, if we expand the result (6.36) in powers of the curvature by taking the next term in the series (6.31)

$$\begin{aligned}\Delta^{(2)}_{ss'}(u,u')&\sqrt{\Delta(u,u')}\\ &= \big(4 + R_{uu}(u)(u-u')^2 + \tfrac{1}{2}\partial_u R_{uu}(u)(u-u')^3\big)\delta_{ss'} + \mathcal{O}(u-u')^4 ,\end{aligned} \tag{6.44}$$

then one finds to order $\mathfrak{R}^{3/2}$,[6] that there is a contribution to the imaginary part of the refractive index involving the derivative of the Ricci tensor:

$$\text{Im } n_{ss'}(u;\omega) = \frac{\omega G_{\text{eff}}}{2\pi \cdot 140 m^2} \cdot \partial_u R_{uu}(u) \delta_{ss'} + \cdots . \tag{6.45}$$

This represents a local quantum contribution to the amplitude of the graviton involving the Ricci tensor of the form

$$\exp\left[-\frac{\omega^2 G_{\text{eff}}}{2\pi \cdot 140 m^2} R_{uu}(u)\right] \tag{6.46}$$

as the graviton propagates. This change in the amplitude is caused by the effect of the local curvature on the wavefunction renormalization of the graviton [46].

[6]Note that a derivative of a component of the Riemann or Ricci tensors is order $\mathfrak{R}^{3/2}$ in our convention.

In order to understand this effect we have to remind ourselves that a physical graviton is a renormalized composite object that consists of a bare graviton plus a cloud of virtual scalar pairs. In flat space, there is a delicate balance between the bare graviton and the virtual cloud of scalars, but in curved space this balance is perturbed by the tidal forces acting on the composite particle induced by the curvature of spacetime. The quantity $\Gamma = 2\omega \,\mathrm{Im}\, n(u;\omega)$ represents the instantaneous rate of production of scalar particle pairs from the gravitons. It is important to realize that this can either be positive or negative as a function of u, since the balance between bare particle and virtual cloud can be upset either way. In particular, in certain backgrounds the graviton can actually amplify as the virtual cloud becomes depleted. This does not break unitarity or violate the optical theorem because the graviton is already a renormalized particle. One way to investigate this, is to imagine turning on the coupling at finite affine time $u = u_0$. In this way, one would see the graviton undergo wavefunction renormalization even in flat space. However, in a gravitational theory, as in QED, this wavefunction renromalization is a UV sensitive process that actually diverges as the cut-off is removed.[7] So the dressing which creates the renormalized graviton is an infinite process and the implication of this is that the graviton may become infinitely "undressed" which means that the amplitude can increase without bound as the graviton becomes undressed by curvature induced tidal forces. More generally the imaginary part can be written in nice way by changing variables to $t = u - u'$ and extending the contour to run from $-\infty$ to $+\infty$:

$$\begin{aligned}&\mathrm{Im}\; n_{ss'}(u;\omega)\\ &= \frac{iG_{\mathrm{eff}}}{2\pi}\int_0^1 d\xi\,[\xi(1-\xi)]^2\int_{-\infty-i0^+}^{+\infty-i0^+}\frac{dt}{t^3}\,e^{-izt}\Delta^{(2)}_{ss'}(u,u-t)\sqrt{\Delta(u,u-t)}\;.\end{aligned} \tag{6.47}$$

A useful consistency check of the result (6.37) can be obtained by taking the external graviton off-shell which is possible in a plane-wave background since it can be done simply by modifying the eikonal phase given in (4.9) as

[7]This effect is described in detail in [53].

follows

$$\Theta = \omega\hat{v} \longrightarrow \omega\hat{v} + \frac{M^2 u}{2\omega} \ , \tag{6.48}$$

where M is the off-shell mass of the graviton. This extra phase can be carried through the one-loop computation of the graviton propagation. This extra phase only affects the non-local contribution from Feynman graph (a) in Figure 6.1 and leads to a modification of the integrand in the refractive index formula in (6.37) of the form[8]

$$\int_{-\infty+i0^+}^{u} \frac{du'}{(u-u')^3} e^{i(z-M^2/2\omega)(u'-u)} \Delta^{(2)}_{ss'}(u,u') \sqrt{\Delta(u,u')} \ . \tag{6.49}$$

The expression for the imaginary part of the refractive index in (6.47) is similarly modified. Now when $M > 2m$, which corresponds to the off-shell graviton being above threshold for decay into pairs of the scalar particle, the imaginary part of the refractive index can be evaluated by completing the contour in (6.47) in the upper-half t-plane.[9] In particular, there is a contribution from the pole at $t = 0$, which is independent of the curvature, of

$$\mathrm{Im}\, n(\omega) = \frac{m^4 G_{\rm eff}}{4\omega^2} \int_0^1 d\xi\, \theta(M^2\xi(1-\xi) - m^2) = \frac{m^4 G_{\rm eff}}{4\omega^2} \sqrt{1 - 4m^2/M^2} \ , \tag{6.50}$$

diagonal in polarization indices, which simply represents the exponential decrease in the off-shell graviton amplitude in flat space due to decay into pairs of the scalars above threshold. The decay rate is given by $2\omega\, \mathrm{Im} n$ in agreement with a conventional flat space calculation of the rate.

There is another way that an imaginary part of the refractive index can be produced which is non-perturbative in the curvature. For a symmetric plane wave where at least one of the eigenvalues of the constant $R^i{}_{uju}$ is negative there is a positive contribution to $\mathrm{Im}\, n(\omega)$, so a decaying amplitude, which is non-perturbative in the curvature. The simplest case to consider is $R^i{}_{uju} = -\sigma^2 \delta_{ij}$. Such a background violates the null energy condition, but provides a useful

[8]Note that the subtractions in (6.37) which become the local contribution to the vacuum polarization are not modified and they are independent of M.

[9]More precisely only for the values of ξ for which $M^2\xi(1-\xi) > m^2$.

example where the imaginary part of the refractive index can be calculated exactly. In this case, $\mathrm{Im}\, n(\omega) = 0$ to all orders in the curvature expansion as can be seen from (6.40) by taking $\sigma \to i\sigma$. In this case, the VVM matrix and related tensor $\Delta^{(2)}$ are obtained by substituting $\sigma \to i\sigma$ in (6.38)

$$\Delta_{ij}(u,u') = \frac{\sigma(u-u')}{\sinh \sigma(u-u')}\delta_{ij} \ , \qquad \Delta^{(2)}_{ss'}(u,u') = \frac{4\sigma^2(u-u')^2}{\sinh^2 \sigma(u-u')}\delta_{ss'} \ . \quad (6.51)$$

The integral in (6.47) can be computed by deforming the contour and picking up the contributions from the poles on the negative imaginary axis at $t = -in\pi/\sigma$, $n = 1, 2, \ldots$. This gives directly

$$\mathrm{Im}\, n(\omega) = \frac{G_{\mathrm{eff}}}{16\omega^2}\int_0^1 d\xi \ \frac{m^4 + 4\sigma^2\omega^2(\xi(1-\xi))^2}{1 + e^{\pi m^2/2\omega\sigma\xi(1-\xi)}} \ , \quad (6.52)$$

which is, indeed, non-perturbative in the curvature. In this case the result is independent of u and so it implies a constant rate of production of pairs of the scalar particles. Such a process is kinematically disallowed in flat space, but there is no such kinematic constraint in curved space. Although this result has been calculated in a background that violates the null energy condition it is generic to plane waves with at least one negative eigenvalue.

Chapter 7

Introduction to De Sitter Space

7.1 De Sitter Physics

Over the past 30 years or so two of the most important advances in the field of cosmology have been the development and success of the theory of inflation [18] and the observation of accelerating cosmological expansion [19] (often referred to as dark energy). Although these might seem to be unrelated topics, with different causes and separated by orders of magnitude in both time and energy scales, they share the common property that both may be modeled by using de Sitter space.

De Sitter space is the maximally symmetric solution to the vacuum Einstein field equations including a positive cosmological constant, discovered by Willem de Sitter [56,57] and independently by Tullio Levi-Civita [58] in 1917. In many models of inflation the inflaton field plays the part of the cosmological constant, driving the exponential growth of the universe. In the present universe the observed 'dark energy' has the same rôle, although the universe should only be seen as asymptotically de Sitter at late times as the usual energy density from matter (including dark matter) and radiation density be-

comes negligible as it is diluted over an ever increasing volume. Therefore de Sitter space is also used as the reference geometry in cosmological models, in which it represents our universe in the absence of matter.

Understanding how flat space quantum field theories are effected by existing in de Sitter space is a very important phenomenological problem, especially in the inflation period where curvature effects could have observable implications today. Investigation of field theory in de Sitter space, using the semi-classical gravity approximation, would also be the first step in understanding how these quantum field theories back-react with the spacetime curvature itself.

Furthermore it is the quantum fluctuations of the inflaton field that are believed to result in the large scale cosmic structure seen today. An understanding of this quantum field theory for the inflaton in the curved de Sitter background is an essential part of understanding the cosmic microwave background power spectrum, that plays a central rôle in much of modern cosmology.

De Sitter space is a very convenient test bed for any study of general curved space physics, as we can take advantage of the high degree of symmetry possessed by de Sitter space. This symmetry allows us to define particles and asymptotic states as is the case in Minkowski space, although this becomes more complicated, when interactions are considered.

A major problem when considering de Sitter space is the time dependence of the spatial coordinates. The dynamical nature of this space means that one must in the very least be careful when defining the vacuum as well as, when interactions are considered, equilibrium states and decay rates.

There are, for free fields at least, a well developed set of techniques for dealing with quantum field theories in de Sitter space [59]. Within this work conducted in Schwinger-Keldysh in(out) states may be defined as those that a regular at $t_0 \to -\infty$ ($t \to \infty$) when m^2 is analytically continued into the upper half plan, $m^2 \to m^2 + i\epsilon$.

For free fields the initial vacuum in state is expressed in terms of the out state modes by using a Bogoliubov transform it is seen in these new modes the this configuration no longer corresponds to a vacuum. Therefore it is valid to say that particles have been created from the vacuum due to the de Sitter expansion, as one can also show that this effect would also lead to non-zero detection rates found by a particle detector. Although this is an interesting and valuable result, it is not the main consideration in this work.[1]

A more complicated problem is that of considering interacting field theories in de sitter space. A surprising early result discovered by Nachtmann [21] was that a particle in de Sitter space may decay into a pair of particles with a greater combined mass than the original particle although this effect is exponentially suppressed by a factor of the de Sitter radius. This violation of the usual sub-additivity condition is due to the lack of the standard conservation of energy in de Sitter spaces, which is itself the result of the fact that there is no timelike Killing vector.

7.2 Some Properties of De Sitter Space

The de Sitter manifold may be identified with a hyperboloid $\{X \in \mathbb{R}^{d+1} : X^2 = X_0^2 - X_1^2 - ... - X_d^2 = -R^2\}$ embedded in a $d+1$ dimensional Minkowski space, where R is the characteristic length scale of the space, the de Sitter radius.

When a point is given by coordinates in the Minkowski space it is shown here as an upper case letter (X^i) and when given in de Sitter coordinates lower case letters (x^i) are used. An important property of the de Sitter manifold dS_d is the existence of antipodal pairs of points related by reflection through

[1]This omission can be justified in several ways, either as the result is already well known and we have nothing to add, or by the consideration of the fact that particle creation via this mechanism can not be related to issues of quantum stability of a de Sitter background as both the in and out states preserve the de Sitter symmetry.

the origin of the de Sitter hyperboloid in the embedding Minkowski space $X^i_A = -X^i$. This is of particular relevance when α-vacua are examined in Chapter.8. These antipodal points are always separated by spatial horizons.

Another useful quantity when considering two spacetime locations in de Sitter space is the scalar invariant variable $Z(x,y) = Z$ given by

$$Z(x,y) = \frac{x \cdot y}{R^2}, \tag{7.1}$$

which may be viewed as the hyperbolic angle in the $d+1$ dimensional Minkowski space and has the property that $Z(x,x) = 1$. This is related to the geodesic distance, $d(x,y)$, or proper time separation for light-like separated points, function given by

$$\cos\frac{d(x,y)}{R} = Z(x,y) \ . \tag{7.2}$$

A result that we will find useful later is that that the function Z is anti-symmetric under the interchange of one of the point point replaced with its anti-podal counterpart.

$$x \cdot y_A = -x_A \cdot y = -Z(x,y) \ . \tag{7.3}$$

One should note that due to the symmetries of de Sitter space one can tell that the two point functions must only be functions of $Z(x,y)$, i.e. $G(x,y) = G(Z)$.

There are three distinct forms of coordinates used for describing de Sitter space. The first of these, the static patch is given by the metric

$$ds^2 = -\left(1 - \frac{r^2}{R^2}\right) dt^2 + \left(1 - \frac{r^2}{R^2}\right)^{-1} dr^2 + r^2 d\Omega^2_{d-2} \ , \tag{7.4}$$

which gives a coordinate system centered on an observer at $r = 0$, with a cosmological horizon at $r = R$.

However as our concern in this thesis is with the spacetime not a specific observer we are more interested in the Poincaré patch and Global coordinates.

The Poincaré (also commonly referred to as the cosmological) patch is used in cosmological calculations as it is a system of co-moving coordinates, covering half of the complete de Sitter manifold

$$ds^2 = -dt^2 + e^{2t/R} d\Omega_{d-1}^2 \, . \tag{7.5}$$

The Global coordinates are geodesically complete and describe the whole de Sitter manifold but do contain causally separated regions. The coordinates are given by

$$ds^2 = -dt^2 + \cosh(2t/R) d\Omega_{d-1}^2 \, . \tag{7.6}$$

7.3 Interacting States and Stability in de Sitter Space

There has been much recent interest in in the stability of de Sitter space when an interacting massive scalar field is added [60–65]. As we know from the Bogoliubov transforms of free field states, particles creation occurs with respect to an initial vacuum configuration as we evolve through time [59]. However as both the in and out states here are de Sitter invariant they can not break the de Sitter symmetry, such that this process could not result in the decay of the de Sitter space.

However when some initial state in an interacting theory is considered it would appear to be possible that, due to the loss of the sub-additivity condition of flat space, particle number could increase at a rate greater than the rate of 'dilution' due to the de Sitter expansion [20]. This would lead to an increase in matter density, which would in turn cause a back-reaction with the curvature in such a way as to result in the decay of the de Sitter space.

The counter argument states that interacting states in de Sitter may be defined in terms of analytic continuation from the Euclidean sphere. It is well

known that quantum field theories on an Euclidean sphere *must* be stable. In particular the long time IR divergences that are proposed to lead to de Sitter decay do not appear in a compact space. When the radial direction of a spherical space is Wick rotated one obtains de Sitter space. It is also possible to analytically continue the free field states in the same way, obtaining the so called Euclidean or Bunch-Davies states.

For interacting massive scalar theories several recent papers [20, 60–67] show how by choosing an appropriate contour it is possible to obtain the full interacting de Sitter theory by analytic continuation from the interacting theory on the sphere — showing how de Sitter space must therefore inherit the stability from the sphere. This leads to a definition of asymptotic states on a sphere given by those obtained as the analytic continuation from the fully interacting states on the sphere. These are in fact the interacting Hartle-Hawking states.

This disagreement obviously leads to contradictions if both arguments are taken at face value. However there are some subtleties that we have yet to consider.

In standard flat space, when calculations involving interactions are conducted, it is often assumed that there are free fields in the asymptotic past and future using an adiabatic switching on and off of the interaction. This leaves us with with asymptotically free unambiguous in and out states with the creation and annihilation operators related by trivial Bogoliubov transformations. However such a procedure in a dynamical spacetime such as de Sitter space would lead to a calculational dependence on the unphysical process of 'switching' on and off of the interaction, i.e. the results acquire a dependence on the process controlling the interaction (although such a case may be desirable in some exotic calculations). This may be interpreted as a result of the fact that the dressing of a particle or even the vacuum in de Sitter space has a time dependence.

The calculations appearing in [20,66,67] are perturbative and are calculated

to a limited order in perturbation, with the coupling gaining a time dependence due to it being switched on at some point in the past. The proof shown in [60–65] is valid for all orders in perturbation theory and has a non-time dependent coupling, as the interacting in and out states are the Hartle-Hawking states obtained from the analytic continuation from the interacting in and out states on the sphere.

This suggests that the divergent results in [20, 66, 67] in which these divergences are said to be indicative of de Sitter decay, are due to the fact that we are considering a different situation in each calculation. Specifically the interacting Hartle-Hawking states obtained from the sphere in are directly examined in [60–65], whereas in [20, 66, 67] the initial value problem considered set the initial conditions to match the free field states at some arbitrary initial surface. This should be interpreted as the coupling being switched on at this initial value Cauchy surface.

Chapter 8

3-D one-loop mean field Calculation

In [20] it is claimed that an instability of de Sitter space is found when the long time evolution of some initial matter content is examined.

To investigate this proposal one of the simplest explicit calculations of this effect is made in this chapter. Here the equation-of-motion of the zero-momentum ground state expectation value is found and solved using Laplace transform techniques.

To further investigate this problem we introduce a more sophisticate technique, giving the equations-of-motion of two point functions known as the Kadanoff-Baym equations, in Chapter.9.

8.1 Amplitude Expansion

The aim of this chapter is, using the simplest possible model, to consider the evolution of a scalar field expectation value in de Sitter space. A massive

self interacting scalar field in the Poincaré patch of a dS_3 (although the key conclusion derived here can easily be generalised to d dimensions) background. An homogeneous initial matter distribution is assumed such that, due to spatial invariance, the field expectation value must take the form

$$\begin{aligned} \langle \phi(t,x) \rangle &= \langle \phi(t) \rangle \ , \\ \phi(t,x) &= \phi(t) + \psi(t,x) \ , \\ \langle \psi(t,p) \rangle &= 0 \ . \end{aligned} \tag{8.1}$$

Therefore it is possible to 'integrate out' these spatially dependent fluctuations given by the $\psi(t,x)$ component of the field. After this coarse graining the equations of motion of the time dependent background field are found using Schwinger-Keldysh formalism.

For the dS_3 metric given by

$$ds^2 = -dt^2 + e^{2t}\left(dx^2 + dy^2\right) \tag{8.2}$$

(such that we are working in the Poincaré patch). As it is shown in Chapter.4 the one loop correction to the Schwinger-Keldysh equations of motion for a scalar field may be found, to linear order in $\phi(t)$, for cubic coupling to be given by

$$\ddot{\phi}(t) + 2\dot{\phi}(t) + m^2\phi(t) + \int_{t_0}^{t} \sqrt{g(t')}dt'\Pi_{SK}(t,t')\phi(t') = 0 \ . \tag{8.3}$$

The Schwinger-Keldysh initial value surface is chosen to be the equal time plane given by $t_0 = 0$

$\Pi_{SK}(t,t')$ is the retarded vacuum polarisation which we calculate in Schwinger-Keldysh perturbation theory using the variation of the diagram shown in Figure 8.1 with respect to ϕ^+. To first order this is simply

$$\Pi_{SK}(t,t') = \lambda^2\left(G_+^2(t,t') - G_-^2(t,t')\right) \ . \tag{8.4}$$

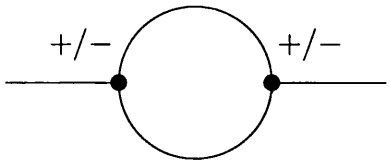

Figure 8.1: The one loop 1PI contribution to the effective action in the 'in-in' state using the Schwinger basis as seen in Figure.4.3

In dS_3 the exact closed form of the massive scalar propagators is well known in real space form [68,69]. This is where this work differs from that in [7] where massless scalar propagators are used. The same normalisations are used and the computational differences arise due to the fact that the massive scalar propagators are not IR divergent as the mass, a protected Casimir operator acts as a natural IR cut off.

The propagators appearing in the calculation are given by

$$\begin{aligned} G_+(t,t') &= \frac{A\sinh\left(\nu\left(\pi - i(t-t')\right)\right)}{\sin i(t-t')}\,, \\ G_-(t,t') &= \frac{A\sinh\left(\nu\left(\pi + i(t-t')\right)\right)}{\sin i(t-t')}\,, \\ G_+^2(t,t') - G_-^2(t,t') &= \frac{A^2\sinh\left(2\nu\pi\right)}{2\sin i(t-t')}\left(e^{-2i\nu(t-t')} - e^{2i\nu(t-t')}\right)\,. \end{aligned} \tag{8.5}$$

where the mass parameter $\nu = \sqrt{m^2 - (d-2)^2/R^2} = \sqrt{m^2 - 1}$ ($d = 3,\ R = 1$) has been introduced with $A = \frac{\Gamma(1+i\nu)\Gamma(1-i\nu)}{4\pi^2}$. It is required that $m^2 > (d-2)^2/R^2$ such that the propagators belong to the principal series. All the separations used here are functions of the quantity $t - t'$ as all spacelike separations are being ignored. Note that these propagators do not reduce to the massless one as m tends to zero, so comparison with the results of [7] is of limited value as it is not expected that these results should match in the massless limit.

A perturbative solution to (8.3) may be found by taking the zero momen-

tum mode to be of the form

$$\phi(t) = \phi_0(t)\left(1 + \delta(t)\right) \ . \tag{8.6}$$

where the free field modes obey the wave equation

$$\ddot{\phi}_0(t) + 2\dot{\phi}_0(t) + m^2\phi_0(t) = 0 \tag{8.7}$$

Substituting (8.6) into (8.3) and applying (8.7) we find the equation of motion for the correction part of (8.6) given by

$$\begin{aligned}\ddot{\delta}(t)\,\phi_0(t) + 2\dot{\delta}(t)\left(\phi_0(t) + \dot{\phi}_0(t)\right) &= \lambda^2 \int_0^t dt' \left(G_+^2(t,t') - G_-^2(t,t')\right)\phi^+(t)\sqrt{g(t')} \\ &= I(t) \ .\end{aligned} \tag{8.8}$$

As in this formalism it is a Schwinger-Keldysh in-in state being calculated, the modes are taken to be the positive frequency Bunch-Davies states

$$\begin{aligned}\phi^+(t) &= \phi(t) \ , \\ \phi_0^+(t) &= \phi_0(t) \ ,\end{aligned} \tag{8.9}$$

with the boundary conditions

$$\begin{aligned}\phi_0^+(0) &= \phi_0 = const \ , \\ \dot{\phi_0^+}(0) &= i\sqrt{m^2+2}\phi_0 \ , \\ \delta^+(0) &= \dot{\delta^+}(0) = 0 \ .\end{aligned} \tag{8.10}$$

From these boundary conditions we obtain the form of the uncorrected zero momentum mode as

$$\phi_0 = \frac{e^{-i\sqrt{m^2+2}t}}{\sqrt{m^2+2}} \ . \tag{8.11}$$

Next the right hand side of (8.8) must be computed. This takes the form

$$I(t) = \frac{A^2 \sinh(2\nu\pi)\lambda^2}{2} \int_0^t \frac{\left(e^{-2i\nu(t-t')} - e^{2i\nu(t-t')}\right)}{\sin i(t-t')} \phi^+(t') e^{2t'} dt' \ . \qquad (8.12)$$

This integral is in the form of a convolution, allowing the use of Laplace transform techniques.

The Laplace transform of a convolution results in the product of the Laplace transform of the two convoluted functions. First we calculate the Laplace transform of the self-energy $(t - t')$ dependent part of the integral. Defining $L(f(t))$ as the Laplace transform of $f(t)$ with respect to the variable s we may now, by examining the poles, see that the Laplace transform of the denominator of the self-energy is given by

$$L\left(\frac{1}{\sinh^2 t}\right) = s\psi(\frac{s}{2}) \ , \qquad (8.13)$$

be rewriting the numerator of the self-energy in terms of exponentials it is clear to see that the Laplace tranform of the total self-energy is given by

$$\Sigma(s) = \frac{A^2 \sinh(2\nu\pi)\lambda^2}{2} \left((s + 2i\nu)\psi(s + 2i\nu) - (s - 2i\nu)\psi(s - 2i\nu)\right) \ . \qquad (8.14)$$

The Laplace transform of the t' (as opposed to $t - t'$) dependent part is given by

$$L\left(\sqrt{g(t')}\phi^+(t')\right) = \frac{1}{(s - 2 + i\sqrt{m^2 + 2})} \ , \qquad (8.15)$$

Therefore the final Laplace transformed result is given by

$$L(I(t)) = \frac{A^2 \sinh(2\nu\pi)\lambda^2 \Sigma(s)}{2(s - 2 + i\sqrt{m^2 + 2})} \ . \qquad (8.16)$$

8.1.1 Inverse Laplace Transform

To find the real space form of the quantum correction to the field expectation we must take the inverse Laplace transform. Using the Bromwich integral,

$$I(t) = 2\pi i \int_{-i\infty+C}^{i\infty+c} L\left(I(t)\right) e^{st} ds \ . \tag{8.17}$$

This, as a contour integral, sums over all the poles to the left hand side of some constant real parameter C, where this constant is taken to be to the right of all the poles.

Looking at (8.16) it becomes apparent that one may split the contributing poles into two distinct groupings, those arising from the poles from the self energy, i.e. the di-gamma function poles and those arising due to the denominator of pole of (8.15).

Self-Energy Poles

The self-energy (8.14) contribution to (8.17) takes the form the poles from the di-gamma function multiplied by some function and as such has three infinite series of poles, one along the negative real axis and the other two parallel to this offset by $\pm 2i\nu$. The poles of the di-gamma function are given by $Residue\left[\psi(n)\right] = -1$, for $n = 0, 1, 2, 3...$ This leaves the sum

$$I_\Sigma(t) = \frac{A^2 \sinh\left(2\nu\pi\right)\lambda^2}{2} \sum_{n=1}^{\infty} \Big(\frac{2ne^{-2(n+i\nu)t}}{-2n - 2i\nu - i\sqrt{m^2+2} - 2} - \frac{2ne^{-2(n-i\nu)t}}{-2n + 2i\nu - i\sqrt{m^2+2} - 2} \Big) \ . \tag{8.18}$$

Which may be evaluated to find the result

$$\begin{aligned} I_\Sigma(t) =& \frac{A^2 \sinh(2\nu\pi)\lambda^2 e^{-2t}}{2(-1+i\nu)(1+3i\nu)(\sqrt{m^2+2}-4i)} \\ &\times \Bigg[-ie^{2i\nu t}(k_1)_2F_1\left(2, \frac{1}{2}-i\frac{i\nu}{2}, \frac{1}{2}-i\frac{i\nu}{2}, e^{-2t}\right) \\ &+ ie^{-2i\nu t}(k_2)_2F_1\left(2, \frac{1}{2}+i\frac{3i\nu}{2}, \frac{3}{2}+i\frac{3i\nu}{2}, e^{-2t}\right)\Bigg] . \end{aligned} \tag{8.19}$$

where

$$\begin{aligned} (k_1) &= \left(4+12i\nu+i\sqrt{m^2+2}-3i\sqrt{m^4+m^2-1}\right) , \\ (k_2) &= \left(4(1+\nu)+i\sqrt{m^2+2}+\sqrt{m^4+m^2-2}\right) . \end{aligned} \tag{8.20}$$

As it is questions of stability that are being asked here it is only the long time behavior, $t \to \infty$ that we are concerned with. In this limit it is clear that due to the prefactors and the argument of e^{-2t} appearing in the hypergeometric functions from (8.19) that the contribution to I dies away rapidly, leaving the expectation value unaffected, by these self-energy poles.

Denominator poles

There is a single pole in the denominator of (8.16) at $s = 2+i\sqrt{m^2+2}$, which gives the contribution from the Bromwich integral of (8.16) as

$$\begin{aligned} I_{den}(t) =& \frac{A^2 \sinh(2\nu\pi)\lambda^2 e^{2t+2i\sqrt{m^2+2}t}}{4} \\ &\times \Big[(2i\nu-2i\sqrt{m^2-2})\psi(2-i\nu+\frac{i}{2}\sqrt{m^2+2}) \\ &-(2i\nu+i\sqrt{m^2+2})\psi(2+i\nu+\frac{i}{2}\sqrt{m^2+2})\Big] . \end{aligned} \tag{8.21}$$

which may be presented in the form

$$I_{den}(t) = e^{2t}\phi_0(t)c(m) , \tag{8.22}$$

where all the constant terms have been collected into c(m).

This gives a term which is exponentially growing as t gets large. Clearly this dominates the contribution from $I(t)$ in the limit $t \to \infty$. Now by taking (8.8) and assuming $I(t)$ is given by (8.22) as all the transient contributions are dropped, the equations of motion for $\delta(t)$ may be solved to find

$$\begin{aligned}\delta(t) =& \frac{c(m)}{4(m^2+2)(3+m^2)}\Bigg(e^{2t}\left(\sqrt{m^2+2}-im^2-2i\right)+i\left(m^2+3\right) \\ & - e^{-2i\sqrt{m^2+2}t}\left(\sqrt{m^2+2}+1\right)\Bigg) .\end{aligned} \tag{8.23}$$

This contains a secular term, i.e. one that grows divergently with time, proportional to e^{2t} which leads to a rapid breakdown of perturbation theory, as it can no longer be assumed that the result is linear in $\phi(t)$, related to $\delta(t)$ by (8.6).

These secular terms are often encountered in non-equilibrium and time dependent situations. In some cases it may be possible to sum over all these secular terms at each order in perturbation theory using a technique known as the 'Dynamical Renormalisation Group'. [22, 70–73].

For the amplitude $\phi(t)$ we may write this, to lowest order in the coupling, in terms of the amplitude at some arbitrary time t^* as

$$\phi(t) = \phi(t^*)\left(1 + (\delta(t) - \delta(t^*))\right) + \dots , \tag{8.24}$$

where the correction $\delta(t)$ may be secular. As the right hand side of this is independent of t^* then,

$$0 = -\phi(t^*)\frac{d\delta(t^*)}{dt^*} + \frac{df(t^*)}{dt^*}(1+\dots) + \dots , \tag{8.25}$$

where ... indicates corrections of higher order in the coupling. Solving (8.25) using the initial conditions $\delta(t_0) = 0$ and setting $t^* = t_0$ leads us to exponen-

tiate these secular terms, such that

$$\phi(t) = \phi_0(t)\,(1 + \delta(t)_{sec}) \rightarrow \phi_0(t)e^{\delta_{sec}(t)} \ . \tag{8.26}$$

Due to the overall sign of the the correction calculated, i.e. our correction is negative, applying (8.26) to the secular terms in (8.23) leaves the corrected field expectation value of the form

$$\phi(t) \propto \phi_0(t)e^{-ke^{2t}} \ , \tag{8.27}$$

where k is some positive constant. This means that due to the interaction our expectation value dies away *extremely* quickly. However this result is in itself not surprising as although the interaction is written in terms of a self coupling field the calculation is exactly the same as would be conducted when our original field is couple to some new extra fields that do not contribute to the expectation. So when considering the effect of self-decay of massive scalars in de Sitter space all that can really be said using this result is that it occurs over surprisingly small time scales, that are in themselves dependent on the couplings.

Many of these short comings may be removed when a higher order perturbative technique is used as is the case in Chapter. 9.

Chapter 9

Kadanoff-Baym Evolution

The results obtained in Chapter.8 show that for an interacting massive scalar theory in de Sitter space one may expect a rapid decay of field expectation values. This implies that the de Sitter curvature has the effect of accelerating particle decay.

The calculation obtaining such a result has several limitations. There is a lack of an ability to describe self decay, as for particles in de Sitter space the decay into multiple copies of the particle, is allowed although the interpretation of this effect in Schwinger-Keldysh formalism is not so simple. Furthermore it is impossible to see thermalisation effects or state occupation numbers, as well as being unable to calculated corrections to the two-point stress tensor required for the examination of back-reaction effects using the technique employed in Chapter. 8. All of these problems may be avoided by examining the two point functions using Kadanoff-Baym equations. These are used in this chapter directly calculate the evolution of some two point functions.

9.1 Numerical Kadanoff-Baym equations in de Sitter space

The study of quantum field theory in time dependent situations is an important area for both our theoretical and practical understanding of non-equilibrium field theory. When considering this time dependence arising due to the background spacetime the prototypical example is that of de Sitter space, which is examined here.

Often, for example in the calculation of an inflaton fluctuation two-point function, massless fields are considered within the Causal or Poincaré patch of de Sitter space. This is appropriate for the situation arising in cosmology where there is only a finite period of de Sitter expansion which, depending on the model in question, may also exist over a region of finite extent. Here the aim is to examine, at least in principle, the stability of quantum field theories in a pure de Sitter background.

Calculations of IR effects by Polyakov and Krotov [20] indicate that the presence of some initial non-vacuum particle state in a self-interacting theory, using global coordinates, leads to explosive particle production. Such particle production would eventually lead to a gravitational back-reaction. This back-reaction would act against the de Sitter curvature 'screening' it away. Such a calculation, including back reaction, is beyond the capabilities of the semi-classical gravity approximation used here.

For an analysis of this the geodesically complete global coordinates are used. This does not suffer from potential violations of unitarity introduced as particles enter and leave a coordinate patch. One should also note that the Poincaré patch glued to regions of Minkowski space, as is often the situation being described by models in Poincaré coordinates, does not correspond to solutions of the vacuum Einstein equations including the cosmological constant, so that it is not appropriate for this kind of calculation.

As the Kadanoff-Baym equations that are used in this chapter need to be implemented numerically we consider the computationally least expensive setting, 2 dimensional de Sitter space. The global coordinates used here are given by the metric

$$ds^2 = -dt^2 + \cosh^2(t) d\theta^2 \,, \tag{9.1}$$

which is now rewritten in the conformal form

$$ds^2 = \sec^2(\eta) \left(-d\eta^2 + d\theta^2\right) \,, \tag{9.2}$$

where the relation between the time coordinates is given by

$$\sinh t = \tan \eta \,. \tag{9.3}$$

It is known that for interacting theories in time dependent backgrounds that the renormalized quantities, such as the mass and wavefunction normalization, obtain a time dependence due to the dynamical dressing/undressing of the bare quantities. With individual states changing with time (that is beyond the usual free field scalings) this makes the study of the evolution of ensemble states even more complicated.

However despite these difficulties one may still hope to make some general qualitative statements about the development of such ensemble states, even if we can not find some kind of dynamical quantum mechanical equivalent to the Maxwell-Boltzmann distribution for de Sitter space (should such an arrangement even exist) is found. For instance when some initial field configuration is considered in a dynamical de Sitter background there are three classes of possible outcomes;[1]

1. Unbounded Decay: the expectation values die away eventually disappearing through some dispersive mechanism.

[1]Note that this is refers to an ensemble of free field states, not the dynamically dressed interacting states.

2. Unbounded Enhancement: the expectation values grow, eventually blowing up indicating a break down of the methodology or potentially a spacetime instability .

3. Thermalization: the expectation value reaches (asymptotically) some stable/finite equilibrium state with a fixed (possibly with a phase) expectation with respect to the free field states.

The Kadanoff-Baym (real time Schwinger-Dyson)equations are obtained with a method that uses the 2PI effective action, in Schwinger-Keldysh formalism for a given theory, to obtain evolution equations for the 2-point functions. This technique is used at a three loop (effective action) level as this has been shown to be of high enough order to examine the effects of thermalization ([8, 74–77] and in a curved spacetime scenario [9, 78]).

For some arbitrary, spatially homogeneous, field configuration we may decompose the propagator

$$G(x,x') = F(x,x') - \frac{i}{2}\rho(x,x')\left[\Theta(t-t') - \Theta(t'-t)\right] \ . \tag{9.4}$$

where $F(x,x')$ is the statistical and $\rho(x,x')$ is the spectral component.[2] These may also be described as the field expectation values

$$\begin{aligned} F(x,x') &= \frac{1}{2}\langle 0|\{\phi(x),\phi(x')\}|0\rangle \\ \rho(x,x') &= i\langle 0|[\phi(x),\phi(x')]|0\rangle \end{aligned} \tag{9.5}$$

The statistical function describes the physical state occupation levels and it is the spectral component that describes the transitions between different excited states.

For a massive scalar theory with a ϕ^4 interaction it may be shown [74] that by extremising the variation of the effectictive action the Kadanoff-Baym

[2]Note that in the notation of Chapter.3 G is the Feynman propagator G_F, F is the Schwinger function G_S and ρ is the Hadamard function $G^{(1)}$.

equations are found. These describe the evolution of these functions from some initial values via the use of the memory integrals

$$\begin{aligned}\left[\partial_\eta^2 + a(\eta)^2 m^2 - \partial_\theta^2 + \Delta M(x)^2\right] F(x,x') &= -\int_{\eta_0}^{\eta} d\eta'' \int d\theta'' \Sigma_\rho(x,x'') F(x'',x') \\ &\quad + \int_{\eta_0}^{\eta'} d\eta'' \int d\theta'' \Sigma_F(x,x'') \rho(x'',x') \ , \\ \left[\partial_\eta^2 + a(\eta)^2 m^2 - \partial_\theta^2 + \Delta M(x)^2\right] \rho(x,x') &= -\int_{\eta_0}^{\eta} d\eta'' \int d\theta'' \Sigma_\rho(x,x'') \rho(x'',x') \ .\end{aligned} \tag{9.6}$$

In the above

$$\Delta M(x)^2 = \frac{a(\eta)^2 \lambda}{2} F(x,x) \ . \tag{9.7}$$

This term appears in (9.6) in the same form as the mass and as such may be seen in a shift in the effective mass of the field given by

$$m^2 \to m^2 + \frac{\lambda}{2} F(x,x) \ . \tag{9.8}$$

Self-energies have also been introduced and are given by

$$\begin{aligned}\Sigma_\rho(x,x'') &= -\frac{a(\eta)^2 a(\eta'')^2 \lambda^2}{2} \rho(x,x'') \left[F(x,x'')^2 - \frac{1}{12}\rho(x,x'')^2\right] \ , \\ \Sigma_F(x,x'') &= -\frac{a(\eta)^2 a(\eta'')^2 \lambda^2}{6} F(x,x'') \left[F(x,x'')^2 - \frac{3}{4}\rho(x,x'')^2\right] \ .\end{aligned} \tag{9.9}$$

Due to the high computational memory requirement of these memory integrals, appearing here numerically, that are required to compute the time evolution of $F(x,x')$ and $\rho(x,x')$, we examine the simplest relevant case. This is a massive (heavy)[3] scalar field in 2-D de Sitter space. The background is described by global conformal coordinates which has spatially spherical sections. The closed spatial component naturally discretizes the spatial momentum modes, which are cut off at some large scale referred to as the 'Planck mass', M_{pl}. A Fourier transform is used to switch between the spatial coor-

[3]Heavy here means that $m^2 > (d-1)^2/4$, such that the propagators of the free theory belong to the principle series.

dinate and momentum space. To allow the numerical computation we further discretize our (conformal) time coordinate. Note that with our discretized momentum states the replacement

$$p^2 \to \left(\frac{M_{pl}}{\pi}\sin\left(\frac{\pi p}{2M_{pl}}\right)\right)^2 , \tag{9.10}$$

must be used.

A fundamental problem with using this type of discretization in a time evolving background is that we have a lattice spacing given by $a(\eta)\delta$, where δ is the time step size. This spacing grows with η such that the finite number of physical momentum modes become red-shifted along with the the cut-off scale. Even when using the physical coordinates this situation is not avoided due to the varying momentum discretization (due to the expanding physical sections) and the changing value of M_{pl} in phyical coordinates. This limits validity of these methods as we run out of 'dynamical range'. In practice this means that we should not trust the numerics generated within this method for the range

$$a(\eta)m > 2 . \tag{9.11}$$

As it is heavy particles (for 2-D $m > 1/2$ in units of the de Sitter radius) that are being investigated here and as the minimum value of $a(\eta) = 1$, this imposes a given a definite range of $0 < \eta \lesssim 1.2$ in which the numerics are expected to be trustworthy. Note this is still an overestimate as the effective mass m increases due to (9.8) further reducing the dynamical range (9.11).

Introducing the Fourier transformed momentum modes of the statistical $F_p(\eta, \eta')$ and spectral $\rho_p(\eta, \eta')$ functions the initial conditions may be chosen

to be

$$\begin{aligned} F_p(0,0) &= 2\left(n_0\delta_{0p}+\frac{1}{2}\right)\Phi_p(\eta_0)\Phi_p^*(\eta_0)\ , \\ F_p(\delta,\delta) &= 2\left(n_0\delta_{0p}+\frac{1}{2}\right)\Phi_p(\eta_0+\delta)\Phi_p^*(\eta_0,\delta)\ , \\ F_p(\delta,0) &= n_0\delta_{0p}\left(\Phi_p(\eta_0+\delta)\Phi_p^*(\eta_0)+\Phi_p(\eta_0)\Phi_p^*(\eta_0+\delta)\right)\ , \\ \rho_p(0,\delta) &= -\delta = \rho_p(\delta,0)\ . \end{aligned} \tag{9.12}$$

This represents the free particle vacuum state with the addition of a matter density given by n_0 where the matter is confined to the $p=0$ groundstate.

These initial conditions are not complete however as due to the mass correction in (9.7), the mass appearing in the field definitions is different to to effective mass in the Kadynoff-Baym equations. This means that we are describing a quenching situation as studied in [79]. To avoid this we modify the definition of the effective mass $\Delta M(x)$, such that on the initial value surface the effective mass is equal to the initial field mass, i.e.

$$\begin{aligned} \Delta M(x) &= a(\eta)^2\frac{\lambda}{2}\sum_p\left(F_p(\eta,\eta)-F_p(\eta_0,\eta_0)\right)\ , \\ m^2 &\to m^2+\frac{\lambda}{2}\sum_p\left(F_p(\eta,\eta)-F_p(\eta_0,\eta_0)\right)\ . \end{aligned} \tag{9.13}$$

As, when the interaction is included, any physical particle acquires a an effective mass we have above chosen the initial conditions such that $m_{eff}(\eta_0) = m_{Init} = m_{bare} = m$. This ensures that we are not observing the relaxation of the field into the configuration with m_{eff} as would otherwise occur in such a quenching scenario. However by being forced into using such time dependent initial conditions it would appear to cast doubt on the appropriateness of the free field vacuum for determining our initial conditions due to the physical dependence on this unphysical matching (i.e. the case we are trying to study is that of a time invariant coupling, whereas we are examining a situation where the coupling is abruptly turned on at some fixed time and the results

depend on this time).

The free field mode functions in the space described are the solutions to

$$\left[\partial_\eta^2 + m^2 \sec^2 \eta + p^2\right] \Phi_p(\eta) = 0 \ , \tag{9.14}$$

with the normalized results are given by

$$\begin{aligned} \Phi_p(\eta) =& c_p P^p_{i\nu-\frac{1}{2}}(i\tan\eta) \ , \qquad \Phi^*_p(\eta) = c_p P^p_{i\nu-\frac{1}{2}}(-i\tan\eta) \ , \\ c_p =& \left[(1-2p+2i\nu)\, P^p_{i\nu+\frac{1}{2}}(0) P^p_{i\nu+\frac{1}{2}} P(0)\right]^{-\frac{1}{2}} \ . \end{aligned} \tag{9.15}$$

9.2 Numerical Evaluation

The aim of this computation is to examine the time evolution of the equal time statistical function (i.e. particle distribution). In the coordinates used the conformal time η has the range $-\frac{\pi}{2} < \eta < \frac{\pi}{2}$ $(-\infty < t < \infty)$, where the numerical evaluation is restricted to the range from the initial value surface $\eta_0 = 0$, up until the time $\eta = 1.2$.[4]

Here we use the values $m = 1$, $n_0 = 1$ (which we compare to the vacuum case $n_0 = 0$). The coupling takes the values $0, 0.1, 2$ and 10. The Planck mass is increased from 50 until numerical convergence is obtained (up to a maximum value of 300) as can be seen in Figure.9.2. The time step size is decreased from 0.01 in an attempt to find the continuum limit down to a minimum value of 0.00125 (where the memory requirements become too large to allow computation).

These results pick up an unphysical phase (related to the fact we are using a time reversible process to try to find a state which is independent of the initial conditions, i.e. the thermal equilibrium is a non time reversible with respect to

[4]We could extend the real time range by starting from the value -1.2 although this would now involve considering both contraction and expansion with respect to the initial surface making separation of the effects more complicated.

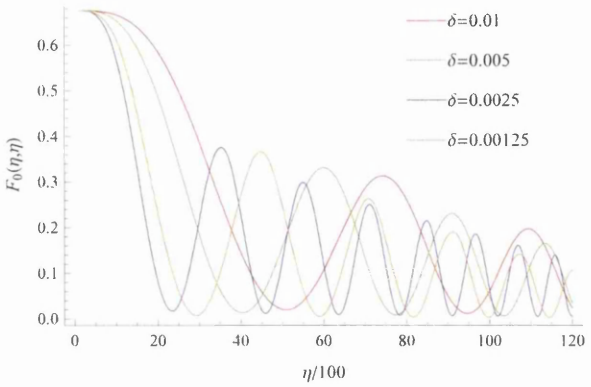

Figure 9.1: We show the zero mode of the statistical function as a function of the conformal time η. The 'convergence' of results as δ, the time step size, is reduced. Using the values $m = 1$, $\lambda = 0.1$, $n_0 = 0$, $p_{max} = 50$ with the values $\delta = 0.01,\ 0.005,\ 0.0025,\ 0.00125$. Although this does not show absolute convergence it does show some stabilization occurring as the phase differences become small. Further analysis of this convergence is beyond the computational capabilities available to the author.

the initial state). This makes direct comparisons between particle distributions at the same time unfeasible due to the differing periodicities appearing in the results as, can be seen in Figure.9.1. To try to minimise this effect we take our results from the last maxima occurring in the $F_0(\eta, \eta)$ function as we increase the number of time steps, before the point the results become numerically unstable.

Other calculations using this methodology in both flat space and curved backgrounds suggest that for any form of equilibrium state to be identified requires a large number of these oscillations to occur. For the range in conformal time this formalism allows it is unlikely that any equilibrium state could be found. However the results here can still act as a test of the feasibility of case 3), by being able to detect any rapid approach to either case 1) or 2).

Figure.(9.5) shows an example of the evolution of the equal time statistical function for both the vacuum and some ground state matter. There is little difference in the late time evolution of the higher momentum states due to the

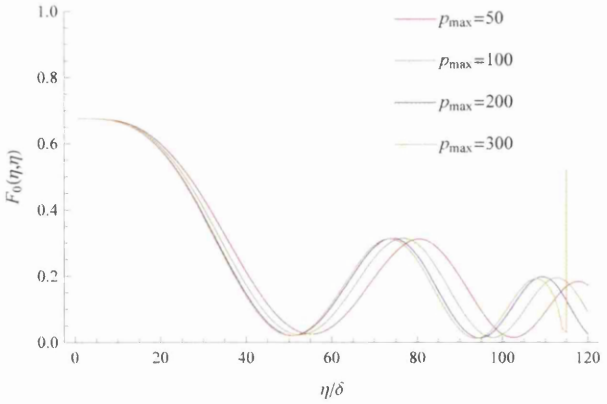

Figure 9.2: This plot shows the equal time zero momentum component of the statistical functions as a function of conformal time and uses the values $\delta = 0.01$, $n_0 = 1$, $m = 1$, $\lambda = 0.1$. We increase the Planck mass, represented by the highest momentum mode, p_{max} and can see that up until very late times, when we expect the results to become unreliable, a value of 200 reproduces the same results as those calculated using a higher M_{pl}. For the comparison of equal time statistical functions the time value is chosen such that it coincides with the final peak in $F_0(\eta, \eta)$ as we increase η appear on this type of plot.

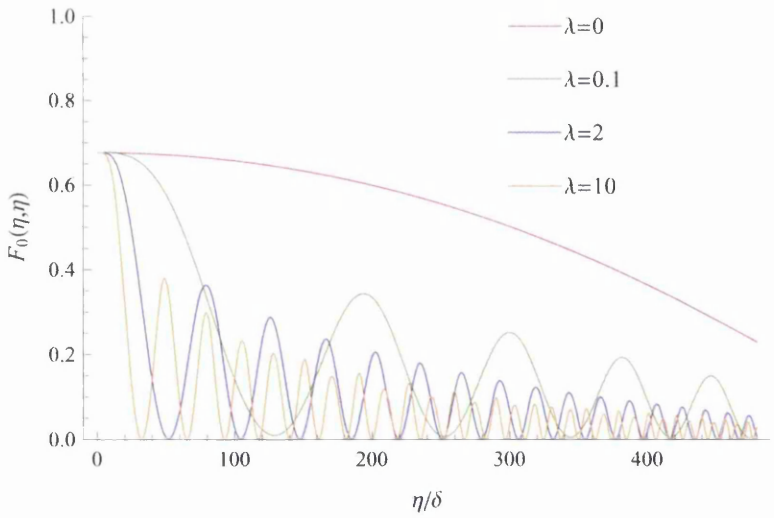

Figure 9.3: The values $m = 1$, $\delta = 0.0025$, $p_{max} = 200$, $n_0 = 0$ are used here with the coupling taking values $\lambda = 0, 0.1, 2, 10$. We see enhanced groundstate vacuum 'decay' with greater coupling.

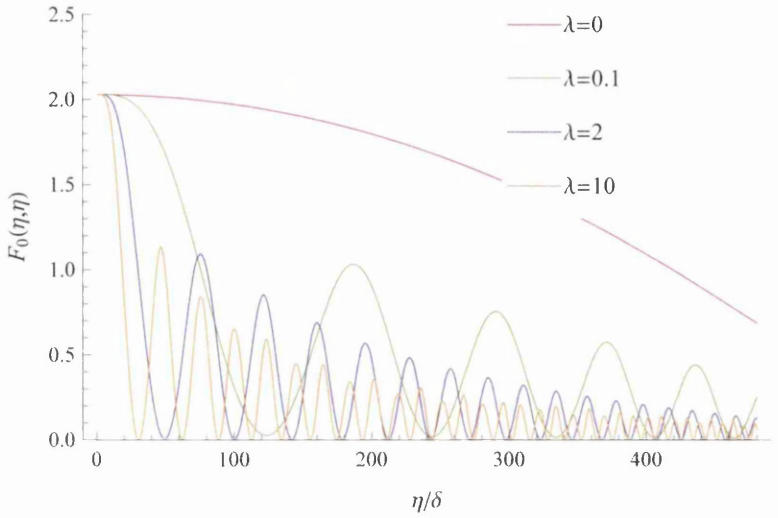

Figure 9.4: The values $m = 1$, $\delta = 0.0025$, $p_{max} = 200$, $n_0 = 1$ are used here with the coupling taking values $\lambda = 0, 0.1, 2, 10$. We see enhanced groundstate vacuum 'decay' with greater coupling.

presence of matter when the result is compared to the vacuum.

One should note that in Figures.9.3&9.4 use values for the coupling given by values as high as 10 (in units of mass). These are not small couplings and as such invalidate the perutbative approximations used although they are still found to be useful in illustrating effects related to increasing the coupling. By using a large N approximation scheme one may also extend into the strong coupling regime, although the equations used here would be slightly modified [79].

The main result that can be found here is depicted in Figures.9.3&9.4. These figures show how the zero momentum mode of the statistical (Schwinger) function 'decays' with respect to the free field state, where this rate of decay increases with increasing coupling. It is unclear however if this decay is towards zero or towards some fixed state scaling with the free field. As this effect occurs for both the Bunch-Davies interacting vacuum case in Figure.9.3 and an initial state containing zero momentum matter Figure.9.4 this suggests the problem does not lie in the system being out of equilibrium as such, but by being

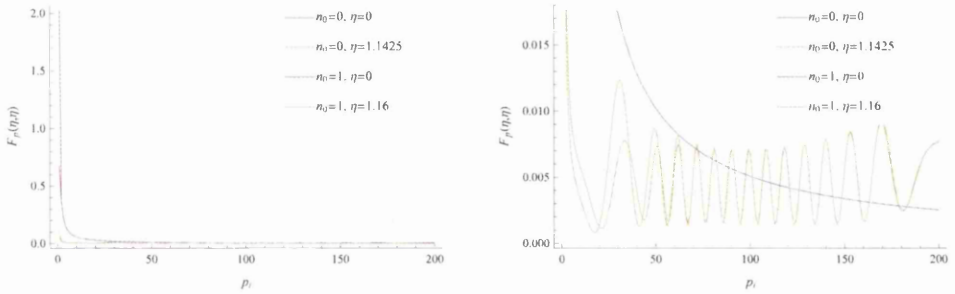

Figure 9.5: This plot shows the the evolution of the equal time statistical function as a function of momentum for both the vacuum and $n_0 = 1$ states. We have used the values $m = 1$, $p_{max} = 200$, $\lambda = 0.1$.

described in the wrong basis. The result shown in Figure.9.5 gives further support to the idea that we are not seeing a result that can be explained as a thermalisation effect as it is seen that the introduction of initial matter has had little effect with respect to vacuum state, particularly when the higher momentum modes are being considered. If thermalisation were to explain the decay of the equal time zero mode statistical function then one would expect much greater populations appearing in the higher momentum modes.

These results would suggests that the overlap between our Bunch-Davies zero mode and the true interacting zero mode is very small, as the system thermalises and tries to approach the true interacting vacuum the occupation levels for our original modes tend to zero.

This result should not be surprising seeing as the scaling of the Bunch-Davies is determined by the conformal scaling of the space time. As any coupling appearing in a 2 dimensional scalar field theory must be massive this shows the coupling would be expected to break the conformal scaling of some interacting state. This would make it interesting to use this method to look at, for instance, a 4 dimensional scalar theory with a quartic coupling, where this coupling now has no classical mass dimension.

9.3 Conclusions

These results are very preliminary and should not be seen as conclusive proof either way for the stability of a massive scalar theory living in a 2-D global de Sitter space. However what has been shown is the apparent effect of vacuum decay in de Sitter space due to the presence of a self-interaction. The explosive matter growth suggested by [20] is not observed here, although, this explosive effect is related to long time interactions and this calculation only runs over a quite small range in real time. The results do appear to agree with the calculations shown in [80], which is consistent with the arguments presented in [63–65, 81]

Although simply throwing more computational time and power at this problem would help improve the range and accuracy of the results presented here it is unlikely such brute force methods would be able to draw any strong conclusions here. This is due to the conformal time limit introduced and an apparently slow approach to thermalization for heavy massive particles . It is unclear how one could introduce a fixed physical momentum cut-off into this formalism, which would be required to increase the dynamical range of this approach.

Chapter 10

Concluding Remarks

This thesis has examined some aspects of interacting quantum field theories in curved spaces. The work is carried out using the semi-classical gravity approximation in which gravitational fluctuations are ignored except in the calculation of the correction to the propagation of a graviton in Chapter.6, were these fluctuations are examined in a controlled manner. The Schwinger-Keldysh formalism is used in much of this work as this methodology is manifestly causal, can cope with out of equilibrium systems and does not require globally defined in and out states.

Within this framework two main questions have been considered. Firstly, how is propagation though a curved space effected for either a photon coupled to the spinor electron field or for a graviton coupled to massive scalars? Secondly is it possible that de Sitter space becomes unstable in the presence of an interacting field with a 'physical' non-zero initial density?

To answer the first question the one loop order correction to the particle's propagation is calculated. It is shown that by calculating within the regime in which the photon or graviton's frequency is much greater than the spatial curvature ($\omega^2 \gg \mathfrak{R}$) and that the loop mass is greater than this curvature ($m^2 \gg \mathfrak{R}$), is equivalent to conducting the calculation in the plane-wave space

time given by the Penrose limit along the particle's trajectory if the original space. It is this simplification that allows an exact but non-trivial result to be calculated within the regime $\omega^2 \gg \mathfrak{R}$, $m^2 \gg \mathfrak{R}$.

It now becomes apparent that the space acts as an optical medium with an effective refractive index. Depending on the space in question this can lead to dispersion effects. As the quantum dressing of a particle involves quantum loop effects, that are non-local, it becomes important to understand how nearby geodesics behave. This may be understood in terms of the null congruence of geodesics around the path of the particle and the cloud of virtual particles (electrons/positrons or massive scalars for the photon and graviton respectively) 'dressing' the bare particles via wavefunction renormalisation.

When geodesics in this null congruence diverge this leads to a greater dressing of the renormalised photon field where the virtual electron cloud is smeared out, leading to the number of real particles increasing within the virtual cloud. When the congruence is convergent this cloud is forced back into the original field leading to an amplification of this field, removing some of the dressing.

The situation becomes more complicated when gravitons are considered. This is, in part due to the introduction of higher order curvature terms in the action (required for renormalising the stress tensor) corresponding to corrections to Einstein gravity, where one would expect such corrections to lead to corrections of the causal structure [27,28]. Also when gravitons are considered the light cones for massless particles, including gravitons, are determined by the full perturbed metric [31].

Arguments regarding the dressing and undressing of the graviton states due to the dressing and undressing of the field may still be made. However a new logarithmic curvature dependence is seen in these calculations. This may be due to a poor choice of gauge for the original graviton modes (in higher curvature gravity for instance the graviton acquires additional degrees of freedom [82]) although is more likely to be a result of the limitations built into the calculation. Some infinite summation of terms may required although

more investigation is required before any conclusions may be drawn.

Now moving onto the second question, that of de Sitter space stability. Taking the lesson that states in curved spaces acquire a spacetime location dependence from the now dynamical dressing of states, leads us to a new view point for this problem.

The potential decay of de Sitter space is proposed, in part, because of the self-decay of a particle into multiple copies of itself, as is allowed in de Sitter space. From here one might propose that this would lead to explosive particle number growth, which could in turn back-react with the curvature screening away the de Sitter curature. Results suggesting such a scenario have been shown by Polyakov and Krotov [20].

This decay is investigated by examining the decay rate for particles in α-vacua states. A mass dependent enhancement of decay into these α-states appears to be shown.

This problem is further investigated in Chapters.8&9 where the expectation value of an initial field configuration is calculated. The initial conditions here are chosen to match those of the free field vacuum with the addition of free field particles, with the interaction turned on at an initial value surface. However as the dressing of the vacuum and particle states is dynamical in a dynamical background, this would imply that our resuits would obtain a physical dependence on the unphysical switching on process. In fact it has been argued [80] that due to the dressing of physical states the overlap between the free and interacting modes could become zero. This would suggest that any initial conditions for an interacting theory set to match a free field conditions would not correspond to a physical field configuration so would bring into question the value of such calculations.

The calculations here are not however conclusive and as such further research is required to make further progress.

This however presents us with many exciting opportunities to improve our understanding of curved space field theories and therefore perhaps, Quantum Gravity.

Clearly further research into the questions raised here could be very useful and interesting.

Bibliography

[1] D. J. Kapner *et al.*, "Tests of the gravitational inverse-square law below the dark-energy length scale," *Phys. Rev. Lett.* **98** (2007) 021101, arXiv:hep-ph/0611184.

[2] J. Shapiro Key, N. J. Cornish, D. N. Spergel, and G. D. Starkman, "Extending the WMAP Bound on the Size of the Universe," *Phys. Rev.* **D75** (2007) 084034, arXiv:astro-ph/0604616.

[3] T. Aoyama, M. Hayakawa, T. Kinoshita, and M. Nio, "Revised value of the eighth-order QED contribution to the anomalous magnetic moment of the electron," *Phys.Rev.* **D77** (2008) 053012, arXiv:0712.2607 [hep-ph].

[4] **Particle Data Group** Collaboration, K. Nakamura *et al.*, "Review of particle physics," *J.Phys.G* **G37** (2010) 075021.

[5] N. Shakura and R. Sunyaev, "Black holes in binary systems. Observational appearance," *Astron.Astrophys.* **24** (1973) 337–355.

[6] S. Weinberg, "Quantum contributions to cosmological correlations," *Phys.Rev.* **D72** (2005) 043514, arXiv:hep-th/0506236 [hep-th].

[7] D. Boyanovsky, R. Holman, and S. Prem Kumar, "Inflaton decay in De Sitter spacetime," *Phys. Rev.* **D56** (1997) 1958–1972, arXiv:hep-ph/9606208.

[8] E. Calzetta and B. Hu, "Thermalization of an interacting quantum field in the CTP-2PI next-to-leading order large N scheme," arXiv:hep-ph/0205271 [hep-ph].

[9] A. Tranberg, "Quantum field thermalization in expanding backgrounds," *JHEP* **0811** (2008) 037, arXiv:0806.3158 [hep-ph].

[10] N. Birrell and P. Davies, "QUANTUM FIELDS IN CURVED SPACE,".

[11] P. Adshead, R. Easther, and E. A. Lim, "The 'in-in' Formalism and Cosmological Perturbations," *Phys.Rev.* **D80** (2009) 083521, arXiv:0904.4207 [hep-th].

[12] K.-i. Kondo and K. Yoshida, "Finite temperature and density QED: Schwinger-Dyson equation in the real time formalism," *Int.J.Mod.Phys.* **A10** (1995) 199–232, arXiv:hep-th/9304018 [hep-th].

[13] L. Ford and R. Woodard, "Stress tensor correlators in the Schwinger-Keldysh formalism," *Class.Quant.Grav.* **22** (2005) 1637–1647, arXiv:gr-qc/0411003 [gr-qc].

[14] T. J. Hollowood and G. M. Shore, "The Refractive index of curved spacetime: The Fate of causality in QED," *Nucl.Phys.* **B795** (2008) 138–171, arXiv:0707.2303 [hep-th].

[15] T. J. Hollowood and G. M. Shore, "The Causal Structure of QED in Curved Spacetime: Analyticity and the Refractive Index," arXiv:0806.1019 [hep-th].

[16] T. J. Hollowood, G. M. Shore, and R. J. Stanley, "The Refractive Index of Curved Spacetime II: QED, Penrose Limits and Black Holes," *JHEP* **0908** (2009) 089, arXiv:0905.0771 [hep-th].

[17] R. Stanley and T. J. Hollowood, "Graviton Propagation and Vacuum Polarization in Curved Space," arXiv:1106.4675 [hep-th]. * Temporary entry *.

[18] A. H. Guth, "The Inflationary Universe: A Possible Solution to the Horizon and Flatness Problems," *Phys.Rev.* **D23** (1981) 347–356.

[19] **Supernova Search Team** Collaboration, A. G. Riess *et al.*, "Observational evidence from supernovae for an accelerating universe and a cosmological constant," *Astron.J.* **116** (1998) 1009–1038, arXiv:astro-ph/9805201 [astro-ph].

[20] D. Krotov and A. M. Polyakov, "Infrared Sensitivity of Unstable Vacua," arXiv:1012.2107 [hep-th]. * Temporary entry *.

[21] O. Nachtmann, "Dynamische stabilitat im de-sitter-raum," *Sitzungsberichte der Osterreichischen Akademie der Wissenschaften, Mathem-Naturw Klasse* (1968) .

[22] D. Boyanovsky, H. J. de Vega, R. Holman, and M. Simionato, "Dynamical renormalization group resummation of finite temperature infrared divergences," *Phys. Rev.* **D60** (1999) 065003, arXiv:hep-ph/9809346.

[23] P. R. Anderson, C. Molina-Paris, and E. Mottola, "Linear response, validity of semiclassical gravity, and the stability of flat space," *Phys. Rev.* **D67** (2003) 024026, arXiv:gr-qc/0209075.

[24] S. Hawking, "Particle Creation by Black Holes," *Commun.Math.Phys.* **43** (1975) 199–220.

[25] E. Witten, "Instability of the Kaluza-Klein Vacuum," *Nucl.Phys.* **B195** (1982) 481.

[26] K. S. Stelle, "Renormalization of Higher Derivative Quantum Gravity," *Phys. Rev.* **D16** (1977) 953–969.

[27] D. M. Hofman, "Higher Derivative Gravity, Causality and Positivity of Energy in a UV complete QFT," *Nucl.Phys.* **B823** (2009) 174–194, arXiv:0907.1625 [hep-th].

[28] V. E. Hubeny, M. Rangamani, and S. F. Ross, "Causally pathological spacetimes are physically relevant," *Int.J.Mod.Phys.* **D14** (2005) 2227–2232, arXiv:gr-qc/0504013 [gr-qc]. Submitted for GRF essay competition.

[29] L. Ford, "Gravitons and light cone fluctuations," *Phys.Rev.* **D51** (1995) 1692–1700, arXiv:gr-qc/9410047 [gr-qc].

[30] L. Ford, "Spacetime in semiclassical gravity," arXiv:gr-qc/0504096 [gr-qc]. To appear in the volume 100 Years of Relativity - Space-time Structure: Einstein and Beyond, A. Ashtekar, ed., to be published by World Scientific.

[31] R. Woodard, "Causal Effective Field Eqns from the Schwinger-Keldysh Formalism ," Jan., 2012.

[32] V. E. Hubeny, M. Rangamani, and S. F. Ross, "Causal structures and holography," *JHEP* **0507** (2005) 037, arXiv:hep-th/0504034 [hep-th].

[33] A. Buchel and R. C. Myers, "Causality of Holographic Hydrodynamics," *JHEP* **0908** (2009) 016, arXiv:0906.2922 [hep-th].

[34] X. O. Camanho, J. D. Edelstein, and M. F. Paulos, "Lovelock theories, holography and the fate of the viscosity bound," *JHEP* **1105** (2011) 127, arXiv:1010.1682 [hep-th].

[35] M. Brigante, H. Liu, R. C. Myers, S. Shenker, and S. Yaida, "The Viscosity Bound and Causality Violation," *Phys.Rev.Lett.* **100** (2008) 191601, arXiv:0802.3318 [hep-th].

[36] G. M. Shore, "Causality and superluminal light," arXiv:gr-qc/0302116.

[37] D. P. Jatkar, L. Leblond, and A. Rajaraman, "On the Decay of Massive Fields in de Sitter," arXiv:1107.3513 [hep-th].

[38] M. G. Jackson and K. Schalm, "Model Independent Signatures of New Physics in the Inflationary Power Spectrum," arXiv:1007.0185 [hep-th].

[39] I. T. Drummond and S. J. Hathrell, "QED Vacuum Polarization in a Background Gravitational Field and Its Effect on the Velocity of Photons," *Phys. Rev.* **D22** (1980) 343.

[40] G. Shore, "'Faster than light' photons in gravitational fields: Causality, anomalies and horizons," *Nucl.Phys.* **B460** (1996) 379–396, arXiv:gr-qc/9504041 [gr-qc].

[41] G. Shore, "Faster than light photons in gravitational fields. 2. Dispersion and vacuum polarization," *Nucl.Phys.* **B633** (2002) 271–294, arXiv:gr-qc/0203034 [gr-qc].

[42] G. Shore, "Superluminality and UV completion," *Nucl.Phys.* **B778** (2007) 219–258, arXiv:hep-th/0701185 [hep-th].

[43] G. M. Shore, "Quantum gravitational optics," *Contemp.Phys.* **44** (2003) 503–521, arXiv:gr-qc/0304059 [gr-qc].

[44] R. Penrose, "Any space-time has a plane wave as a limit," *Differential geometry and relativity,* (1976) 271–275.

[45] T. J. Hollowood and G. M. Shore, "Causality and Micro-Causality in Curved Spacetime," *Phys.Lett.* **B655** (2007) 67–74, arXiv:0707.2302 [hep-th].

[46] T. J. Hollowood and G. M. Shore, "The Effect of Gravitational Tidal Forces on Vacuum Polarization: How to Undress a Photon," *Phys.Lett.* **B691** (2010) 279–284, arXiv:1006.0145 [hep-th].

[47] T. J. Hollowood and G. M. Shore, "'Superluminal' Photon Propagation in QED in Curved Spacetime is Dispersive and Causal," arXiv:1006.1238 [hep-th].

[48] M. Blau, "Plane waves and Penrose limits," *Lectures given at the 2004 Saalburg/Wolfesdorf Summer School* (2004) .

[49] M. Blau, D. Frank, and S. Weiss, "Fermi coordinates and Penrose limits," *Class.Quant.Grav.* **23** (2006) 3993–4010, arXiv:hep-th/0603109 [hep-th].

[50] D. E. Diaz and H. Dorn, "Propagators and WKB-exactness in the plane wave limit of AdS x S," *JHEP* **08** (2004) 008, arXiv:hep-th/0406240.

[51] S. F. Ross and G. Titchener, "Time-dependent spacetimes in AdS/CFT: Bubble and black hole," *JHEP* **0502** (2005) 021, arXiv:hep-th/0411128 [hep-th].

[52] J. A. Hutasoit, S. Prem Kumar, and J. Rafferty, "Real time response on dS(3): The Topological AdS Black Hole and the Bubble," *JHEP* **0904** (2009) 063, arXiv:0902.1658 [hep-th].

[53] T. Hollowood and G. M. Shore, "The Effect of Gravitational Tidal Forces on Renormalized Qunatum Fields," *to appear* .

[54] A. Higuchi, D. Marolf, and I. A. Morrison, "de Sitter invariance of the dS graviton vacuum," arXiv:1107.2712 [hep-th]. * Temporary entry *.

[55] M. Cahen and N. Wallach, "Lorentzian symmetric space," *Bull.Amer.Math.Soc.* **76, Number 3** (1970) 585–591.

[56] W. de Sitter, "On the relativity of inertia. Remarks concerning Einstein's latest hypothesis," *Koninklijke Nederlandse Akademie van Weteschappen Proceedings Series B Physical Sciences* **19** (1917) 1217–1225.

[57] W. de Sitter, "On the curvature of space," *Koninklijke Nederlandse Akademie van Weteschappen Proceedings Series B Physical Sciences* **20** (1918) 229–243.

[58] T. Levi-Civita, "Realt fisica di alcuni spaz normali del bianchi," *Reale Accademia Dei Lincei* **26** (1917) 519–531.

[59] E. Mottola, "Particle Creation in de Sitter Space," *Phys.Rev.* **D31** (1985) 754.

[60] D. Marolf and I. A. Morrison, "The IR stability of de Sitter QFT: results at all orders," arXiv:1010.5327 [gr-qc].

[61] D. Marolf and I. A. Morrison, "The IR stability of de Sitter: Loop corrections to scalar propagators," arXiv:1006.0035 [Unknown].

[62] D. Marolf and L. A. Pando Zayas, "On the singularity structure and stability of plane waves," *JHEP* **01** (2003) 076, arXiv:hep-th/0210309.

[63] S. Hollands, "Correlators, Feynman diagrams, and quantum no-hair in deSitter spacetime," arXiv:1010.5367 [gr-qc].

[64] S. Hollands, "Massless interacting quantum fields in deSitter spacetime," arXiv:1105.1996 [gr-qc]. * Temporary entry *.

[65] A. Higuchi, D. Marolf, and I. A. Morrison, "On the Equivalence between Euclidean and In-In Formalisms in de Sitter QFT," *Phys.Rev.* **D83** (2011) 084029, arXiv:1012.3415 [gr-qc].

[66] A. Polyakov, "De Sitter space and eternity," *Nucl.Phys.* **B797** (2008) 199–217, arXiv:0709.2899 [hep-th].

[67] A. M. Polyakov, "Decay of Vacuum Energy," *Nucl. Phys.* **B834** (2010) 316–329, arXiv:0912.5503 [Unknown].

[68] R. Bousso, A. Maloney, and A. Strominger, "Conformal vacua and entropy in de Sitter space," *Phys. Rev.* **D65** (2002) 104039, arXiv:hep-th/0112218.

[69] J. Bros, H. Epstein, M. Gaudin, U. Moschella, and V. Pasquier, "Triangular invariants, three-point functions and particle stability on the de Sitter universe," *Commun. Math. Phys.* **295** (2010) 261–288, arXiv:0901.4223 [hep-th].

[70] F. Tanaka, "Coherent Representation of Dynamical Renormalization Group in Bose Systems," *Prog.Theor.Phys.* **54** (1975) 1679–1692.

[71] L.-Y. Chen, N. Goldenfeld, and Y. Oono, "The Renormalization group and singular perturbations: Multiple scales, boundary layers and reductive perturbation theory," *Phys. Rev.* **E54** (1996) 376–394, arXiv:hep-th/9506161.

[72] D. Boyanovsky and H. de Vega, "Dynamical renormalization group approach to relaxation in quantum field theory," *Annals Phys.* **307** (2003) 335–371, arXiv:hep-ph/0302055 [hep-ph].

[73] D. Boyanovsky, H. J. De Vega, D. S. Lee, S.-Y. Wang, and H. L. Yu, "Dynamical renormalization group approach to the Altarelli- Parisi equations," *Phys. Rev.* **D65** (2002) 045014, arXiv:hep-ph/0108180.

[74] J. M. Cornwall, R. Jackiw, and E. Tomboulis, "Effective Action for Composite Operators," *Phys.Rev.* **D10** (1974) 2428–2445.

[75] K.-c. Chou, Z.-b. Su, B.-l. Hao, and L. Yu, "Equilibrium and Nonequilibrium Formalisms Made Unified," *Phys.Rept.* **118** (1985) 1.

[76] J. Berges and J. Cox, "Thermalization of quantum fields from time reversal invariant evolution equations," *Phys.Lett.* **B517** (2001) 369–374, arXiv:hep-ph/0006160 [hep-ph].

[77] G. Aarts and J. Berges, "Nonequilibrium time evolution of the spectral function in quantum field theory," *Phys.Rev.* **D64** (2001) 105010, arXiv:hep-ph/0103049 [hep-ph].

[78] A. Hohenegger, A. Kartavtsev, and M. Lindner, "Deriving Boltzmann Equations from Kadanoff-Baym Equations in Curved Space-Time," *Phys.Rev.* **D78** (2008) 085027, arXiv:0807.4551 [hep-ph].

[79] J. Berges, "Controlled nonperturbative dynamics of quantum fields out-of-equilibrium," *Nucl.Phys.* **A699** (2002) 847–886, arXiv:hep-ph/0105311 [hep-ph].

[80] D. Boyanovsky and R. Holman, "On the Perturbative Stability of Quantum Field Theories in de Sitter Space," *JHEP* **1105** (2011) 047, arXiv:1103.4648 [astro-ph.CO]. * Temporary entry *.

[81] D. Marolf and I. A. Morrison, "The IR stability of de Sitter QFT: Physical initial conditions," *Gen. Relativ. Gravit.* (2011) , arXiv:1104.4343 [gr-qc].

[82] L. H. Ford, "Quantum Vacuum Energy in a Closed Universe," *Phys. Rev.* **D14** (1976) 3304–3313.